Dust Explosion Experiments

Measurements of Explosion Indices of Graphite Dust in Hydrogen-Containing Atmospheres

A. Denkevits

Institut für Kern- und Energietechnik
Programm Kernfusion

Mai 2005

Forschungszentrum Karlsruhe

in der Helmholtz-Gemeinschaft

Wissenschaftliche Berichte

FZKA 7114

Dust Explosion Experiments

Measurements of Explosion Indices of Graphite Dust in Hydrogen-Containing Atmospheres

Report on EFDA Subtask TW4-TSS-SEA5.2

A. Denkevits

Institut für Kern- und Energietechnik
Programm Kernfusion

Abstract

To address the hazard of combined hydrogen/dust explosions in ITER, the maximum overpressures and rates of pressure rise are measured using a standard method of 20-l sphere of hybrid hydrogen/graphite dust mixtures. The hydrogen concentration is varied from 4 to 18 vol. %. The tested graphite dust concentrations range from 25 to 300 g/m^3. To ignite the mixtures, strong 10 kJ chemical igniters and electric sparks are used.

When ignited by the chemical igniters, the H_2/graphite dust/air mixtures produce higher overpressures than the hydrogen/air mixtures. At low dust concentrations two separate phases of the mixture explosion process can be distinguished: an initial phase of igniter/hydrogen explosion followed by a slower dust-explosion phase. At high dust concentrations only one fast phase is observed, in which hydrogen and dust explode like a monofuel. The pressure rise rates in this case are higher that those measured for pure hydrogen/air explosions.

Electric spark ignition can induce the combined hydrogen/graphite dust explosions at 10 vol. % of hydrogen and higher. The combined explosions have also two phases, if hydrogen concentration is lower 12 vol. %. At 14 vol. % and higher the hybrid mixtures explode faster than hydrogen alone.

Staubexplosionsexperimente
Messungen der Explosionskenngrößen von Graphitstaub in Wasserstoff-Luft Mischungen

Zusammenfassung

Um das Gefahrenpotential von kombinierten Wasserstoff/Staub Explosionen zu untersuchen, werden maximale Überdrücke und Druckanstiegsraten für hybride Wasserstoff/Graphitstaub Mischungen mit der Standardmethode der 20-Liter Kugel gemessen. Der Wasserstoffanteil variiert dabei zwischen 4 und 18 Volumenprozent, die Graphitstaubkonzentrationen zwischen 25 und 300 g/m^3. Zur Zündung werden 10 kJ starke chemische Zünder sowie elektrische Funken benützt.

Bei Zündung mit chemischen Zündern sind die gemessenen Überdrücke höher als für Wasserstoff/Luft Mischungen. Bei niedrigen Staubkonzentrationen kann man dabei zwei Explosionsphasen unterscheiden: eine Anfangsphase mit Zünder/Wasserstoff Explosion, gefolgt von einer langsameren Staubexplosionsphase. Dagegen wird bei hohen Staubkonzentrationen nur eine einzige Phase beobachtet, in der Wasserstoff und Staub wie ein Monobrennstoff explodieren. In diesem letzteren Fall sind die Druckanstiegsraten höher als für reine Wasserstoffexplosionen.

Zündung mit elektrischen Funken kann kombinierte Wasserstoff/Graphitstaub Explosionen bei Wasserstoffkonzentrationen von 10 Volumenprozent und höher induzieren. Liegt die Wasserstoffkonzentration unter 12 Volumenprozent, so haben diese vereinten Explosionen ebenfalls zwei Phasen. Bei einem Wasserstoffanteil von 14 Volumenprozent und höher explodieren diese hybriden Mischungen schneller als Wasserstoff allein.

Executive summary

This work addresses the hazard of combined hydrogen/dust explosions in ITER. Two aspects of the problem are concerned: whether the ITER-relevant dusts mitigate or enhance hydrogen explosions, and the possibility of dust explosion initiation by hydrogen combustion. To investigate these issues, the explosion behaviour of fine graphite dust/hydrogen/air mixtures ignited by either strong chemical igniters or electric sparks is studied using the standard 20-l sphere method.

With this aim the existing DUSTEX facility has been modified to allow tests with hydrogen. The explosion indices of four-micron graphite dust were measured in hydrogen-containing atmospheres at 1 bar initial pressure and ambient initial temperature. The dust was tested in the 25-300 g/m^3 concentration range, and the hydrogen content varied from 4 to 18 vol. %. Both strong 10 kJ chemical igniters and electric sparks were used to ignite the mixtures. The maximum overpressures generated during the explosions and maximum rate of pressure rise were measured as functions of hydrogen content and dust concentrations.

Adding hydrogen to dust cloud atmospheres makes the 4-μm graphite dust explosible by 10 kJ igniters at any tested concentrations. At low concentrations from 4 to 8 vol. %, hydrogen acts like an additional igniter. The explosion process of hybrid dust/hydrogen/air mixtures is similar to the explosion of dust/air mixture. If the dust concentration is low, fast hydrogen explosion induced by the chemical igniter is followed by slower dust explosion. With increasing concentrations the dust explodes faster, and the two explosions overlap. At medium hydrogen concentrations from 8 to 12 vol. %, some part of the dust explodes together with hydrogen participating in the fast explosion phase. At higher hydrogen concentrations, from 14 to 18 vol. %, most of the dust is involved in the fast phase; dust and hydrogen explode together like a monofuel.

At all tested combinations of hydrogen/dust concentrations the maximum overpressures are higher than those produced by hydrogen or dust alone. At low hydrogen concentrations maximum rates of pressure rise for the hybrid mixtures are lower than those measured for the corresponding hydrogen/air mixtures. At higher hydrogen concentrations the maximum rates of pressure rise for the hybrid mixtures are higher than those for the hydrogen/air mixtures.

The hydrogen/graphite dust mixtures can be ignited by electric spark at medium and high hydrogen concentrations only. In case of 8 vol. % hydrogen, the electric spark ignites only the hydrogen constituent of the fuel mixtures; the graphite dust is not involved in the explosion process at any tested dust concentrations. In this case the dust acts as a heat-sink agent

decreasing the maximum overpressure and rate of pressure rise. At medium hydrogen concentrations (10 to 12 vol. %) both hydrogen- and graphite dust-constituents can be induced to explode by electric spark. Like in case of strong ignition, the hybrid explosion has two phases. Initially the spark ignites the hydrogen which explodes like it does without dust. Then the graphite dust starts to react, if the dust concentration is high enough. The dust Lower Explosion concentration Limit is 75 g/m^3 for 10 and 10.5 vol. % hydrogen. With increasing dust concentrations the dust constituent explodes faster generating higher overpressures. For these hydrogen concentrations there are also the dust Upper Explosion concentration Limits for dust explosion development; these UELs are 150 and 175 g/m^3 for 10 and 10.5 vol. % [H_2], respectively. With 11 vol. % hydrogen added, the dust/air mixtures exploded from 50 to 250 g/m^3.

At low hydrogen concentrations the maximum rates of pressure rise in the hybrid mixtures are generally lower that the corresponding values of hydrogen/air mixtures.

At hydrogen concentrations from 14 to 18 vol. % there is only one fast phase for the hybrid mixture explosions. The maximum rates of pressure rise are higher than those measured without dust.

Contents

Introduction

This work continues the study of explosion properties of ITER-relevant dusts which was started in 2002. The explosion indices of graphite dusts [1], tungsten dusts and graphite-tungsten dust mixtures [2] have been measured by a standard method using a 20-l sphere [3, 4]. In this method the tested dust sample is dispersed inside the spherical chamber of 20 l volume, and then the dust cloud is ignited at the sphere centre. The pressure evolution in the chamber during the explosion process is recorded, and two explosion characteristics, so called 'explosion indices', are derived from the pressure-time curve. The two indices are the maximum overpressure and the maximum pressure rise rate which are used to rank the dust explosion severity [3].

Three different graphite dusts were tested of 4 μm, 30 μm, and 45 μm characteristic particle size [1]. They were tested under standard conditions, i.e. at 1 bar initial pressure and room temperature. The other method conditions imply rather conservative results. The used dispersion method causes a very high initial turbulence of the dust cloud, which is expected to enhance the explosion severity. Then, a very strong ignition source – chemical igniters of 10 kJ release energy – are used, which can result in so called 'overdriven explosions' in a relatively small chamber volume.

The dusts were tested over a wide dust-in-air concentration range. The measured overpressures reached about 6.6 bar and depended only slightly on the dust particle size. The maximum rates of pressure rise varied from 250 bar/s for the finest tested dust down to 80 bar/s for the coarsest. Another important explosion characteristic – the Lower Explosion concentration Limit LEL – was measured. It also appeared to depend strongly on the dust particle size, decreasing from 120 g/m^3 for 45 μm dust to 70 g/m^3 for 4 μm dust. The sensitivity of the graphite dust explosions to the ignition energy was also tested. The definition of 'explosive' dust was taken as it is given in [3]. This standard defines a dust as being explosive if it can be induced to explode by an igniter of 1 to 2 kJ energy. The finest tested dust could be triggered to explode by 2 kJ igniter and not by a 1 kJ igniter. The coarser dusts did not explode with a 2 kJ igniter [1].

Tungsten being another ITER-relevant dust material, three tungsten dusts of 1 μm, 5 μm, and 12 μm characteristic particle size were tested. Five- and twelve-micron dusts could not be exploded under the standard conditions described above. One-micron dust exploded in the concentration range from 450 g/m^3 (LEL) to 7500 g/m^3 (the highest tested concentration). The maximum measured overpressure was 4.7 bar, and the maximum pressure rise rate was 260 bar/s.

To investigate interaction effects in the explosion of ITER-relevant dust mixtures, graphite/tungsten dust mixtures were also tested. The four test mixtures were composed of 4-μm graphite and 1-μm tungsten dust having the tungsten-to-carbon molar ratios of W/C=1/30, 1/4, 1/1, and 3/1. The maximum overpressures, maximum pressure rise rates, and LELs of the mixtures were measured. With increasing tungsten content, the maximum overpressure decreased from 6.6 bar (pure graphite) to 4.7 bar (pure tungsten), while the maximum rate of pressure rise had a pronounced peak of 360 bar/s at W/C=1/1, i.e. 1.5 times higher than that for pure graphite and tungsten dust alone. This mixture could be exploded by 2 kJ igniters and was very close to explosion when ignited by 1 kJ igniters [2].

Though some tested dusts could be classified as explosive according to the standard [3], the minimum ignition energy needed was about 1-2 kJ. Such a strong local ignition source seems rather unrealistic under ITER accident conditions. More probably, the graphite and tungsten dusts could participate in an explosion due to the combustion of hydrogen occurring in ITER accident scenarios. Hydrogen can be ignited by a weak ignition source like a small electric spark, and the energy delivered in the course of the hydrogen combustion might be enough to ignite the dusts [5]. The combined explosion of hydrogen and dust under ITER accident conditions is of interest not only in this view. Dispersed dust can also influence a sustained regime of hydrogen explosion. The dust can either enhance the explosion violence, since it may provide additional chemical energy, or it can mitigate the explosion acting as a heat-sink or by competing with hydrogen for the limited atmospheric oxygen.

The combined combustion of flammable gas admixed to dispersed dust, which mixture is usually referred to as 'hybrid mixture', is reviewed by Eckhoff [6]. Several investigations reported a substantial influence of small percentages of combustible gas added to the air on the LELs [7-9]. For example, adding 2 vol. % of methane reduces LEL of coal dusts with 14 % volatiles from 200 g/m^3 to about 70 g/m^3 [7]. The same effect was observed for maize starch dust and hydrogen: 4 vol. % of added hydrogen reduced the dust LEL from 70 g/m^3 (pure air) to about 35 g/m^3, and even hydrogen amounts below the flammability limit caused a noticeable decrease of the dust LEL [8]. When 1 vol. % propane was added to iron dust cloud atmosphere, it caused to 200 to 100 g/m^3 reduction of LEL compared with the pure-air dust cloud [9]. Another relevant aspect was how the combustible gas influences the minimum ignition energy of dust clouds [7, 10, 11]. Adding 3 vol. % of methane can reduce the minimum spark energy needed to ignite coal dust clouds by factors of the order of 100 [10]. It was found that the dust concentration most sensitive to ignition decreased systematically with increasing combustible gas content in the air [7]: for 31 % volatile coal dust the most sensitive dust concentration dropped from 750 g/m^3 in

pure air to 200 g/m^3 when 3.5 vol. % of methane were added. For a coal dust containing 18 % moisture and 12 % ash, the minimum ignition energy decreased from 300 mJ without methane to about 30-50 mJ for 2 vol. % of methane [11]. It was also reported in this work that both maximum pressure and rate of pressure rise in a closed 20-l chamber increased by 30 % if 3 vol. % of methane was added to the air. A significant decrease of optimum dust concentrations was also observed: from 600 g/m^3 without methane to 300 g/m^3 with 3 vol. % of methane. The influence of small fractions of methane in air on maximum explosion pressure and pressure rise rate was studied in 1 m^3 vessel with 10 kJ pyrotechnical igniters [12]. An increase in the methane concentration to 5 vol. % caused a substantial increase in the maximum rate of pressure rise from 70 to 250 bar/s. Another study using a 20-l chamber addressed the influence of small amounts of xylene, toluene, and hexane on the maximum pressure rise rate of exploding organic dust-air mixtures [13]. A pronounced influence was observed even for gas concentrations, which were only about 10 % of the gas minimum explosive concentration in air. For example, a sharp increase in the maximum rate of pressure rise – from 50 bar/s up to 300-400 bar/s – was measured for 250 g/m^3 dust by raising the xylene concentration from 5 to 10 % of its lower flammability limit. A comprehensive study of the explosion indices of hybrid mixtures of organic dust/propane is reported in [14] with the following conclusions:

- hybrid mixtures are easier to ignite and explode with greater severity than pure dust-air mixtures;

- non-explosible dust-air mixtures and non-explosible flammable gas -air mixtures can form explosible hybrid mixtures;

- while addition of flammable gas to the combustible atmosphere raises maximum explosion pressure to some extent, the maximum rate of pressure rise of the combustible dust increases considerably, even though its concentration is below the LEL;

- the minimum ignition energy and the limiting oxygen concentration of the hybrid mixture are determined by the combustible substance with the lowest limit value.

All these results show that the combination of gaseous and solid fuels can change both the ignitability of the mixture and the elementary processes of its combustion, which can result in significant effects on the macroscopic explosion behaviour. It is therefore necessary to experimentally investigate the explosion properties of ITER-relevant hybrid fuel mixtures.

The aim of the present work is to provide the first fundamental data for combined hydrogen/dust explosion process in ITER. Especial attention is focused on the possibility of ITER-relevant dust explosions triggered by low-energy ignition sources. With this purpose, the explosion indices of

4 μm graphite dust ignited in hydrogen-containing atmospheres are measured in the DUSTEX facility using the standard 20-l sphere method. Both strong chemical igniters and electric spark ignition are used to investigate the effect of ignition type and energy. The influence of hydrogen concentration on the dust explosibility is studied.

Test facility

The scheme of the DUSTEX test facility is shown in Fig. 1. The main part of the test facility is a spherical explosion chamber combined with a dust storage container (see Fig. 2). A dust cloud is formed inside the chamber and then ignited at the centre. To form the cloud, a dust sample is placed first into the dust container, then the container is pressurised with compressed air, and at the test start the dust sample is injected inside the sphere with a portion of compressed air via a dust outlet valve. Since the amount of the injecting air is quite comparable with that in the sphere, the sphere is pre-evacuated to provide the standard pressure inside the sphere after dust injection at the moment of ignition.

The test chamber and the container are made of stainless steel and are rated to 30 bar static pressure. The test chamber inner volume is 20 l, and that of the dust container is 0.6 l. The dust container opens to the chamber via a dust outlet valve through the entry at the chamber bottom of about 5 cm^2 cross-section and a dispersion nozzle. The nozzle is used to facilitate the dust dispersion process. Normally, the valve shuts the chamber off from the dust container; in this position it keeps separated both the pressure in the chamber down to several millibars and in the dust container up to 30 bar. The dust outlet valve is opened and closed pneumatically by a short blast of 20 bar compressed air via two solenoid valves, which are activated electrically. The chamber has a bayonet-clamped flange at its top to provide access for cleaning, two flanged openings at its equator, an outlet connecting it to a vacuum pump/atmosphere, and an inlet used to supply hydrogen to the inside. The inlet and outlet ports are closed by ball valves withstanding the maximum design explosion pressure. Two electrode rods are inserted in the upper flange about 3 cm apart. They are used to fix chemical igniters or spark electrodes at the sphere centre and provide ignition voltage. The two pressure transducers are mounted at the two equatorial flanges with their faces flush with the inner wall of the sphere.

The chamber has a jacket with flowing cooling water to keep the chamber wall temperature the same from test to test. The water cooling system is a closed loop; it consists of a heat-insulated water tank, a refrigerator cooling the water in the system to 20° C, and a water pump supplying the water from the tank to the chamber jacket at 1 l/min rate.

The vacuum outlet is connected to a vacuum pump providing 5 mbar evacuation pressure. The vacuum line can be opened to ambient atmosphere. A pressure transducer is fitted in the vacuum line to measure the evacuation pressure; it is also used to prepare gas mixtures in the chamber before an explosion test by the partial pressure method.

To pressurize the dust storage container, dry air from a compressed air bottle kept at 40-150 bar pressure is used. First, the compressed air is supplied from the gas bottle station outdoors via a pipeline into an intermediate vessel of about 10 l volume placed near the chamber. This vessel is necessary to compensate for changing weather conditions and to measure precisely the air dispersion pressure. Hydrogen is supplied directly into the sphere from a hydrogen bottle via a separate line.

The pressure evolution during the explosion is measured with two fast pressure transducers to ensure correct measurements and allow for self checking. The used pressure transducers are piezoelectric gauges, type Kistler 701A (70 kHz natural frequency, 0.1 % uncertainty). Because the piezoelectric pressure transducers are heat-sensitive, their membranes are protected by silicon lubricate. To measure the pressure inside the sphere during gas mixture preparation, a piezoresistive pressure transducer JUMO dTRANS p01 is installed close to the vacuum outlet ball-valve. The measurement range is 0-1 bar, the accuracy is 0.5 %. The air dispersion pressure in the dust storage container and intermediate vessel is measured by JUMO dTRANS p30 pressure transducer in the range 0-25 bar with 0.5 % accuracy. The initial temperature of dispersing air is measured by a resistance thermometer (not shown in the figure) with 0.1° C accuracy.

To ignite the tested mixtures, two types of igniters are used: usual chemical igniters and electric sparks. The chemical (pyrotechnical) igniters are composed of 40 wt% zirconium, 30 wt% barium nitrate, and 30 wt% barium peroxide. A chemical igniter is activated electrically by low-voltage source and provides a dense cloud of hot dispersed particles and very little gas.

For electric spark ignition, a special unit has been designed and fabricated. It consists of a high-frequency transformer with high voltage ratio and a controlling scheme. The unit can provide a train of unipolar half-sine voltage pulses. The pulse amplitude is up to 15 kV; the frequency is up to 15 kHz. Both the amplitude and frequency are tunable. The spark unit output is connected to the electrode rods at the chamber top flange. At the opposite rod ends inside the chamber two spark electrodes are fixed with the inter-electrode gap at the sphere centre. The spark electrodes are made of 2 mm diameter stainless steel wire and sharpened to a point. In the performed tests the gap between the spark electrodes was varied from 0.8 to 2 mm; the spark voltage – from 1 to

3 kV, and the spark duration – from 5 to 50 ms. The hydrogen/air test results did not depend on the spark parameters.

The pressure transducer outputs are digitized and recorded by a data acquisition system based on a 12-bit ADC controller installed in IBM PCs (Keithley KPCI-3103 type, up to 400 kHz sampling rate). In the experiments described here the sampling rate is 5 kHz; 2,000 to 5,000 measurements per channel/shot are stored depending on the explosion process duration. Simultaneously, the timings of the dust outlet valve operation and of the ignition activation current are recorded.

The facility is operated by a central control unit. At the test start this unit triggers the data acquisition board, activates the dust outlet valve to open and close, and switches on the ignition circuit. It sets the timing of the dust outlet valve, the time delay of the ignition activation and the ignition pulse duration. In addition, the control unit blocks the dust outlet valve and the ignition circuit power supply if the bayonet flange at the top of the vessel or the outlet ball-valve is not closed.

Testing procedure

The tests described in this report are conducted under standard conditions [3]. To disperse the dust sample placed in the dust storage container, the container is filled with compressed air to 21 bar. The initial pressure inside the chamber at the moment of ignition is 1 bar; to provide this value, the pressure in the sphere before the injection must be 0.4 bar. At the start of the test the dust outlet valve is opened for 90 ms and then closed. At this moment pressure inside the chamber and in the dust container are both 1 bar. Ten milliseconds later the ignition is activated. If the dust outlet valve runs properly, the pressure inside the sphere starts to rise 40 ms after the test start, so the time delay between start of pressure rise and ignition is 60 ms.

In the described tests the 4 μm graphite dust is used; some information on the dust can be found in [1]. Before charging the container, the dust samples are weighed with 0.01 g accuracy. Typical sample masses are 0.5-5 g. All the dust-in-air concentrations reported here are calculated as the sample mass divided by 20 l. After a dust sample is placed into the storage container and a pair of chemical igniters or spark electrodes is fixed to the electrode rods, the container is pressurized to 21±0.1 bar with dry compressed air using the intermediate storage vessel to let the air obtain the constant room temperature.
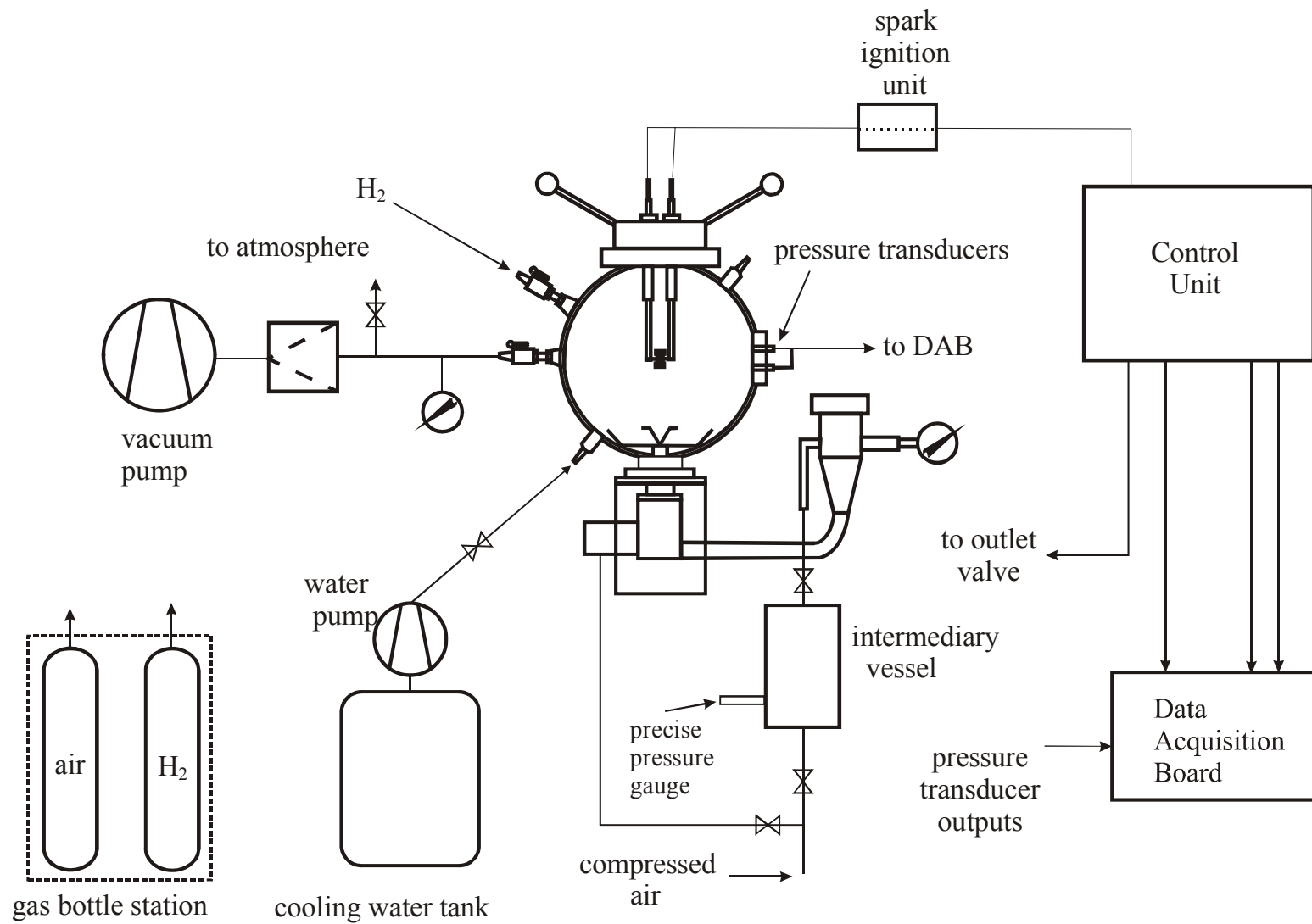
Figure 1. Scheme of DUSTEX facility
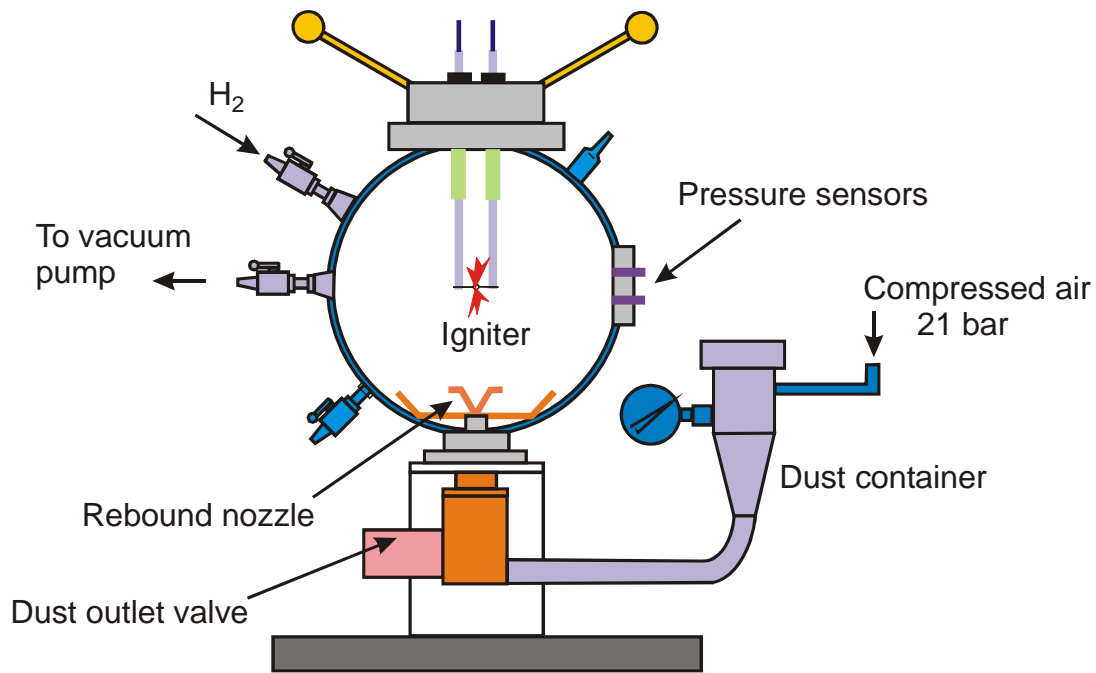
Figure 2. Scheme of 20-l-sphere.

Next, the gas mixture in the combustion chamber is prepared. The chamber is evacuated to 5-7 mbar, then the necessary amount of hydrogen is filled into the chamber (40-200 ± 5 mbar), and then the ambient air is added to the chamber to reach the pressure of 400 mbar.

Before each test the chamber is cleaned thoroughly by a vacuum cleaner and then by rinsing it with a compressed air. After each test series the complete assembly of the chamber, dust outlet valve and dust container is dismounted and cleaned.

Test results

The test results are summarized in Table 1. Here C_{dust} is the graphite dust concentration; $[H_2]$ is hydrogen mole fraction in the mixture in percent; in the column '**Ignition**' ES indicates electric spark igniter and 10 kJ – the chemical igniter, P_m is measured maximum overpressure, and dP/dt_m is maximum rate of pressure rise.

The maximum overpressure values P_{ex} recorded in a test are different from the values P_m presented in Table 1 and reported below. Two effects are taken into account: (a) mixture cooling as the flame front approaches the chamber wall, and (b) the additional pressure generated by the chemical igniter. The first one is important if P_{ex} exceeds 5.5 bar; the second one – if P_{ex} is

below 5.5 bar. The reported values for P_m are derived from the formulas recommended by the sphere manufacturer[15]:

$$P_m = 0.775 \bullet P_{ex}^{1.15} \qquad\qquad \text{if } P_{ex} > 5.5 \text{ bar;} \qquad (1)$$

$$P_m = 5.5 \bullet (P_{ex} - P_{ci}) / (5.5 - P_{ci}) \text{ (bar)} \qquad \text{if } P_{ex} > 5.5 \text{ bar} \qquad (2)$$

Here P_{ci} is the pressure generated by the chemical igniters themselves in a blind test with no dust or hydrogen. Neglecting heat losses, P_{ci} is proportional to the ignition energy IE. Our blind tests with 10 kJ igniters give 1.1 bar overpressure, and $P_{ci} = 1.1 \bullet IE/10,000$ (bar). In the blind tests with electric spark ignition the measured values for P_{ci} were below the accuracy of pressure measurements, and therefore the spark ignition energy was taken to be zero in the data processing.

Another effect of the chemical igniter is important in case of "slow" explosions with less than 150 bar/s pressure rise rate. T the effect of 10 kJ igniters is about 100 bar/s and terminated after 50 ms. So for slow explosions with the pressure rise rates lower 150 bar/s the values of $(dP/dt)_m$ are derived at the moment 50 ms after ignition. In some tests it is impossible to distinguish the effect of the tested fuel, either it is quite low or because of high-level noise. These tests are marked by n/d (not determined).

Table 1. Results of the tests with hydrogen/graphite dust hybrid mixtures.

[H$_2$], % vol.	C$_{dust}$, g/m^3	Ignition	P$_m$, bar	dP/dt$_m$, bar/s	Number of tests
4		ES	0.1	n/d	2
6	0	ES	0.1	n/d	1
7	0	ES	0.1	n/d	1
8	0	ES	2.6	200	3
10	0	ES	3.2	355	2
10.5	0	ES	3.5	460	1
11	0	ES	3.6	530	2
12	0	ES	3.8	600	2
14	0	ES	4.3	830	2
16	0	ES	4.7	970	3
18	0	ES	5.1	1125	2
4	0	10 kJ	0.5	n/d	2
6	0	10 kJ	1.5	n/d	2
8	0	10 kJ	2.5	376	3
10	0	10 kJ	3.2	591	1
12	0	10 kJ	3.8	828	2
14	0	10 kJ	4.5	942	2
16	0	10 kJ	4.8	1168	2
18	0	10 kJ	5.2	1318	2
4	25	10 kJ	1.3	n/d	1
4	50	10 kJ	3.9	90	1
4	100	10 kJ	6.2	150	1
4	125	10 kJ	6.8	190	1
4	150	10 kJ	7.3	250	1
4	175	10 kJ	6.9	265	1
4	200	10 kJ	6.6	210	1
4	250	10 kJ	6.5	200	1

* n/d – not determined

Table 1 (continued). Results of the tests with hydrogen/graphite dust hybrid mixtures.

[H$_2$], % vol.	C$_{dust}$, g/m^3	Ignition	P$_m$, bar	dP/dt$_m$, bar/s	Number of tests
6	25	10 kJ	2.3	n/d	1
6	50	10 kJ	4.7	145	1
6	75	10 kJ	6.1	200	1
6	100	10 kJ	6.8	240	1
6	150	10 kJ	7.5	340	1
6	200	10 kJ	7.1	330	1
6	250	10 kJ	6.4	250	1
8	25	10 kJ	3.8	440	1
8	50	10 kJ	5.4	440	1
8	75	10 kJ	6.6	450	1
8	100	10 kJ	7.5	370	2
8	125	10 kJ	7.3	370	1
8	150	10 kJ	7.3	470	3
8	175	10 kJ	7.2	430	3
8	200	10 kJ	7.2	430	2
8	250	10 kJ	6.7	370	1
10	25	10 kJ	4.5	590	1
10	50	10 kJ	5.2	470	1
10	75	10 kJ	6.8	490	3
10	85	10 kJ	7.1	550	1
10	100	10 kJ	7.3	570	2
10	125	10 kJ	7.3	565	2
10	150	10 kJ	7.1	540	2
10	200	10 kJ	6.7	505	1
12	25	10 kJ	5.3	720	1
12	50	10 kJ	6.5	690	1
12	75	10 kJ	7.1	600	1
12	100	10 kJ	7.4	680	1
12	125	10 kJ	7.6	750	1
12	150	10 kJ	7.4	790	1
12	175	10 kJ	7.4	790	1
12	200	10 kJ	7.1	770	1
12	250	10 kJ	6.8	740	1

Table 1 (continued). Results of the tests with hydrogen/graphite dust hybrid mixtures.

[H$_2$], % vol.	C$_{dust}$, g/m^3	Ignition	P$_m$, bar	dP/dt$_m$, bar/s	Number of tests
14	25	10 kJ	5.9	990	1
14	50	10 kJ	6.8	1130	1
14	75	10 kJ	7.4	950	2
14	100	10 kJ	7.6	1350	3
14	125	10 kJ	7.6	1220	2
14	150	10 kJ	7.2	1280	2
14	200	10 kJ	7.0	1140	2
14	250	10 kJ	6.7	1020	1
16	25	10 kJ	6.2	1300	1
16	50	10 kJ	6.9	1200	1
16	75	10 kJ	7.4	1360	2
16	100	10 kJ	7.5	1430	2
16	125	10 kJ	7.4	1360	1
16	150	10 kJ	7.4	1420	2
16	175	10 kJ	7.2	1430	1
16	200	10 kJ	6.8	1270	1
16	250	10 kJ	6.5	1200	1
18	25	10 kJ	6.3	1400	1
18	50	10 kJ	7.0	1400	1
18	75	10 kJ	7.3	1430	1
18	100	10 kJ	7.4	1600	1
18	125	10 kJ	7.3	1540	1
18	150	10 kJ	7.2	1480	1
18	175	10 kJ	7.0	1480	1
18	200	10 kJ	6.8	1420	1
18	250	10 kJ	6.7	1430	1

Table 1 (continued). Results of the tests with hydrogen/graphite dust hybrid mixtures.

[H$_2$], % vol.	C$_{dust}$, g/m^3	Ignition	P$_m$, bar	dP/dt$_m$, bar/s	Number of tests
8	100	ES	2.0	140	1
8	150	ES	1.9	120	1
8	175	ES	1.9	110	1
8	200	ES	1.9	85	1
8	250	ES	1.8	90	1
10	25	ES	3.7	420	1
10	25	ES	3.2	360	1
10	50	ES	3.2	390	1
10	75	ES	5.4	320	1
10	100	ES	3.0	360	1
10	100	ES	6.2	320	1
10	125	ES	6.4	340	1
10	125	ES	6.5	280	1
10	125	ES	3.0	300	1
10	125	ES	6.4	330	1
10	135	ES	2.9	330	1
10	150	ES	2.9	340	1
10.5	25	ES	3.5	430	1
10.5	50	ES	3.3	390	1
10.5	75	ES	5.3	350	1
10.5	100	ES	6.1	365	1
10.5	125	ES	6.3	330	1
10.5	150	ES	5.8	260	1
10.5	175	ES	3.0	320	1

Table 1 (continued). Results of the tests with hydrogen/graphite dust hybrid mixtures.

[H$_2$], % vol.	C$_{dust}$, g/m^3	Ignition	P$_m$, bar	dP/dt$_m$, bar/s	Number of tests
11	25	ES	3.5	450	1
11	50	ES	4.2	450	1
11	75	ES	6.4	350	1
11	100	ES	6.6	355	1
11	125	ES	6.8	360	1
11	150	ES	6.2	410	1
11	175	ES	6.0	390	1
11	200	ES	6.4	390	1
11	225	ES	5.9	350	1
11	250	ES	5.1	340	1
11	300	ES	0	0	1
12	25	ES	5.4	590	1
12	50	ES	6.6	710	1
12	75	ES	6.9	550	1
12	100	ES	7.2	550	1
14	25	ES	5.8	950	1
14	50	ES	6.6	910	1
14	75	ES	7.2	1010	1
14	100	ES	7.4	950	1
16	25	ES	6.0	1100	1
16	50	ES	6.7	1230	1
16	75	ES	7.3	1280	2
16	100	ES	7.3	1140	1
18	25	ES	6.2	1260	1
18	50	ES	7.0	1400	1
18	75	ES	7.2	1400	1
18	100	ES	7.3	1290	1

Hydrogen-air tests

The test series were started with hydrogen/air mixtures. The investigated range of hydrogen concentration was 4 vol. % (close to the lower flammability limit of hydrogen) to 18 vol. % of hydrogen; the mixtures were ignited either by a 10 kJ chemical igniter or an electric spark. The results are presented in Fig. 3 where maximum overpressures and maximum rates of pressure rise are shown. The pressure-time curves recorded in the tests with electric spark ignition at hydrogen concentrations [H_2]= 8, 12, and 18 vol. % are shown in Fig. 4. About 40 ms after the start of the test, the pressure in the chamber begins to rise due to air injection and reaches 1 bar about 60 ms later. At 100 ms after the start of the test the mixture is ignited, and the pressure increases sharply during the explosion until the flame front arrives at the chamber wall. At this moment the pressure reaches its maximum value; hereafter it decreases as the combustion products cool. With increasing hydrogen concentration the time of combustion in the 20-l sphere decreases from about 35 ms for [H_2]=8 vol. % to 10 ms for [H_2]=18 vol. % (Fig. 4, right), the maximum overpressure increases from 2.6 to 5.1 bar (Fig. 4, left), and the maximum rate of pressure rise – from 200 to 1100 bar/s, correspondingly (Fig. 4, right).

Similar experiments were performed in a closed spherical bomb of 11.4 l volume to measure the laminar burning velocities of hydrogen-air mixtures [16]. The tests were carried out under quiescent initial conditions using weak electric spark ignition. The tested hydrogen concentrations varied form 8 to 67 vol. % The highest laminar burning velocity of about 2.8 m/s was measured for [H_2]=40 vol. % The combustion process duration in this test was about 100 ms. Comparing with the 35 ms combustion time of 8 vol. % hydrogen/air mixture reported here, one can say that the fastest regime in 11.5. l sphere under quiescent initial conditions is three times longer than the slowest one in the 20 l sphere with highly turbulent atmosphere.

If ignited by a 10 kJ igniter, the hydrogen burnt out completely in all the tests (4-18 vol. % [H_2]). If ignited by an electric spark, hydrogen burned only starting from 8 vol. % concentration (see Fig. 3). The measured maximum overpressures in the electric spark ignition tests are essentially the same, within the measurement accuracy, as those obtained with the 10-kJ ignited mixtures. This means that Eq. (2) correctly takes into account the pressure input of the igniters. Maximum rates of pressure rise measured in the strong ignition tests are systematically higher than those measured in the electric spark ignition tests (see Fig. 3, right). This effect can be explained by the additional turbulence due to hot-particle jets from the chemical igniters.
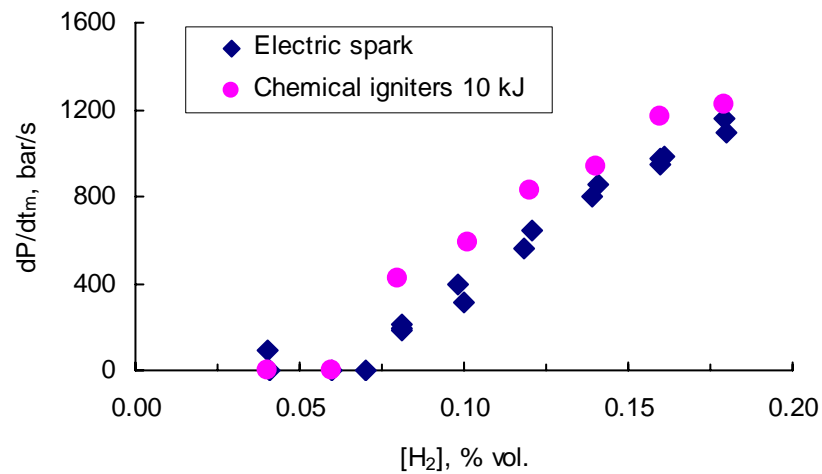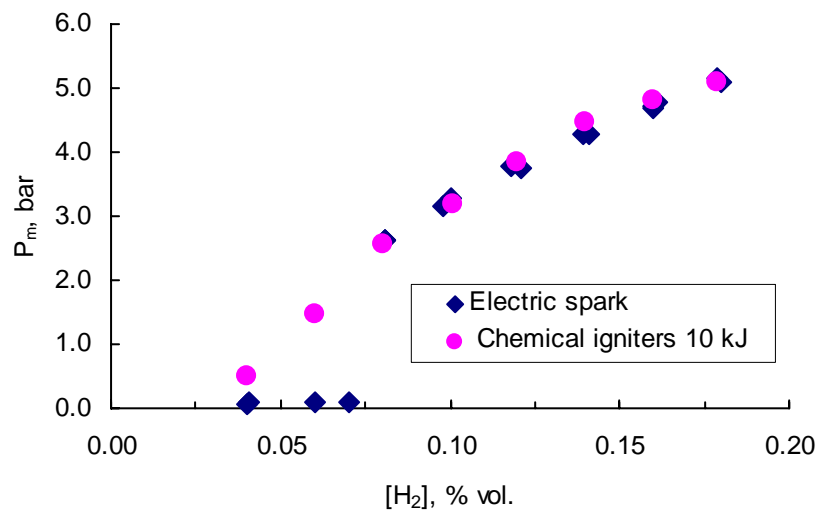
Figure 3. Maximum overpressures (left) and rates of pressure rise (right) measured in hydrogen-air tests. Diamonds: tests with electric spark ignition; circles: tests with 10 kJ chemical igniters.
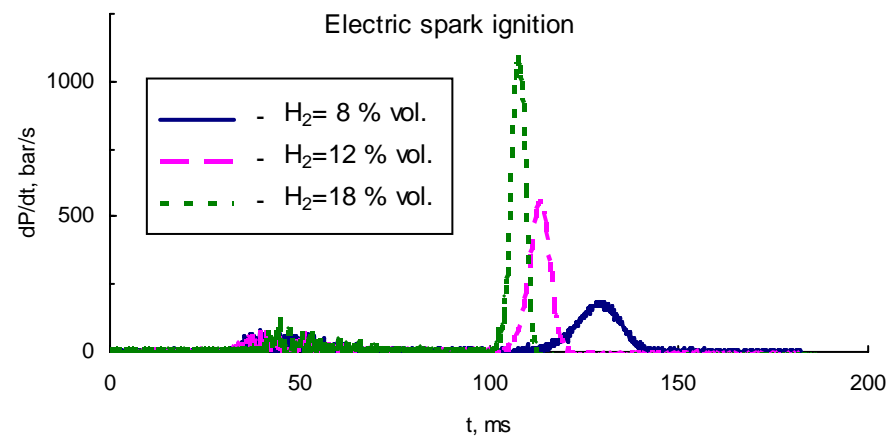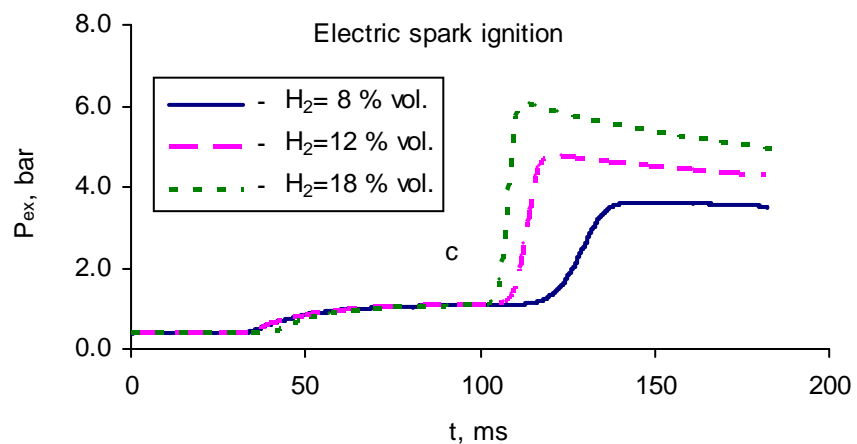
Figure 4. Pressure-time curves (left) and corresponding rates of pressure rise (right) for 8, 12, and 18 vol. % of hydrogen--air mixtures. Electric spark ignition.

Hydrogen-graphite dust-air tests

Strong ignition

The measured maximum overpressures and maximum pressure rise rates in the test series with **4 vol. % of hydrogen** added to graphite dust/air clouds are plotted in Fig. 5 versus dust concentration. The tested dust concentration range is 25-250 g/m^3. The maximum overpressure in the test without dust at the same hydrogen concentration is indicated in Fig. 5a by the horizontal line. Even at the lowest tested concentration of 25 g/m^3 the dust explodes together with hydrogen adding 0.5-1 bar to the explosion overpressure P_m. This can be clearly seen from Fig 6a, where the pressure-time curves with and without dust are compared. Maximum rate of pressure rise cannot be determined either for H_2/air or H_2/C/air mixtures at these concentrations, because the effect of the 10 kJ igniter prevails. The dP/dt curve is shown in Fig. 6b. The first peak occurred at 40 ms is due to the dispersing air injection; the second one is a combination of the igniter and mixture combustion. As the dP/dt of the10 kJ igniters itself is about 100 bar/s, it is difficult to distinguish from this signal if the mixture is burned out volumetrically due to the hot-particle jets of the chemical igniter or a defined flame surface propagated throughout the mixture. Since the 4 % mixture did not ignite by the electric spark, it appears probable that the hydrogen burn is driven by the exploding chemical igniter.

At the dust concentration of 50 g/m^3 the maximum overpressure is 3.9 bar (Fig. 5). This is appreciably higher than that produced by 4 % hydrogen only (about 0.5 bar), so the rest is due to the dust combustion. The pressure-time curve recorded in the test and the corresponding dP/dt(t) are plotted in Fig. 7. The second peak at the dP/dt curve reflects the effect of the igniters. Different from the previous case, there is now a third smooth peak in pressure rise rate near 120 ms. It means that after the igniter has burnt out, there is a slower stable combustion of the mixture. The maximum overpressure is quite high, and the maximum pressure rise rate during the mixture combustion reaches 100 bar/s, i.e. it can be classified as self-sustained explosion. Notice that Lower Explosion concentration Limit LEL measured previously for this dust is 70 g/m^3 [1]; at this concentration without hydrogen the overpressure is less than 0.4 bar.

With increasing dust concentrations the pressure-time curves become more and more similar to those obtained in pure dust-air explosions (see Figs 8-11). The maximum overpressure and pressure rise rate reach their maxima P_{max} and dP/dt_{max} at the dust concentration about 200 g/m^3, 7.3 bar and 265 bar/s, correspondingly. This differs from 250 g/m^3 optimum graphite dust concentration without hydrogen [1]. In general, the small amount of hydrogen in these tests acts like an additional chemical igniter. It consumes only a small amount of oxygen and delivers

additional combustion energy, the energy delivery rate being significantly higher as compared to the rate of the dust combustion. This results in a higher consumption rate of the dust and lowers its optimum concentration.
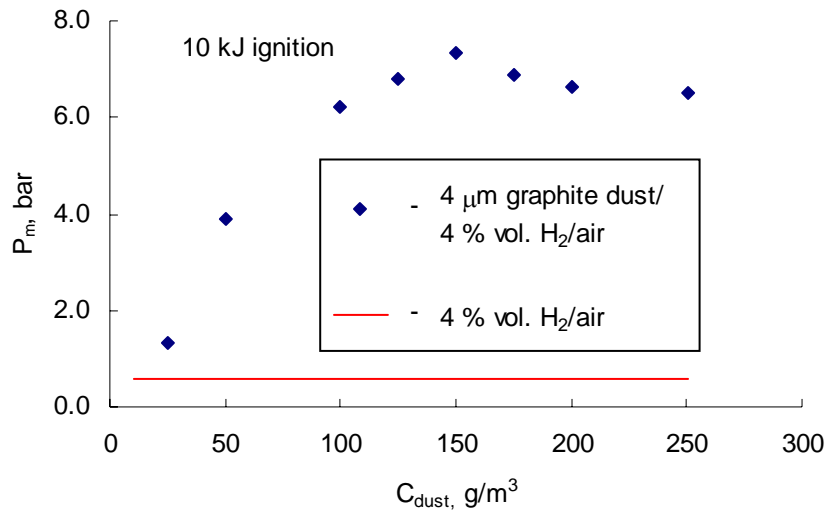

(a)
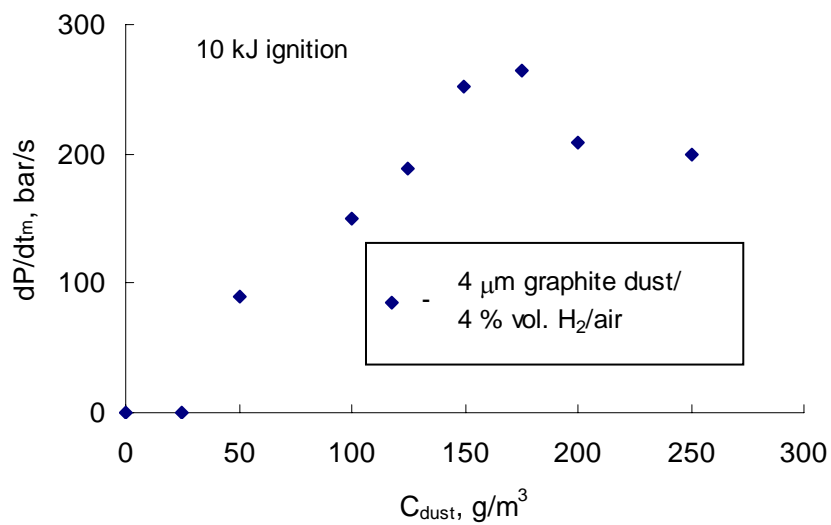
(b)

Figure 5. Maximum overpressures (a) and rates of pressure rise (b) measured in combined hydrogen/graphite dust (4μm) explosions.
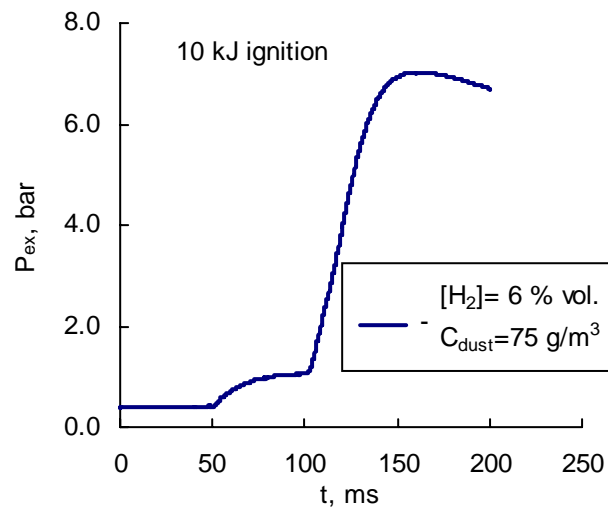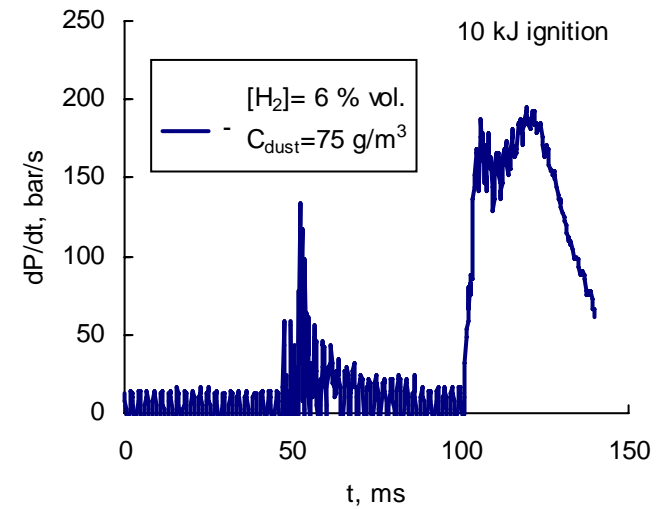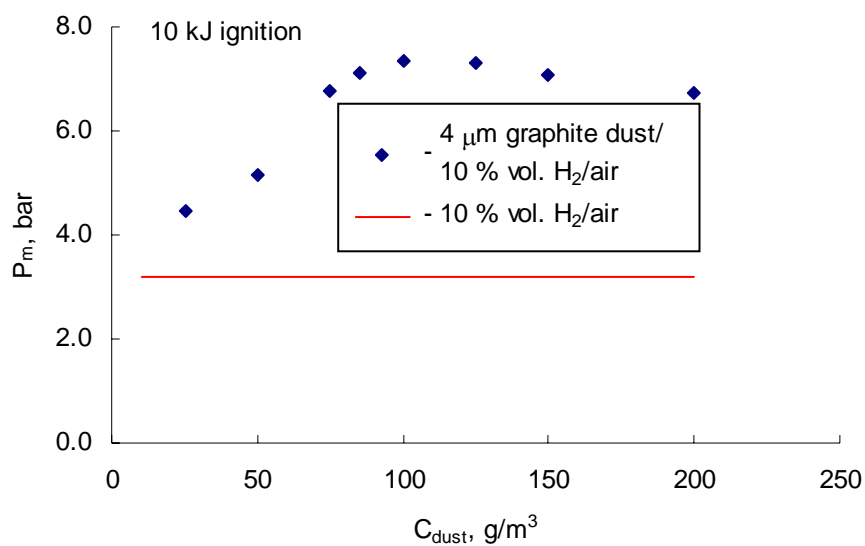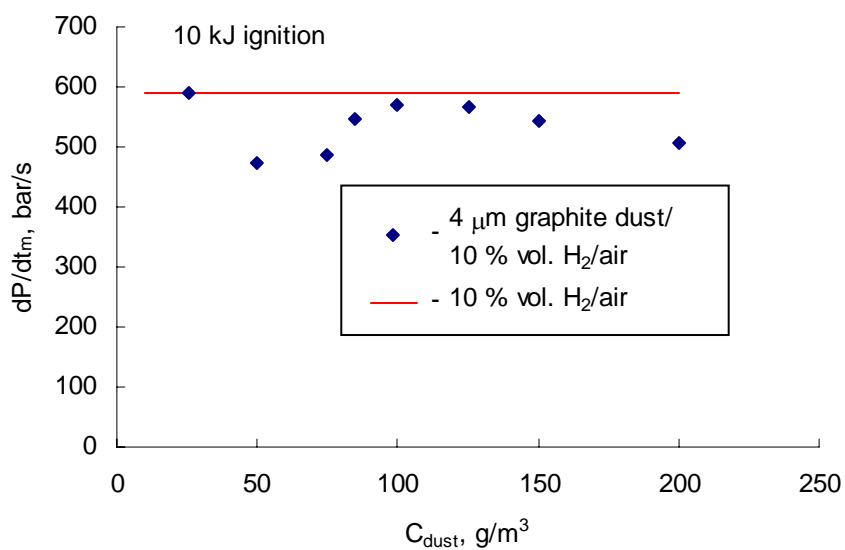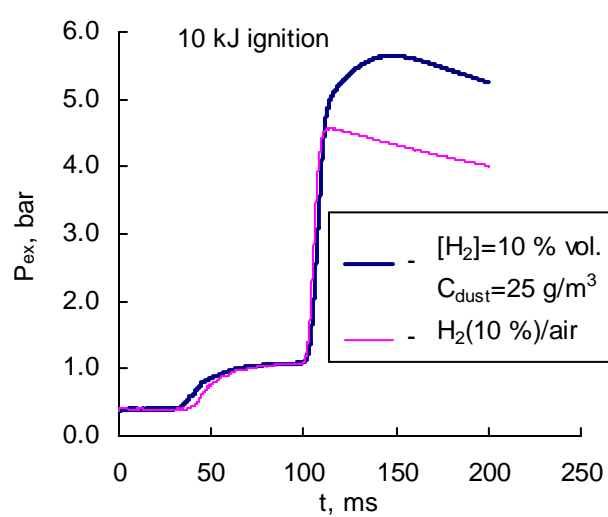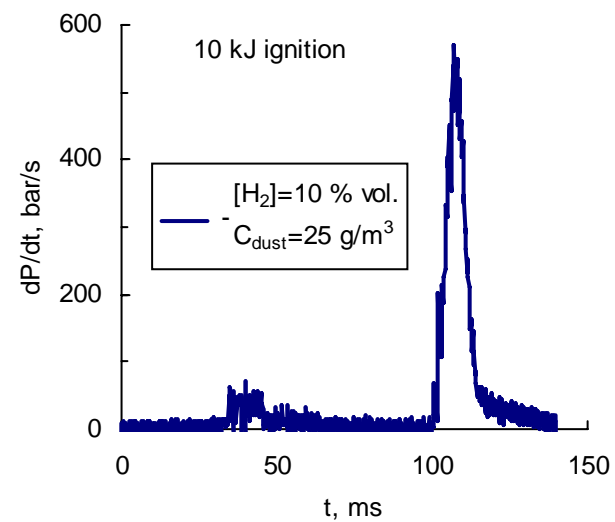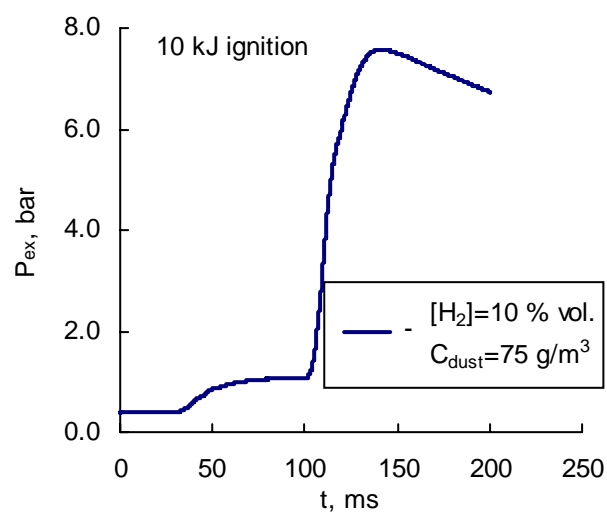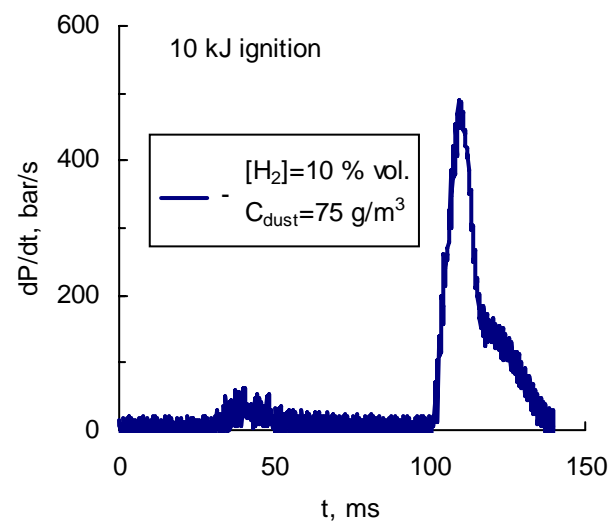Hydrogen concentration – 4 vol. %, ignition – 10 kJ chemical igniters.
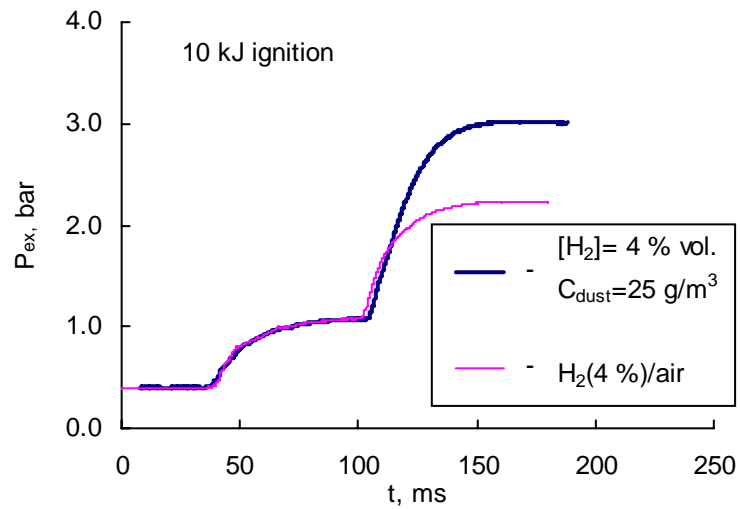
(a)
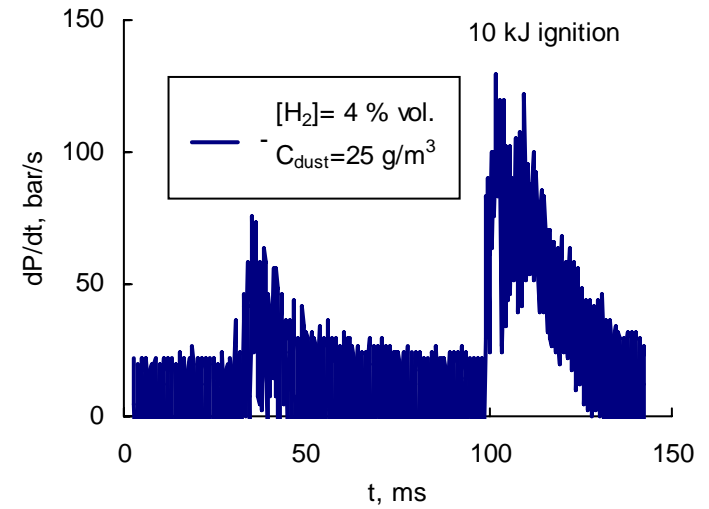
(b)

Figure 6. Pressure-time curve (a) and its derivative (b) for combined hydrogen/graphite dust explosion. $[H_2]$=4 vol. %, C_{dust}=25 g/m^3.
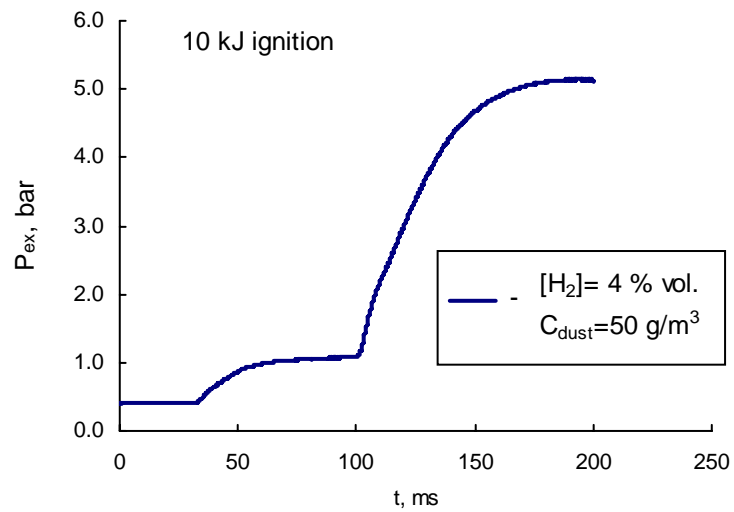
(a)
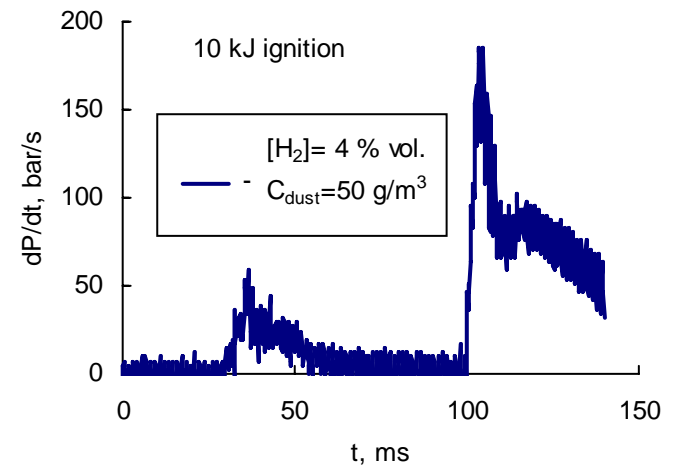
(b)

Figure 7. Pressure-time curve (a) and its derivative (b) for combined hydrogen/graphite dust explosion. $[H_2]$=4 vol. %, C_{dust}=50 g/m^3.
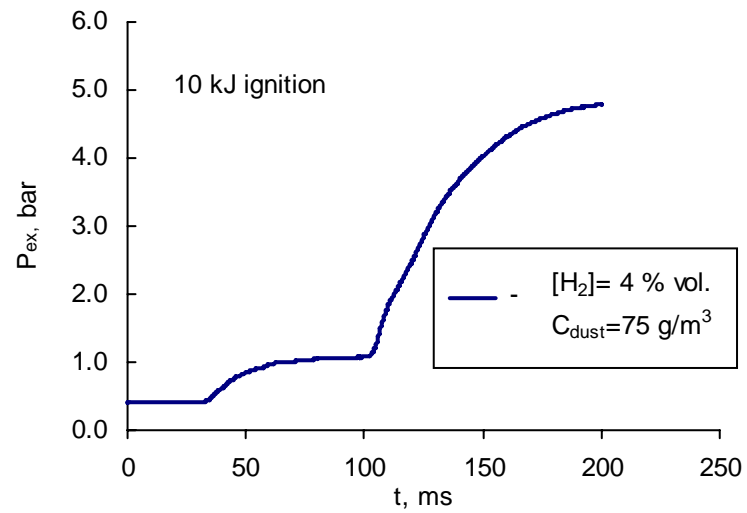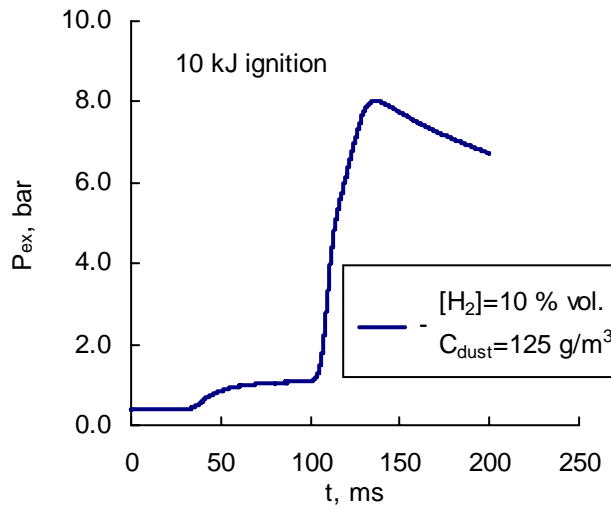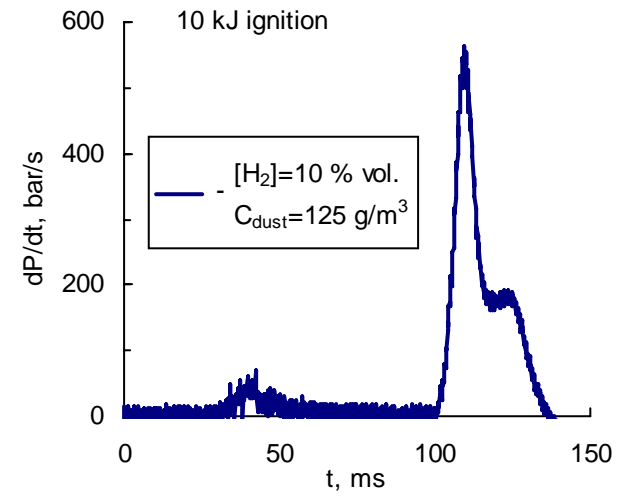
(a)
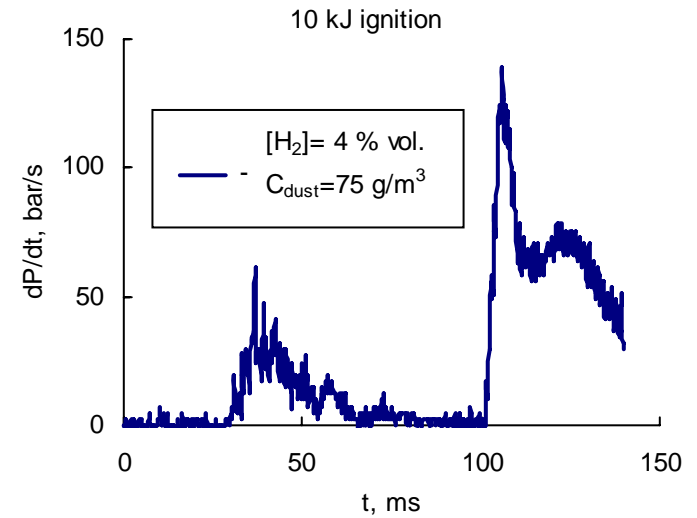
(b)

Figure 8. Pressure-time curve (a) and its derivative (b) for combined hydrogen/graphite dust explosion. [H$_2$]=4 vol. %, C$_{dust}$=75 g/m^3.
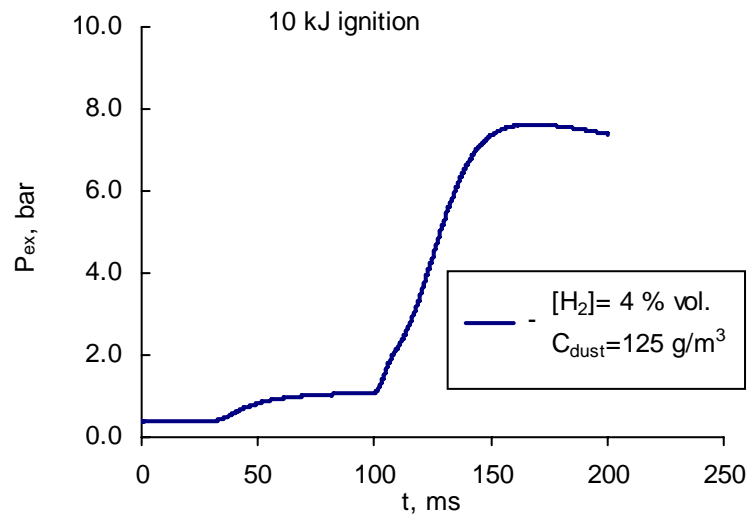
(a)
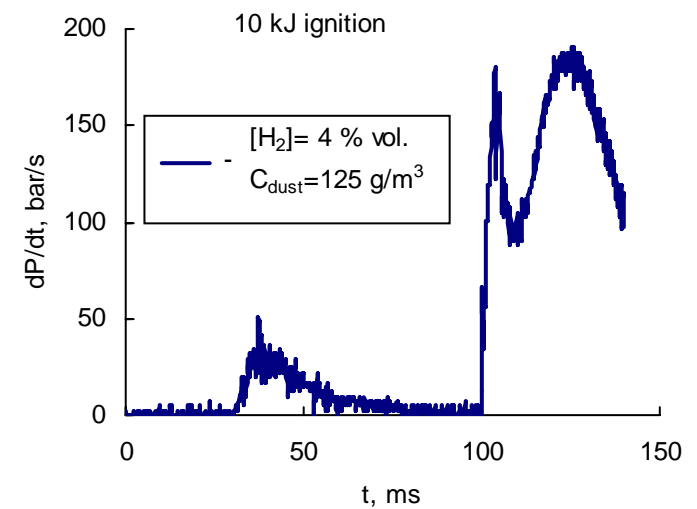
(b)

Figure 9. Pressure-time curve (a) and its derivative (b) for combined hydrogen/graphite dust explosion. [H$_2$]=4 vol. %, C$_{dust}$=125 g/m^3.
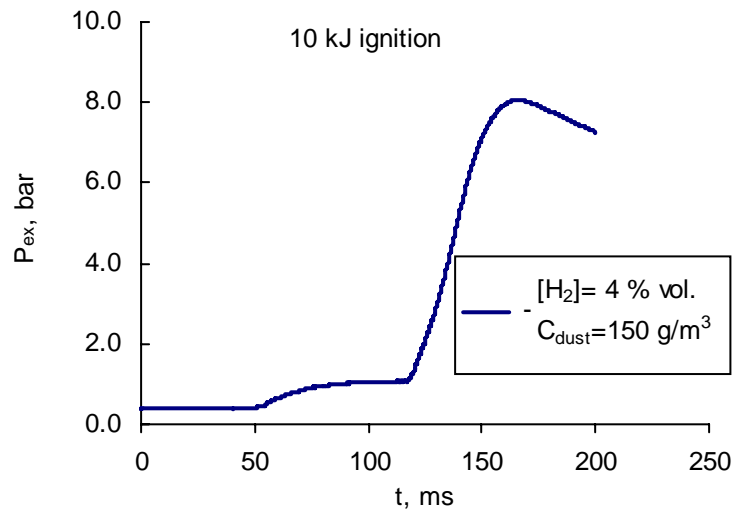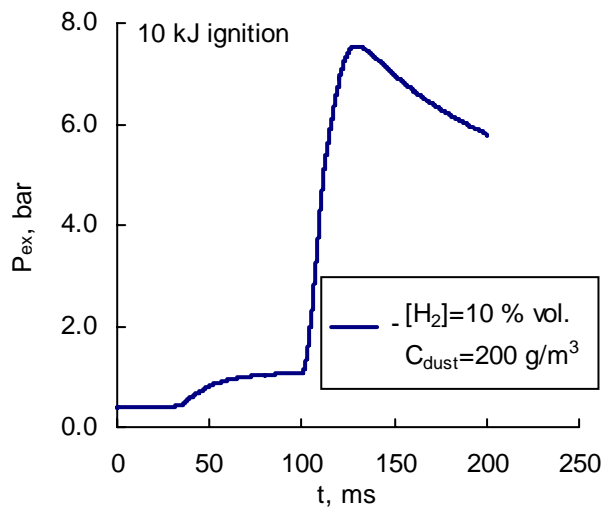
<center>(a)</center>
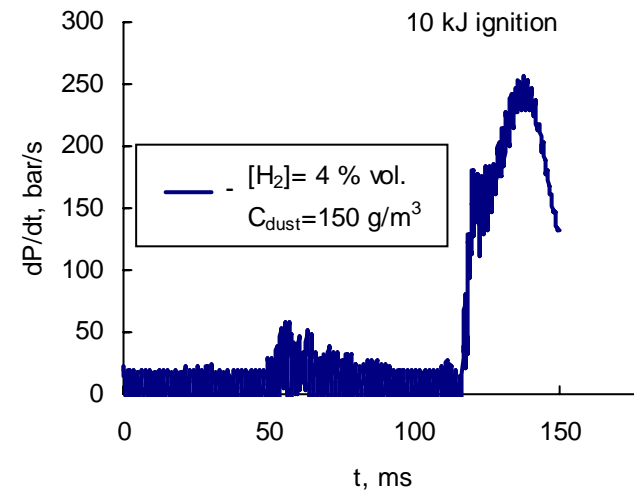
<center>(b)</center>

Figure 10. Pressure-time curve (a) and its derivative (b) for combined hydrogen/graphite dust explosion. $[H_2]$=4 vol. %, C_{dust}=150 g/m^3.
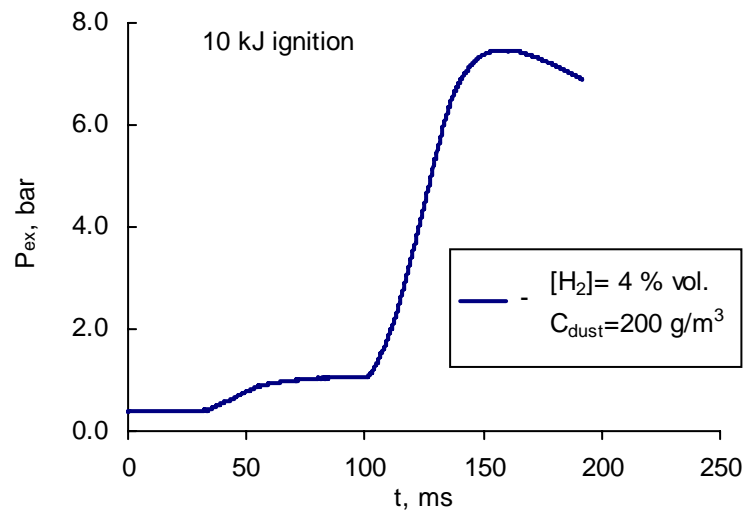
<center>(a)</center>
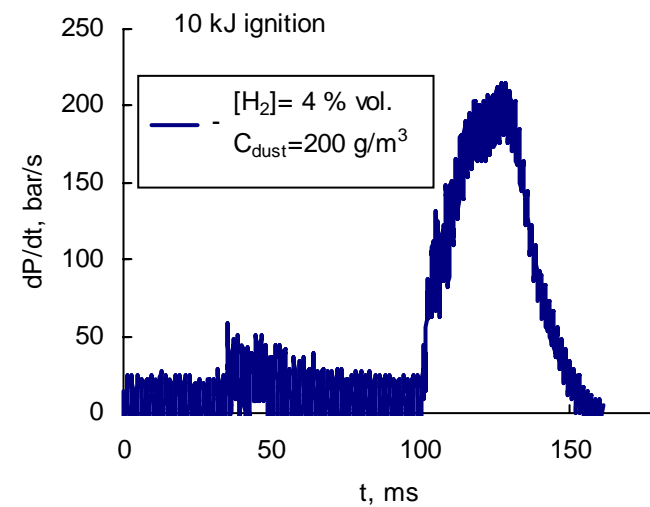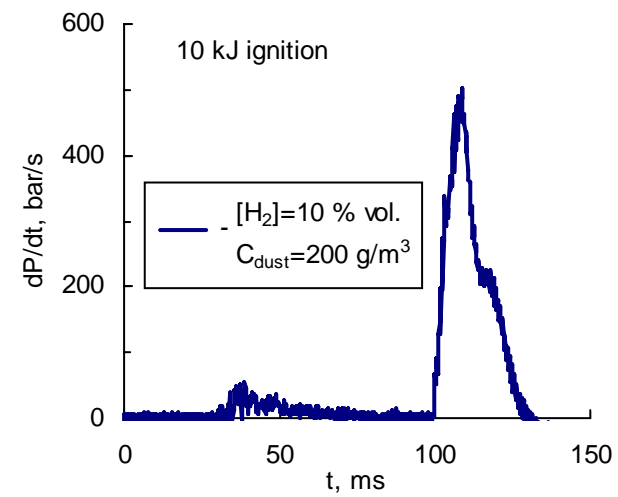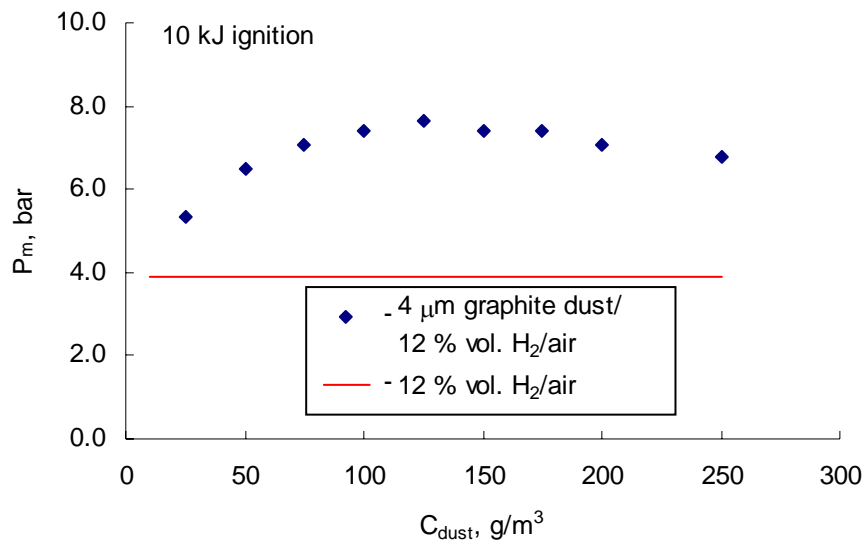

<center>(b)</center>

Figure 11. Pressure-time curve (a) and its derivative (b) for combined hydrogen/graphite dust explosion. $[H_2]$=4 vol. %, C_{dust}=200 g/m^3.

At **6 vol. % of hydrogen** the H_2/graphite dust/air mixtures explode qualitatively in a similar way. The maximum overpressures and rates of pressure rise are plotted in Fig. 12; some examples of the corresponding pressure-time curves are presented in Figs. 13-16. The maximum overpressures are higher for all the tested dust concentrations (25-250 g/m^3) than that observed in the test without dust (indicated by the horizontal lines in Fig. 12)). However, at 25 g/m^3 graphite dust concentration the maximum overpressure is about 1 bar higher than in case of 4 vol. % hydrogen content. Moreover, at this dust concentration the third peak of the dP/dt(t) curve, which represents the dust combustion after operation of the chemical igniters, is clearly distinguishable. The third and second peaks of the dP/dt(t) curve become equal at 75 g/m^3 dust concentration as compared to 125 g/m^3 in case of $[H_2]$= 4 vol. % The optimum dust concentration is slightly lower at 6 vol.% $[H_2]$, around 150 g/m^3; the corresponding explosion indices P_{max} and dP/dt$_{max}$ are noticeably higher than without hydrogen – 7.4 bar and 340 bar/s, compared to 6.6 bar and 250 bar/s without hydrogen. However, the addition of 6 vol. % of hydrogen does not change qualitatively the regime of graphite dust explosion.

Figures 17 and 18 show the dependences of (a) maximum overpressures and (b) maximum rates of pressure rise on the dust concentration with **8 and 10 vol. % of hydrogen**, respectively. Horizontal red lines indicate the values obtained without dust. At 8 vol. % $[H_2]$ the explosion indices P_{max} and dP/dt$_{max}$ are 7.5 bar and 470 bar/s, correspondingly. At this hydrogen concentration maximum rate of pressure rise as a function of dust concentration dP/dt$_m(C_{dust})$ changes its behaviour. With increasing dust concentration it decreases first, then rises, reaches another maximum and then decreases again. Starting from 10 vol. % $[H_2]$, the combined explosion of hydrogen and graphite dust changes, as it can be seen from the pressure-time curves (Figs. 19-22). It is still possible to distinguish two stages of the hybrid explosion: first a fast stage "chemical igniters + hydrogen" and then a subsequent slower stage of predominantly dust combustion. The second explosion peak – third on the dP/dt curve – is still seen. However, it is at no dust concentration higher than the first one. The most part of energy is delivered during the first fast stage of explosion. One can say that hydrogen combustion begins to prevail over graphite dust combustion.

At **12 vol. % of hydrogen** the maximum overpressure over the tested dust concentrations P_{max} is 7.6 bar, the maximum rate of pressure rise dP/dt$_{max}$ is about 800 bar/s (see Fig. 23). Over all dust concentration range tested, the maximum overpressures P_m are higher than the value 3.9 bar measured for hydrogen without dust. Maximum rate of pressure rise dP/dt$_m$ decreases first with dust concentration increasing to 75 g/m^3 and then rises reaching the second maximum at about

170 g/m^3 graphite dust. At all tested dust concentrations it is lower than dP/dt$_m$ measured for 12 vol. % H$_2$/air mixture.
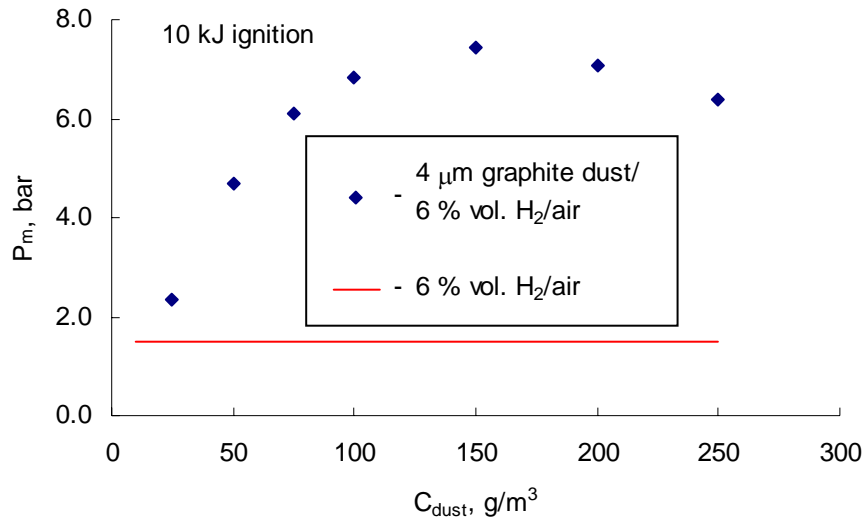

(a)
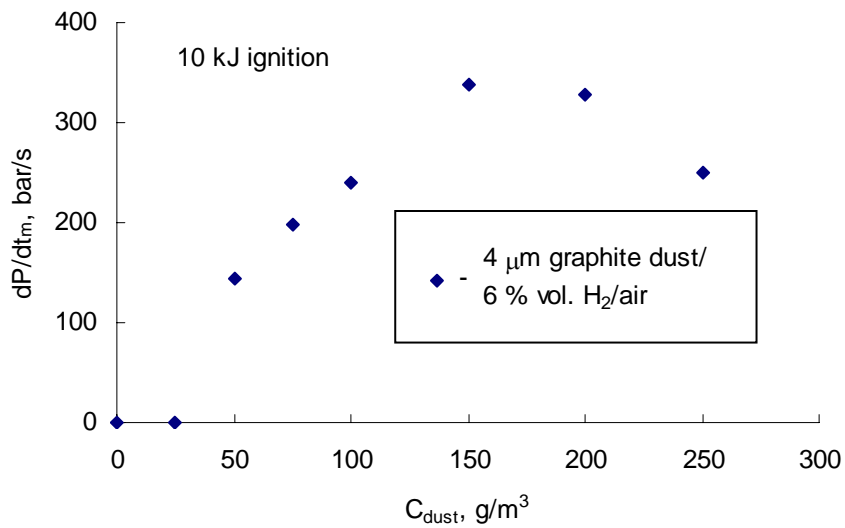
(b)

Figure 12. Maximum overpressures (a) and rates of pressure rise (b) measured in combined hydrogen/graphite dust (4μm) explosions.

Hydrogen concentration – 6 vol. %, ignition – 10 kJ chemical igniters.
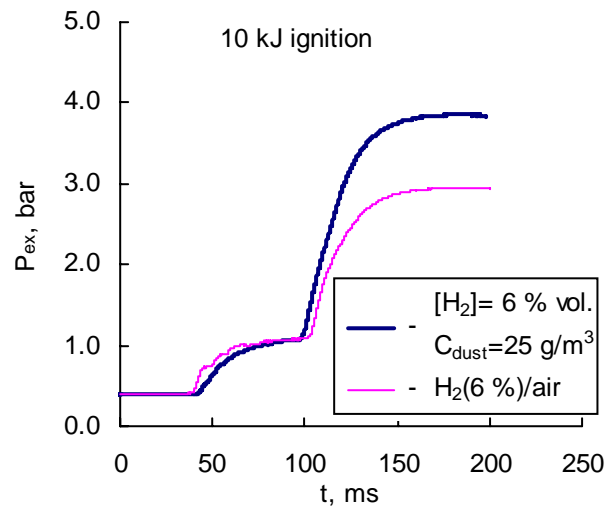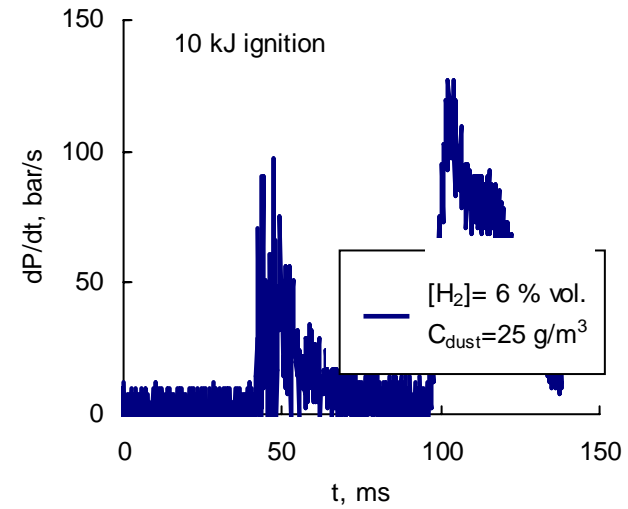
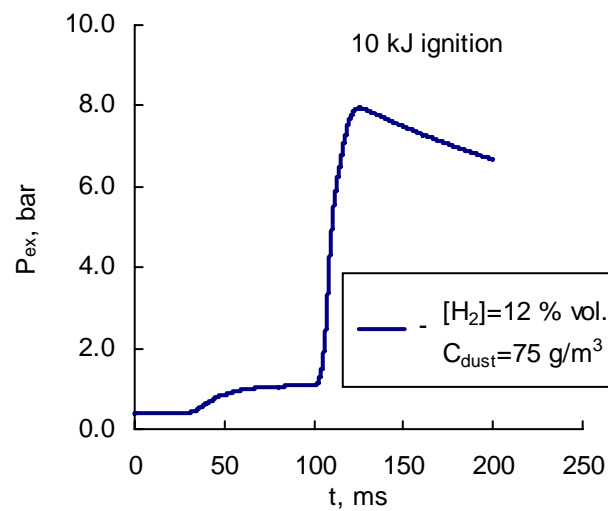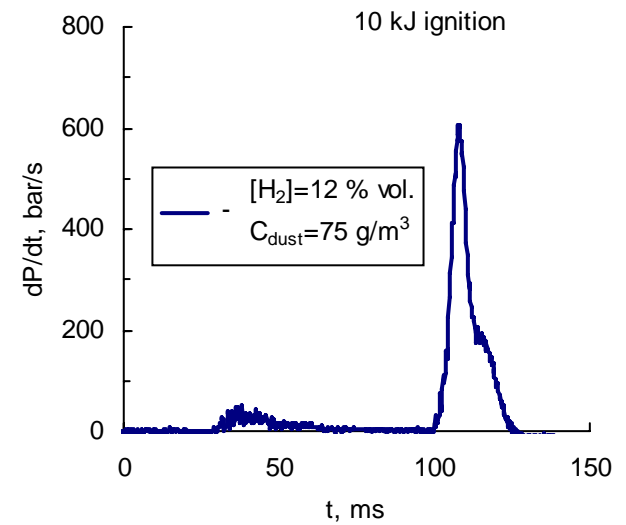Figure 13. Pressure-time curve (a) and its derivative (b) for combined hydrogen/graphite dust explosion. $[H_2]$=6 vol. %, C_{dust}=25 g/m^3.

Figure 14. Pressure-time curve (a) and its derivative (b) for combined hydrogen/graphite dust explosion. $[H_2]$=6 vol. %, C_{dust}=75 g/m^3.
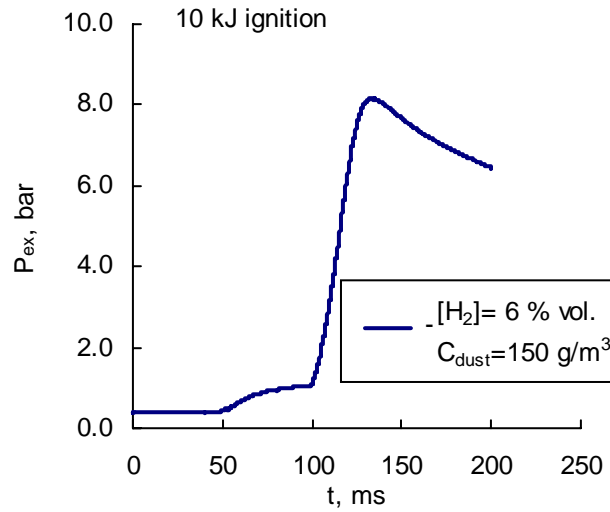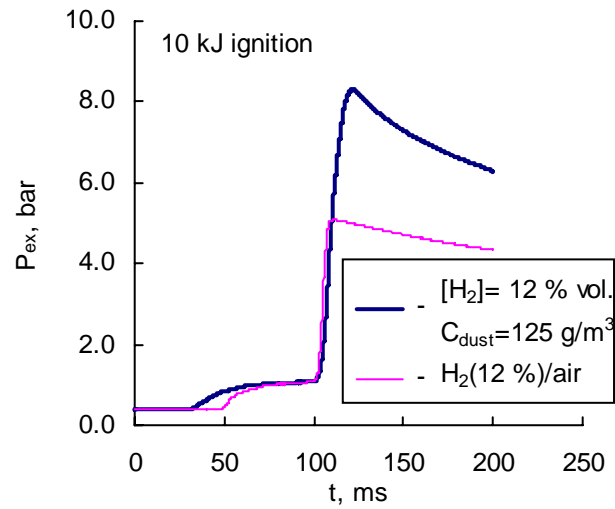
(a)
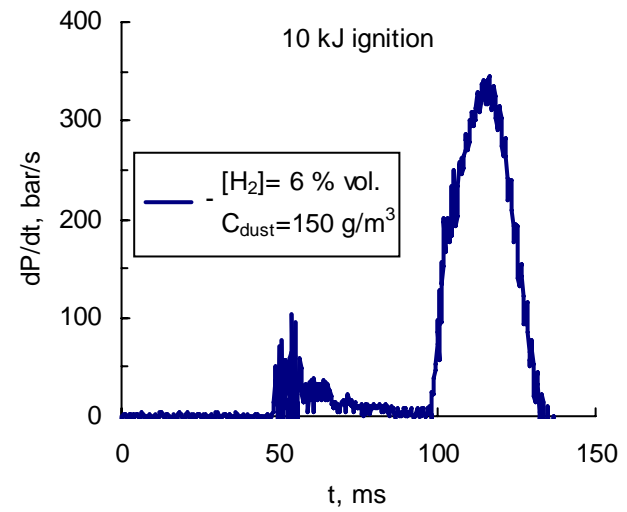
(b)

Figure 15. Pressure-time curve (a) and its derivative (b) for combined hydrogen/graphite dust explosion. [H$_2$]=6 vol. %, C$_{dust}$=150 g/m^3.
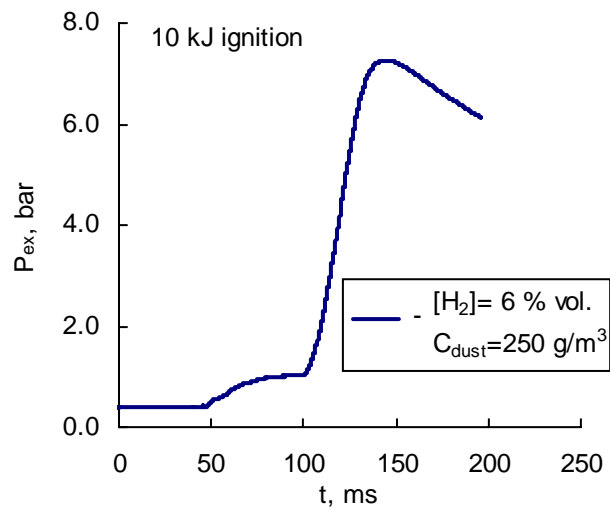
(a)
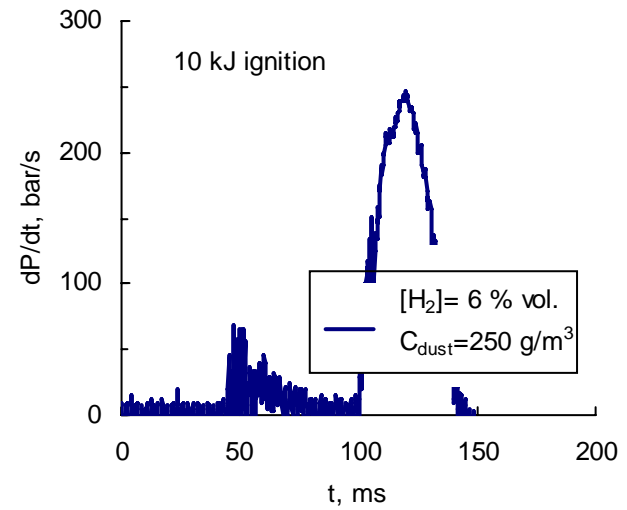
(b)

Figure 16. Pressure-time curve (a) and its derivative (b) for combined hydrogen/graphite dust explosion. [H$_2$]=6 vol. %, C$_{dust}$=250 g/m^3.
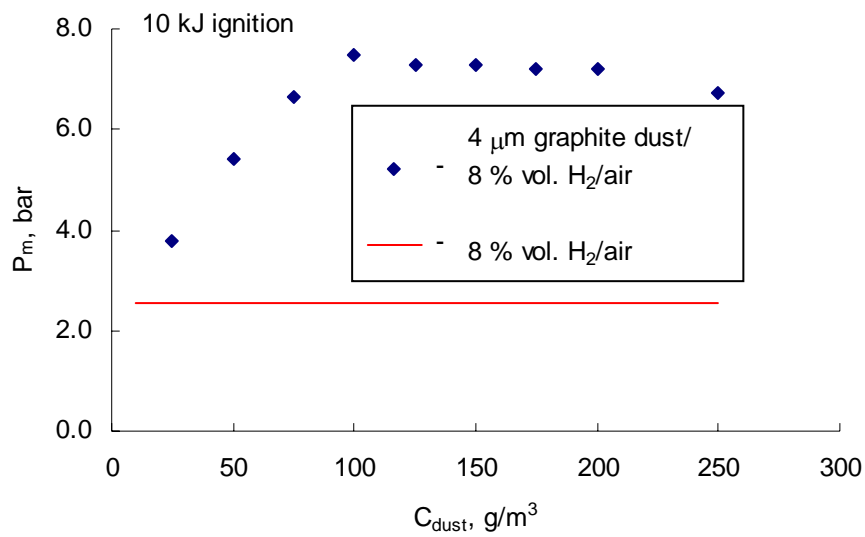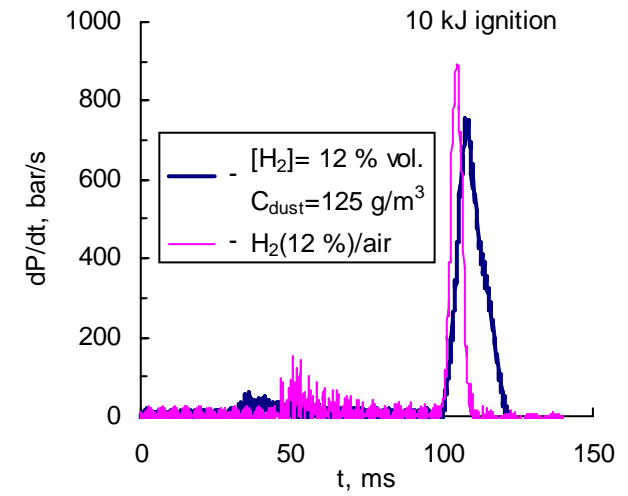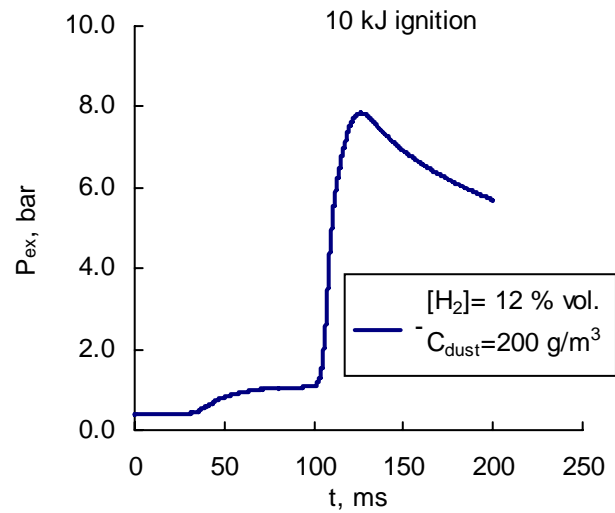
(a)
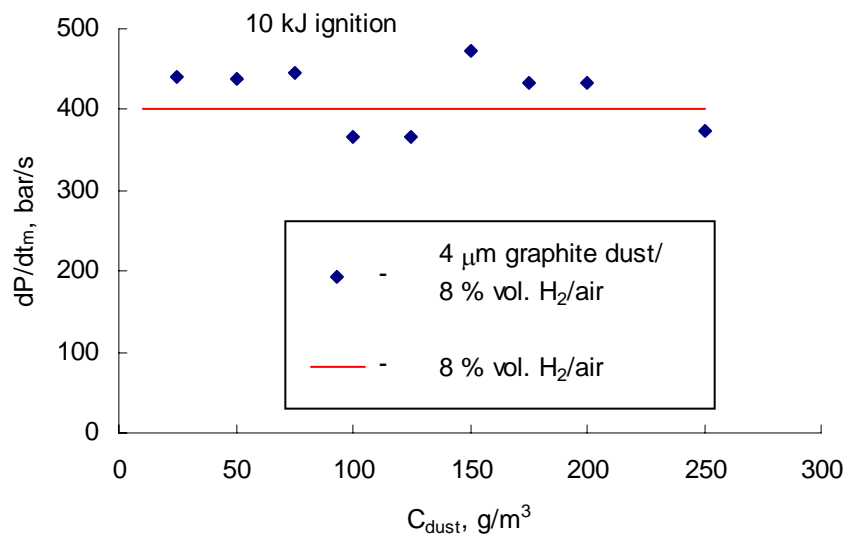
(b)

Figure 17. Maximum overpressures (a) and rates of pressure rise (b) measured in combined
hydrogen/graphite dust (4μm) explosions.
Hydrogen concentration – 8 vol. %, ignition – 10 kJ chemical igniters.

(a)

(b)

Figure 18. Maximum overpressures (a) and rates of pressure rise (b) measured in combined
hydrogen/graphite dust (4μm) explosions.
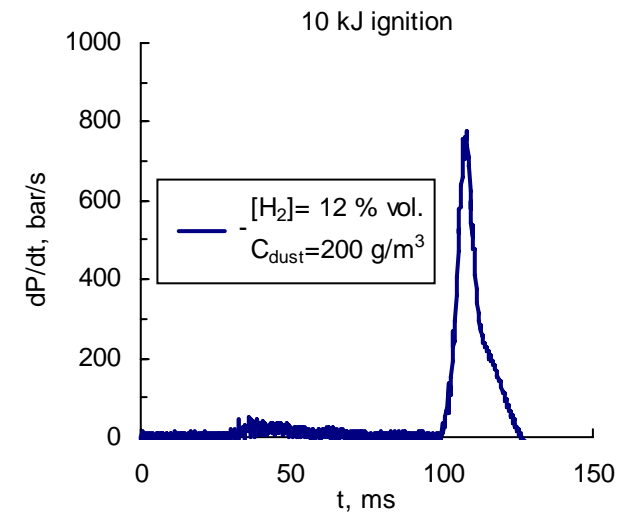Hydrogen concentration – 10 vol. %, ignition – 10 kJ chemical igniters.

Figure 19. Pressure-time curve (a) and its derivative (b) for combined hydrogen/graphite dust explosion. $[H_2]$=10 vol. %, C_{dust}=25 g/m^3.
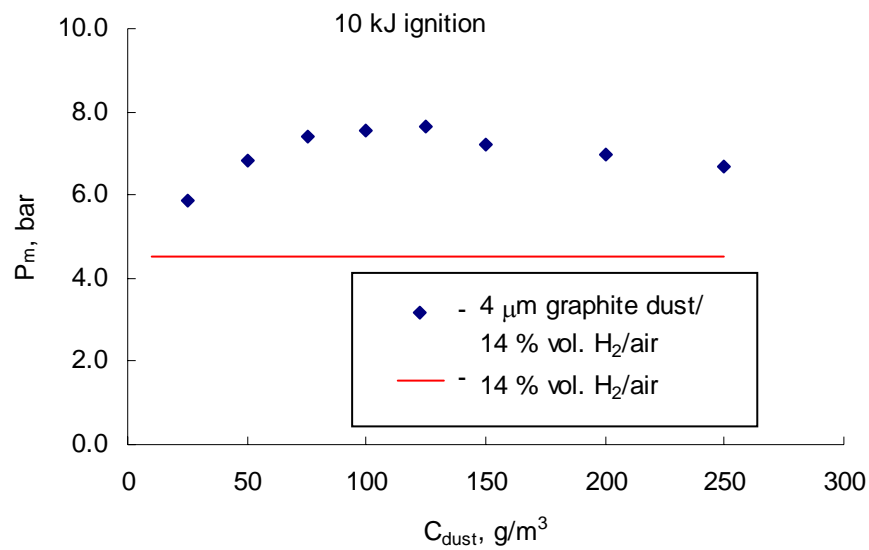

Figure 20. Pressure-time curve (a) and its derivative (b) for combined hydrogen/graphite dust explosion. $[H_2]$=10 vol. %, C_{dust}= 75 g/m^3.

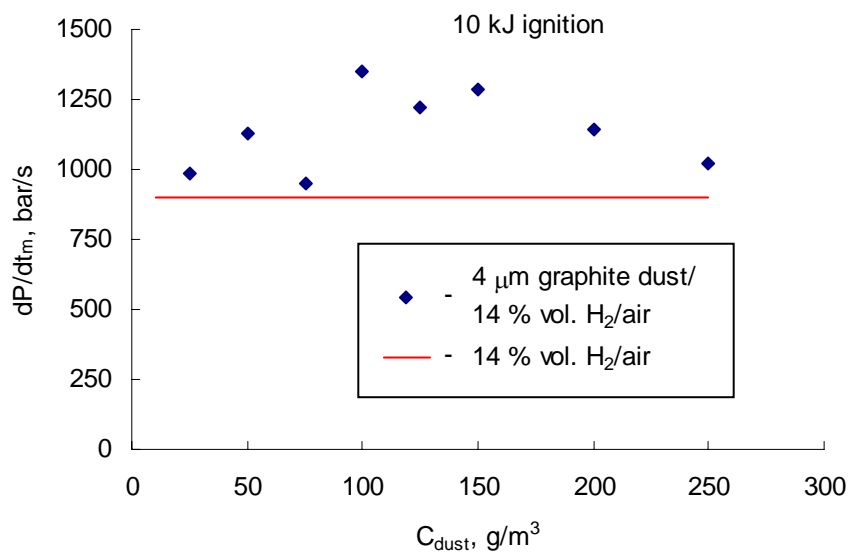(a)   (b)

Figure 21. Pressure-time curve (a) and its derivative (b) for combined hydrogen/graphite dust explosion. $[H_2]$=10 vol. %, C_{dust}=125 g/m^3.
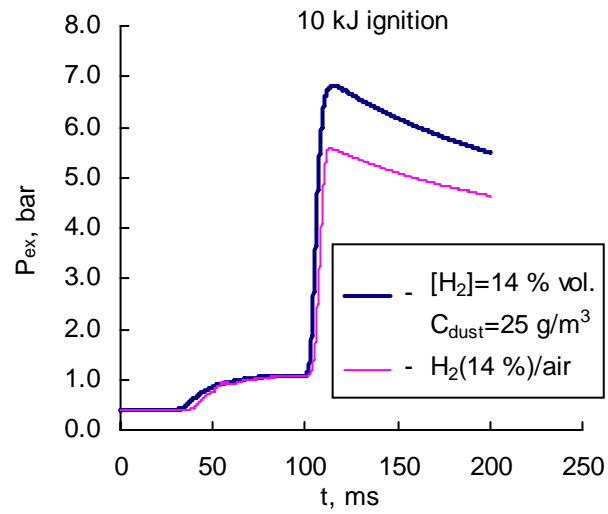

(a)   (b)

Figure 22. Pressure-time curve (a) and its derivative (b) for combined hydrogen/graphite dust explosion. $[H_2]$=10 vol. %, C_{dust}=200 g/m^3.

In the test series with 12 vol. % H_2 the mode of the hybrid mixture explosions looks more like that of hydrogen/air mixture explosions than with 10 vol. % H_2. This can be seen from Figs. 24-27, where the pressure-time curves recorded in this tests series are shown. At 25 g/m^3 dust concentration the dust essentially burns out during the first fast stage (Fig. 24). At 75 g/m^3 concentration a fraction of the dust burns during the 15 ms following the first stage of 10 ms duration (Fig. 25). At 125 g/m^3 it is rather hard to distinguish between the two stages, both the P(t) and dP/dt(t) are qualitatively of the same shape as those for the H_2/air mixture (Fig. 26). At 200 g/m^3 the second slow phase can be distinguished again (Fig. 27).

The maximum overpressure and rate of pressure rise for **14 vol. % of hydrogen** are plotted in Fig. 28 versus dust concentration. From this hydrogen concentration on, the combustion of the H_2/graphite dust/air mixtures has no second slow stage. The dust and hydrogen burn together as a monophase fuel. It can be seen from Figs. 29 and 30, where P(t) and dP/dt(t) curves are plotted for the dust concentrations 25 and 250 g/m^3 at 14 vol. % H_2, and Figs. 33 and 34 with the curves for the dust concentrations 25 and 250 g/m^3 at 18 vol. % H_2. Inside this range the curves look qualitatively the same. The pressure-time curves have the sharp peak structure typical for fast-burning gases with a thin flame front. The difference between 'pure hydrogen' case and 'hydrogen/dust' case is only in the pressure amplitude, the combustion duration is almost the same in both cases. In addition, starting from 14 vol. % H_2, the hydrogen/dust/air mixtures explode faster than the hydrogen/air mixtures at the same hydrogen concentration. This can be seen from Figs. 28, 31, and 32, where maximum overpressures and rates of pressure rise are plotted versus dust concentration at 14, 16, and 18 vol. % H_2, respectively.

The measured maximum overpressures and maximum rates of pressure rise are summarized as functions of dust concentration in Fig. 35. The same results are plotted in Figs. 36-40 as function of hydrogen concentration. At dust concentration below 100 g/m^3 even small amounts of added hydrogen make the dust-air mixtures explosible by a strong ignition source. With increasing hydrogen concentration both the maximum overpressure and the maximum rate of pressure rise increase also. At higher dust concentrations the maximum overpressure is essentially independent on hydrogen concentration, except where the dust/hydrogen fuel is not rich enough to consume all the oxygen in air. When this happens, an increase in the hydrogen concentration results in higher rates of pressure rise, i.e. faster explosions. From 14 vol. % of hydrogen on, the maximum rate of pressure rise is generally higher at all dust concentrations than that of the corresponding hydrogen-air mixture. This is not a trivial result, as one could expect as well that the heat-sink influence of the unburned dust might prevail.

(a)
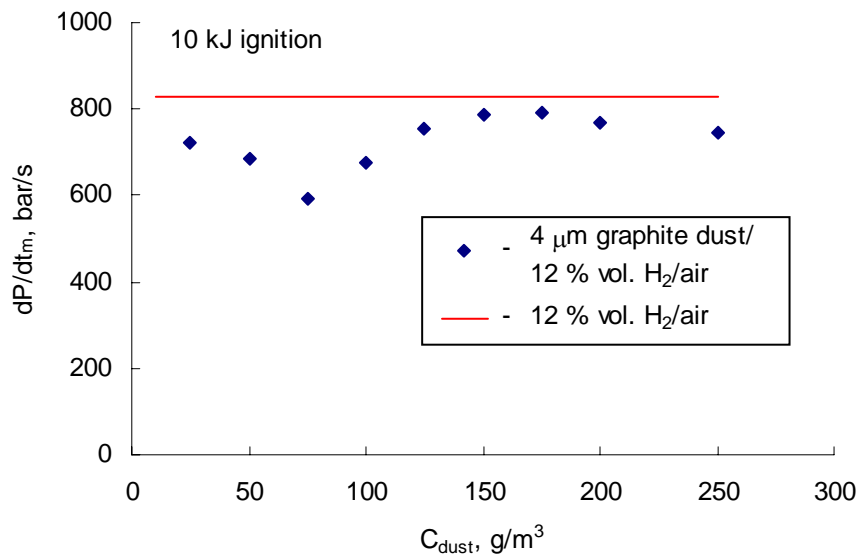
(b)

Figure 23. Maximum overpressures (a) and rates of pressure rise (b) measured in combined hydrogen/graphite dust (4μm) explosions.
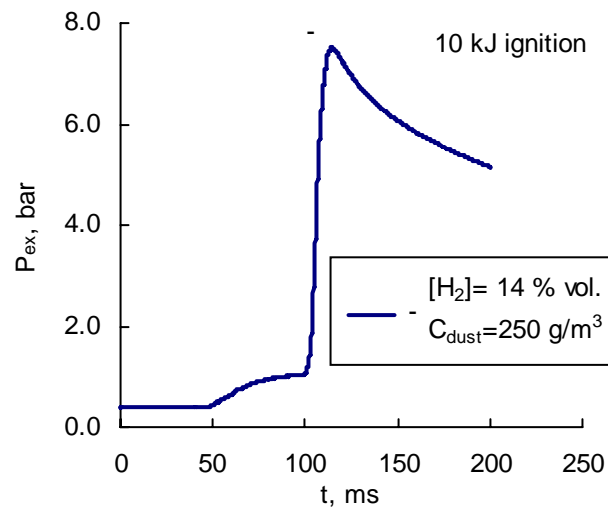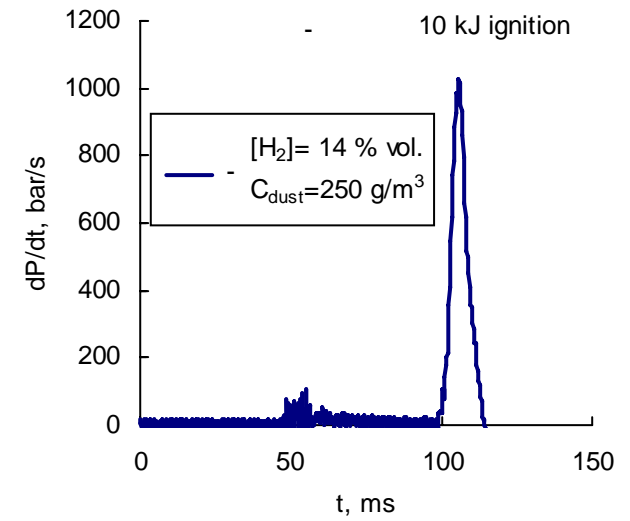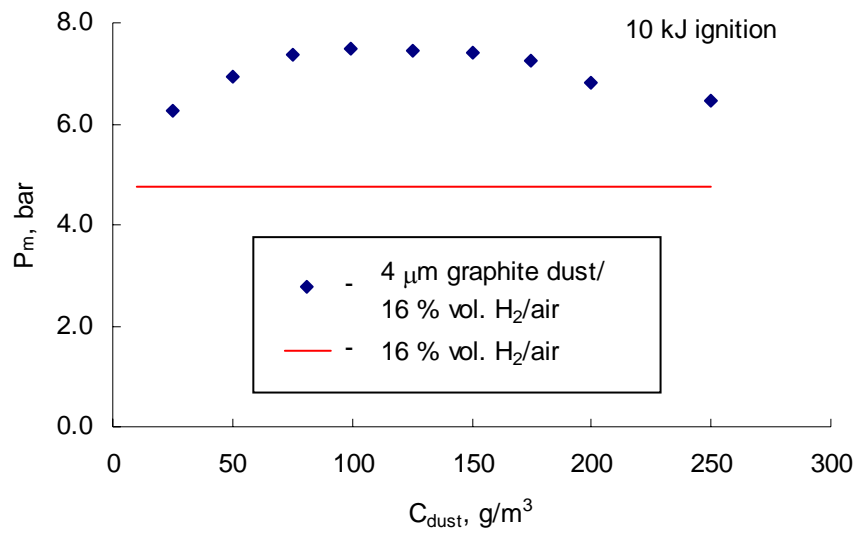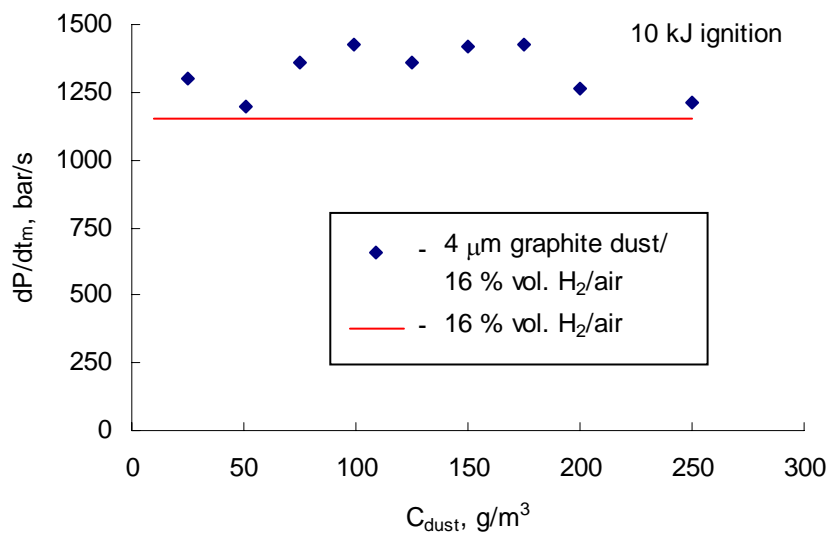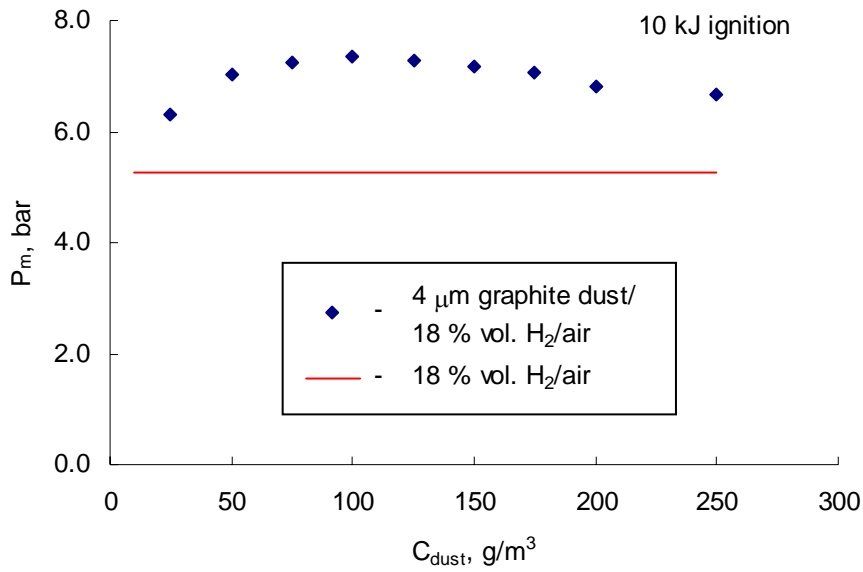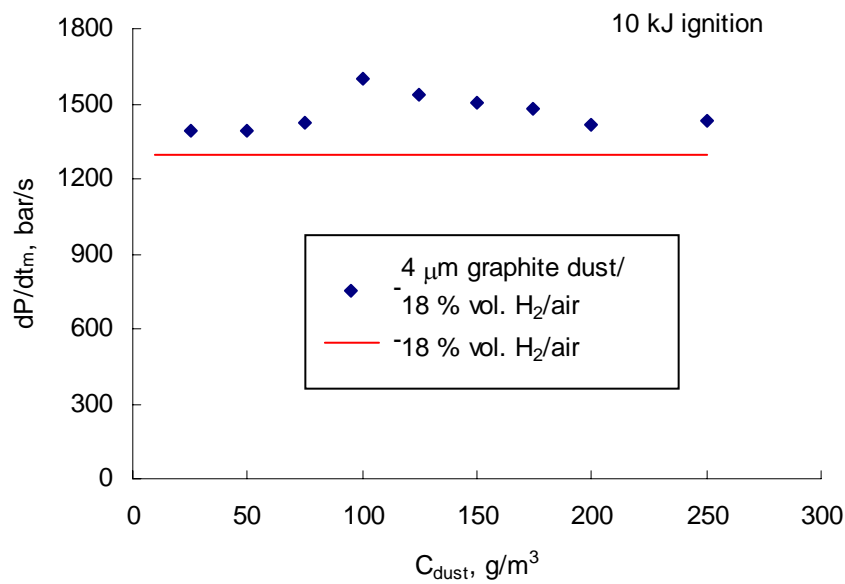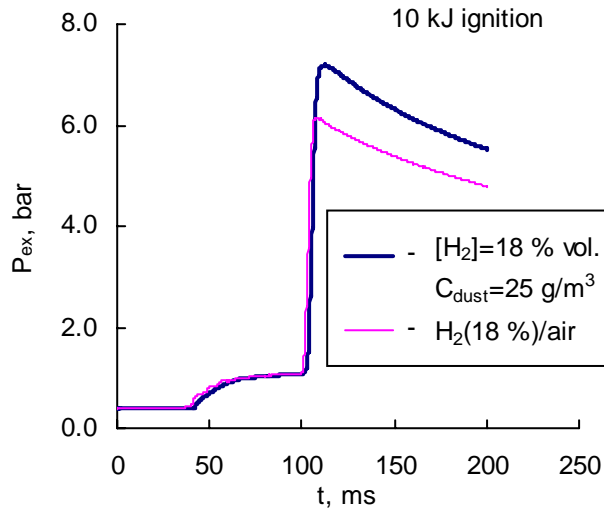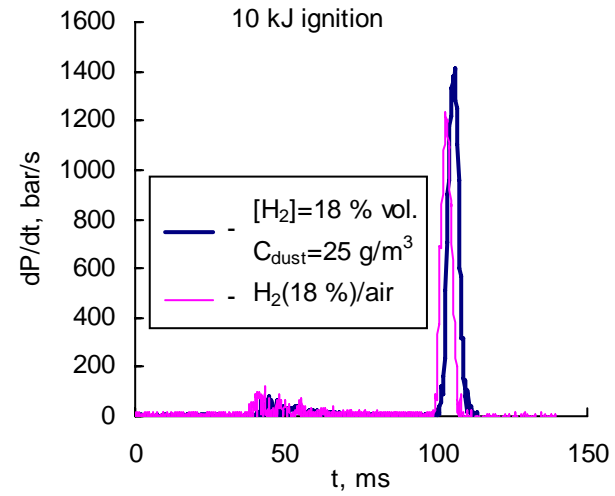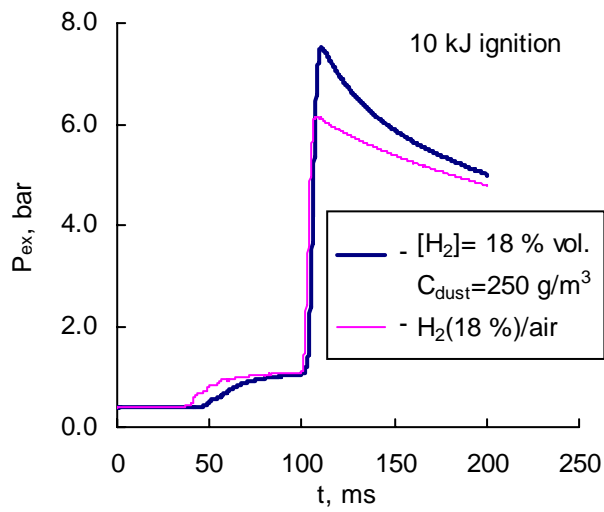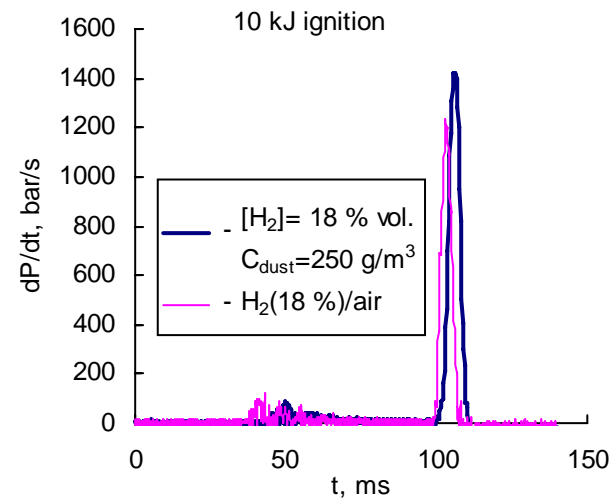Hydrogen concentration – 12 vol. %, ignition – 10 kJ chemical igniters.
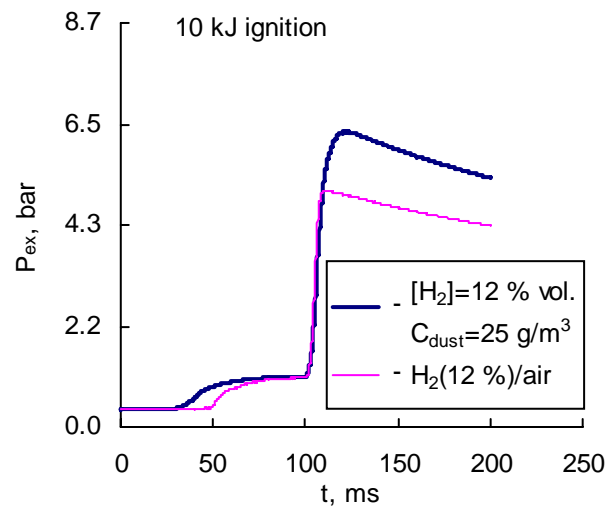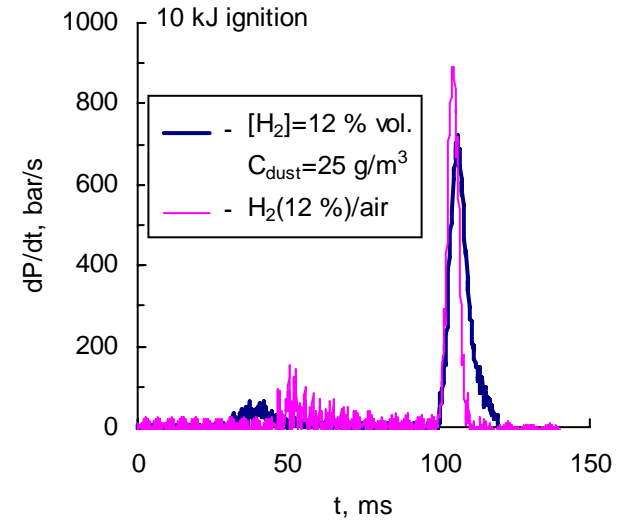
Figure 24. Pressure-time curve (a) and its derivative (b) for combined hydrogen/graphite dust explosion. $[H_2]$=12 vol. %, C_{dust}= 25 g/m^3.


Figure 25. Pressure-time curve (a) and its derivative (b) for combined hydrogen/graphite dust explosion. $[H_2]$=12 vol. %, C_{dust}= 75 g/m^3.

(a)   (b)

Figure 26. Pressure-time curve (a) and its derivative (b) for combined hydrogen/graphite dust explosion. [H$_2$]=12 vol. %, C$_{dust}$=125 g/m^3.

(a)   (b)

Figure 27. Pressure-time curve (a) and its derivative (b) for combined hydrogen/graphite dust explosion. [H$_2$]=12 vol. %, C$_{dust}$=200 g/m^3.

(a)

(b)

Figure 28. Maximum overpressures (a) and rates of pressure rise (b) measured in combined hydrogen/graphite dust (4μm) explosions.
Hydrogen concentration – 14 vol. %, ignition – 10 kJ chemical igniters.
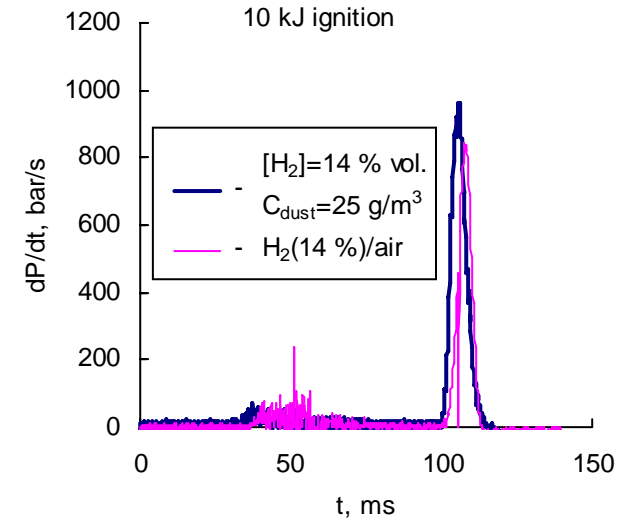
(a)   (b)

Figure 29. Pressure-time curve (a) and its derivative (b) for combined hydrogen/graphite dust explosion. $[H_2]$=14 vol. %, C_{dust}= 25 g/m^3.

(a)   (b)

Figure 30. Pressure-time curve (a) and its derivative (b) for combined hydrogen/graphite dust explosion. $[H_2]$=14 vol. %, C_{dust}=250 g/m^3.

(a)

(b)

Figure 31. Maximum overpressures (a) and rates of pressure rise (b) measured in combined hydrogen/graphite dust (4μm) explosions.
Hydrogen concentration – 16 vol. %, ignition – 10 kJ chemical igniters.

(a)

(b)

Figure 32. Maximum overpressures (a) and rates of pressure rise (b) measured in combined hydrogen/graphite dust (4μm) explosions.
Hydrogen concentration – 18 vol. %, ignition – 10 kJ chemical igniters.

Figure 33. Pressure-time curve (a) and its derivative (b) for combined hydrogen/graphite dust explosion. $[H_2]$=18 vol. %, C_{dust}= 25 g/m^3.

Figure 34. Pressure-time curve (a) and its derivative (b) for combined hydrogen/graphite dust explosion. $[H_2]$=18 vol. %, C_{dust}=250 g/m^3.
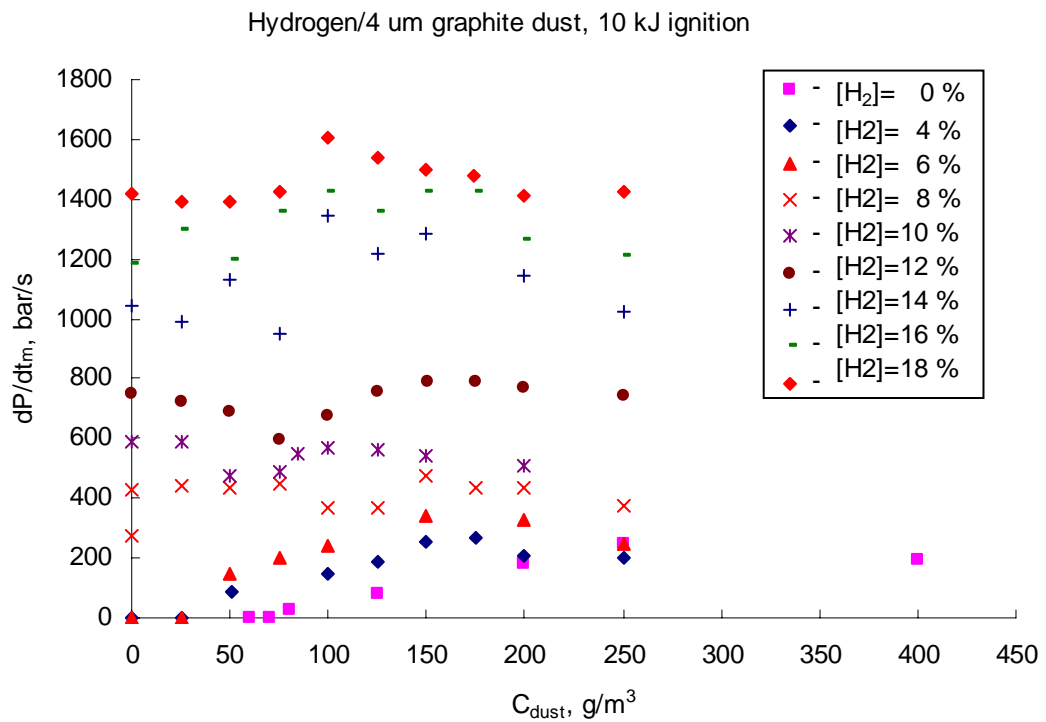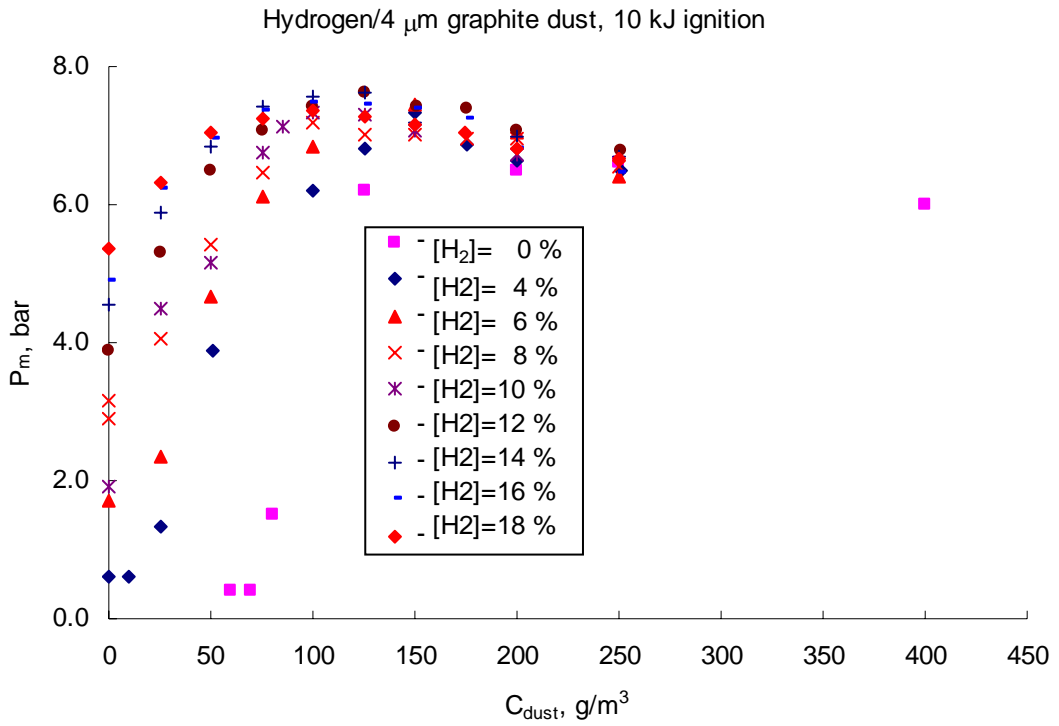
Figure 35. Summary of maximum overpressure (a) and rate of pressure rise (b) measurements for hydrogen/graphite dust/air mixtures ignited by 10 kJ chemical igniters.
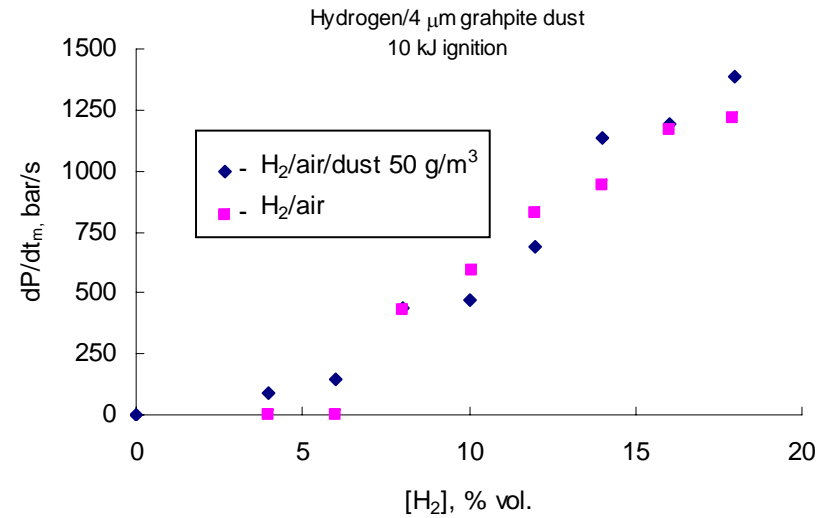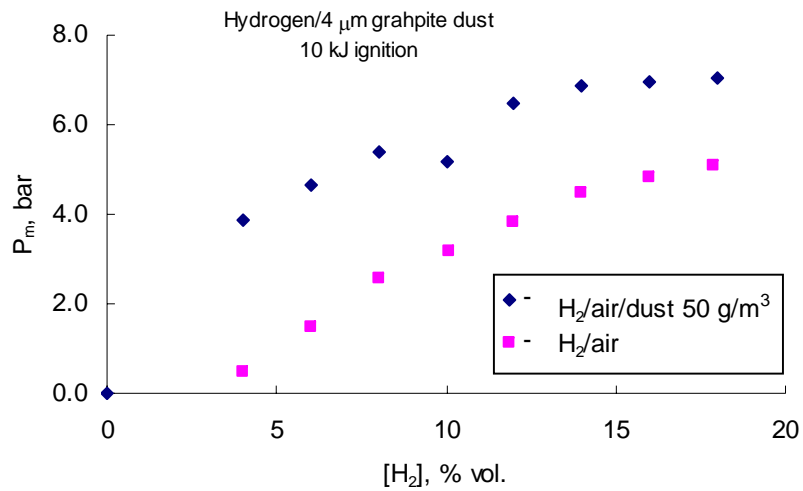
(a)

(b)

Figure 36. Maximum overpressure (a) and rate of pressure rise (b) versus hydrogen concentration. Graphite dust 4 μm, C_{dust}=50 g/m^3. 10 kJ ignition.
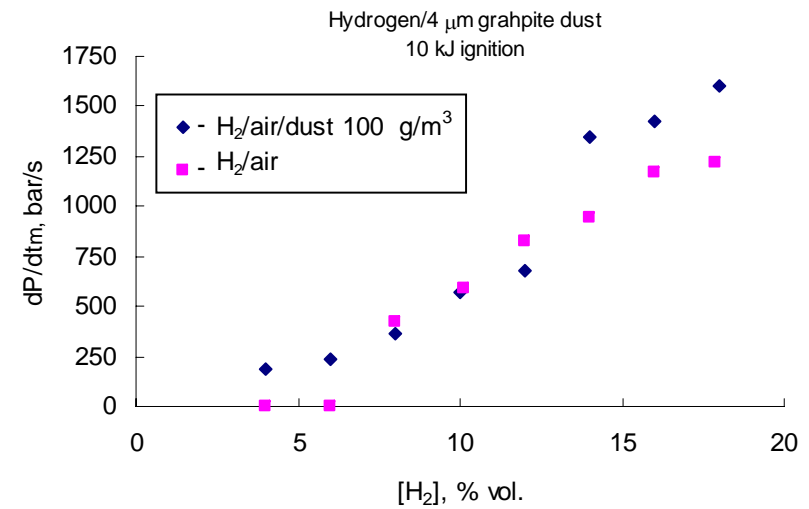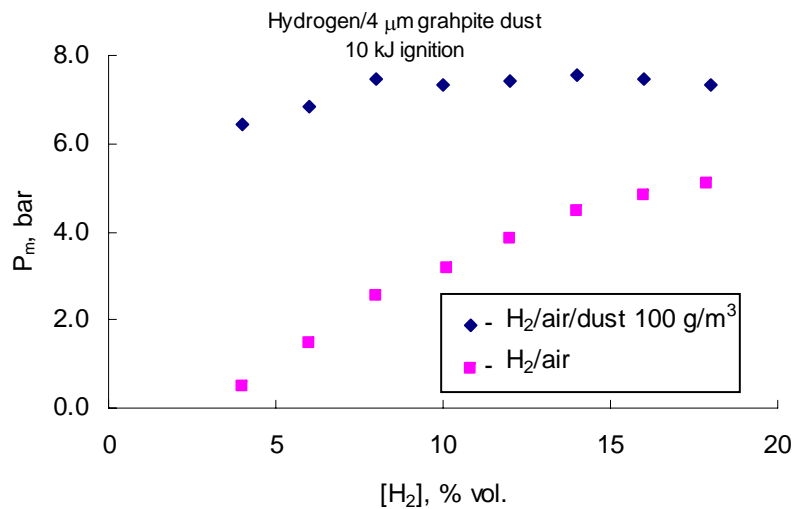
(a)

(b)

Figure 37. Maximum overpressure (a) and rate of pressure rise (b) versus hydrogen concentration. Graphite dust 4 μm, C_{dust}=100 g/m^3, 10 kJ ignition.
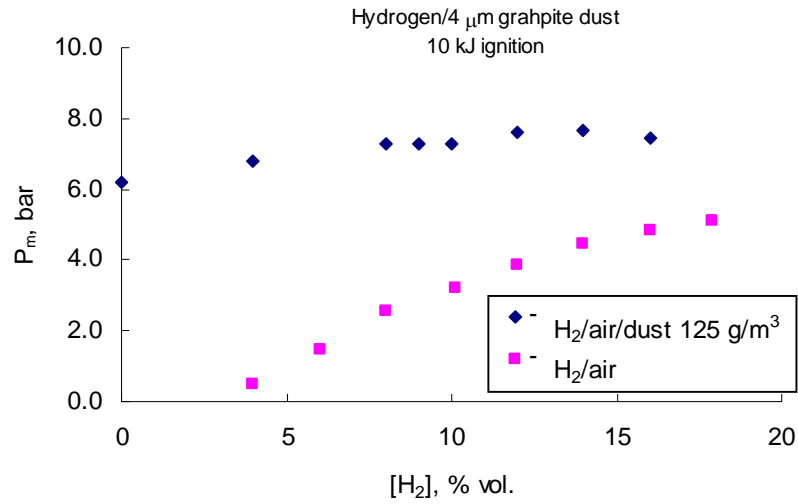
<center>(a)</center>
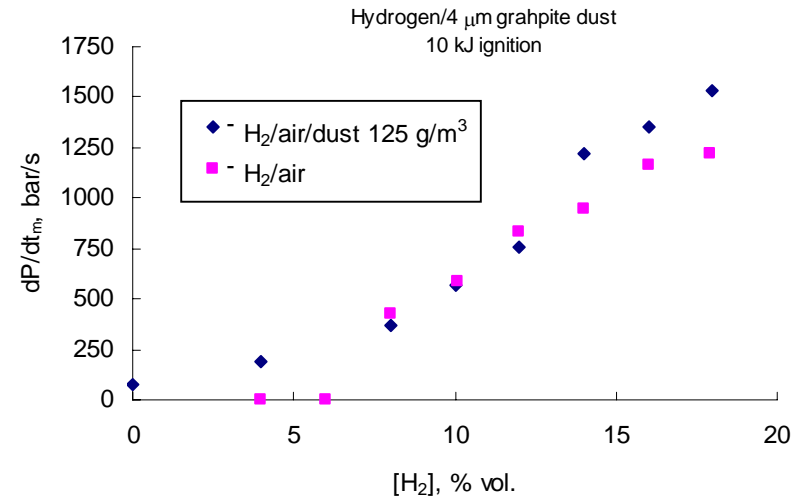
<center>(b)</center>

Figure 38. Maximum overpressure (a) and rate of pressure rise (b) versus hydrogen concentration. Graphite dust 4 µm, C_{dust}=125 g/m^3, 10 kJ ignition.
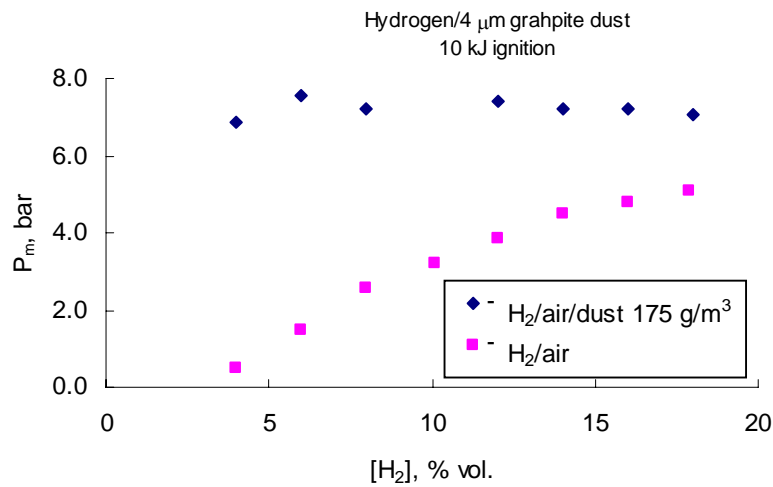
<center>(a)</center>
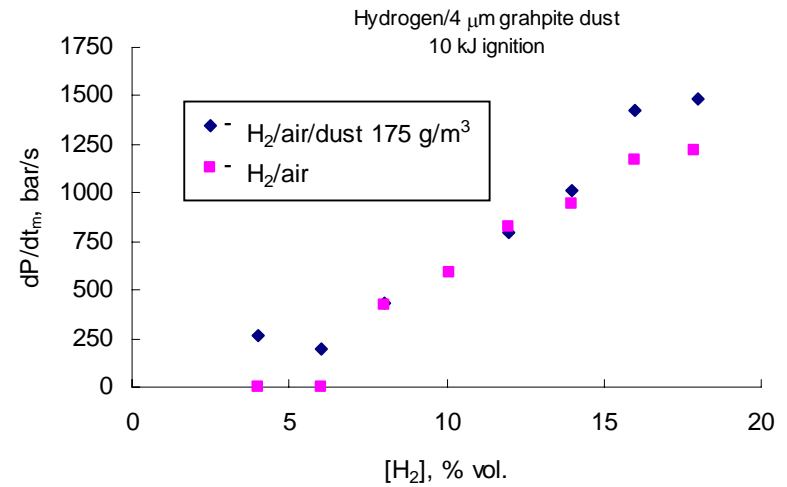
<center>(b)</center>

Figure 39. Maximum overpressure (a) and rate of pressure rise (b) versus hydrogen concentration. Graphite dust 4 µm, C_{dust}=125 g/m^3, 10 kJ ignition.
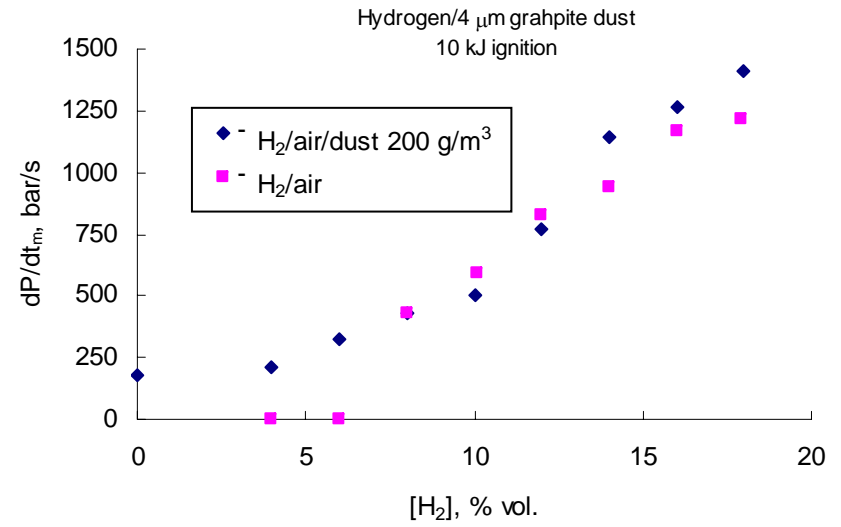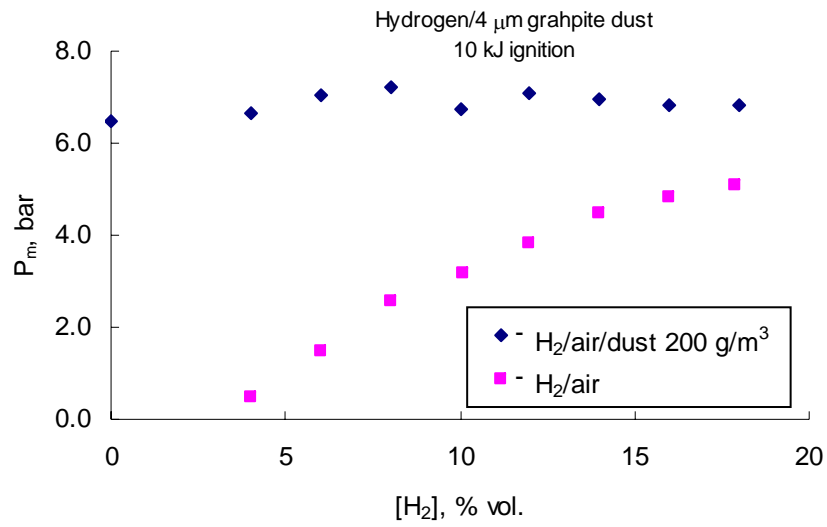
(a)   (b)

Figure 40. Maximum overpressure (a) and rate of pressure rise (b) versus hydrogen concentration. Graphite dust 4 μm, C_{dust}=200 g/m^3, 10 kJ ignition.

Electric spark ignition

The tests with electric spark ignition have been performed starting from **8 vol. % of hydrogen** added to the dust-air cloud. The results are presented in Fig. 41, where the maximum overpressure and the maximum pressure rise rate are plotted versus dust concentration. The tested graphite dust concentration range is 100-250 g/m^3. The pressure-time curves and dP/dt(t) curves for 100 and 200 g/m^3 dust concentrations are plotted in Figs. 42 (a) and (b), respectively, together with the curves recorded in the test with 8 vol. % hydrogen and no dust. As it is seen from these figures, with increase in the dust concentration the mixture burns slower producing lower maximum pressures. The dust contribution to pressure generation is negative; it acts as a heat-sink. In all tests of this series only hydrogen is ignited and explodes; the dust is not involved in the combustion process.

With **10 vol. % of hydrogen** added into the chamber, a similar regime of the dust/air/hydrogen mixture explosion is observed for 25 and 50 g/m^3 of graphite dust. The maximum overpressures are almost the same as that recorded in the test with the same hydrogen concentration and no dust (Fig. 43a); the pressure-time curves recorded in tests with and without dust are practically identical indicating again the inert dust behaviour. However, the mixture '75 g/m^3 graphite dust/10 vol. % hydrogen/air' burns quite different. The maximum overpressure in this test is 2 bar higher than without dust. The pressure-time curve resembles those obtained in the tests with slow explosions of the graphite dust [1]: after ignition the pressure rises fast for 10 ms, then remains constant, and rises again slowly during about 90 ms (Fig. 44a). This can be clearly seen from the dP/dt(t) curve which shows a first sharp peak of 300 bar/s amplitude (hydrogen explosion) and 60 ms later the second wide peak of 50 bar/s amplitude. At the next tested dust concentration of 100 g/m^3 the 'slow dust explosion' phase of the hybrid fuel combustion process is also observed. The maximum overpressure is significantly higher (6.2 bar against 3.2 bar without dust), and the dust explosion is also noticeably faster, the second peak amplitude reaching 80 bar/s (Fig. 45). The next higher concentration of 125 g/m^3 gives an even faster dust explosion; now the second peak of the dP/dt(t) curve reaches 110 bar/s (Fig. 46). There were three tests made at this combination of dust/hydrogen concentrations. In one of them there was no dust explosion phase; in the other two the dust explosion was observed (see Fig. 43a). At the next higher tested concentration of 150 g/m^3 there was only a fast hydrogen explosion (Fig. 47). This test was not repeated.

The maximum overpressures and the maximum rates of pressure rise measured in the tests with **12 vol. % of hydrogen** are plotted versus dust concentration in Fig. 48. The tested

concentrations are 25, 50, 75, and 100 g/m^3. The pressure-time curves recorded in the tests with 25 and 100 g/m^3 dust concentrations are shown in Fig. 49. In all these tests both hydrogen and dust exploded. At 25, 50, and 75 g/m^3 the explosion has only one fast phase, when hydrogen and dust burn like a single fuel with the same time scale. At 100 g/m^3 there is so much dust (and oxygen) that the graphite dust continues burning after the fast "hydrogen" stage has been completed. This is indicated by the 'slow tail' seen at the dP/dt(t) curve in Fig. 49b. In all these tests the maximum overpressures are appreciably higher than that observed in the corresponding test without dust. The maximum rate of pressure rise is at the same level as in the hydrogen/air test for all tested dust concentrations, except for 50 g/m^3, where it is 1.5 times higher.

The test results for **14 vol. % of hydrogen** and 25, 50, 75, and 100 g/m^3 graphite dust concentrations are presented in Fig. 50. The maximum overpressures and rates of pressure rise are higher than in the corresponding tests without dust. All explosions are fast; they show no second slow phase. This can be seen from Fig. 51, where the pressure-time curves recorded in the tests with 14 vol. % of hydrogen and 25 and 100 g/m^{3}' dust concentrations are presented. The records for the corresponding test without dust are also presented.

The same trends are observed in the tests with **16 and 18 vol. % of hydrogen**. The tested concentrations are 25, 50, 75, and 100 g/m^3. In these tests the maximum overpressures and the maximum rates of pressure rise are again higher than those measured in the corresponding hydrogen/air tests (Figs. 52 and 54). All hybrid mixtures tested at these hydrogen concentrations and the given range of dust concentrations explode like a monofuel in a single fast reaction (Figs. 53 and 55).
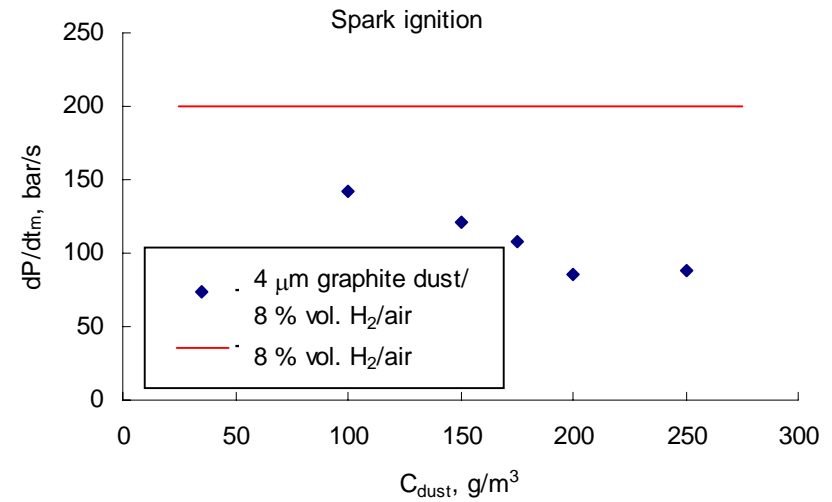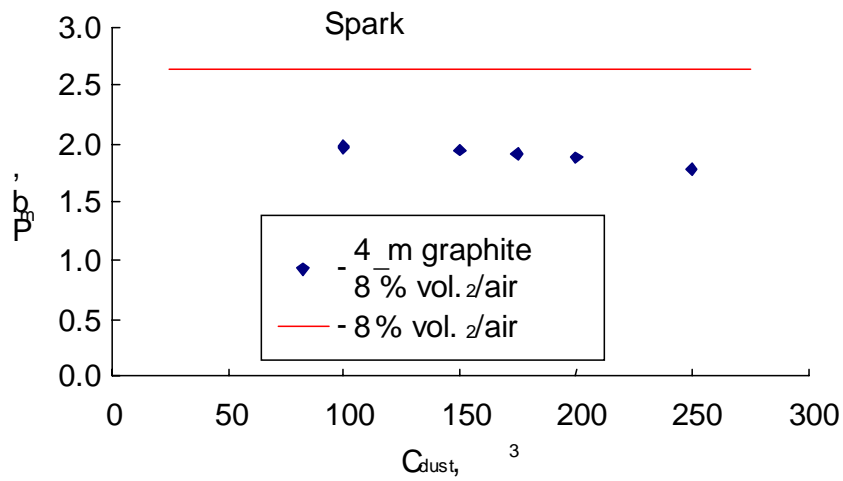
(a)

(b)

Figure 41. Maximum overpressures (a) and rates of pressure rise (b) measured in combined hydrogen/graphite dust (4μm) explosions. Hydrogen concentration – 8 vol. %, ignition – electric spark.
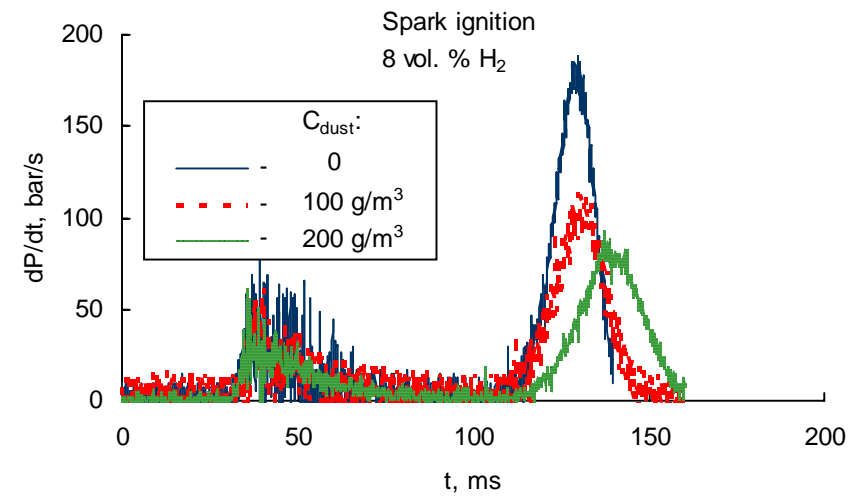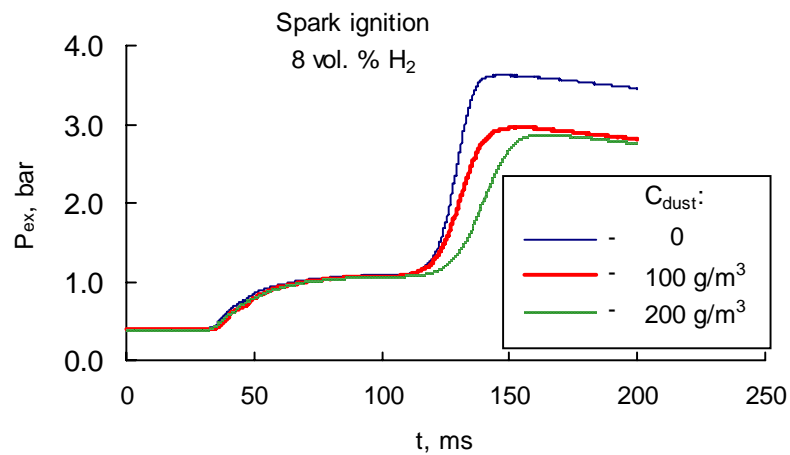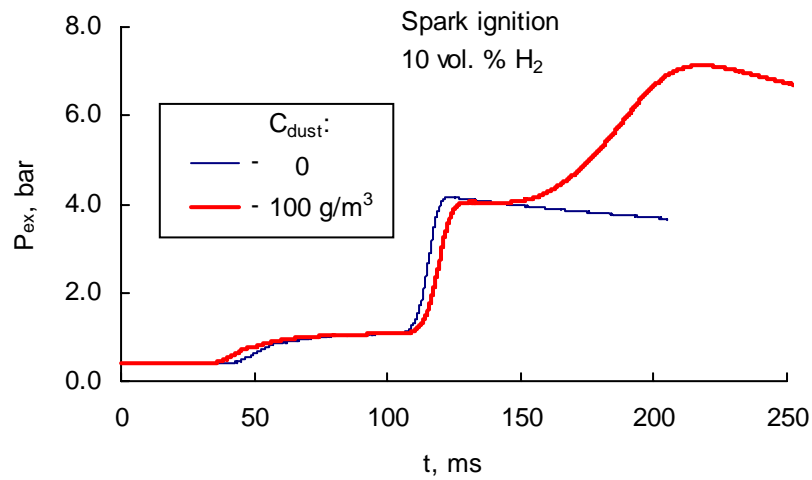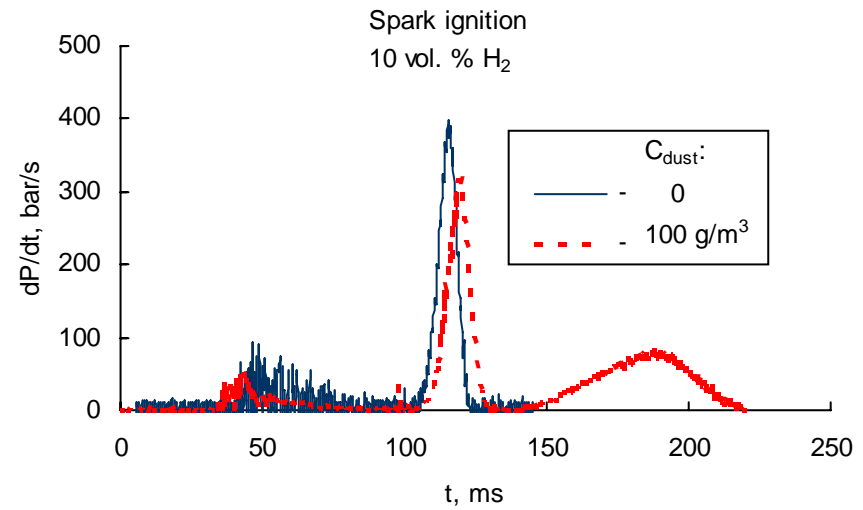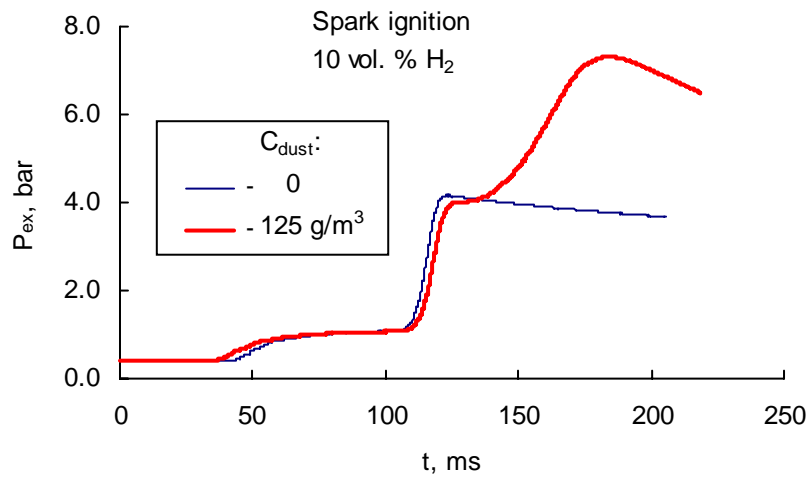

(a)
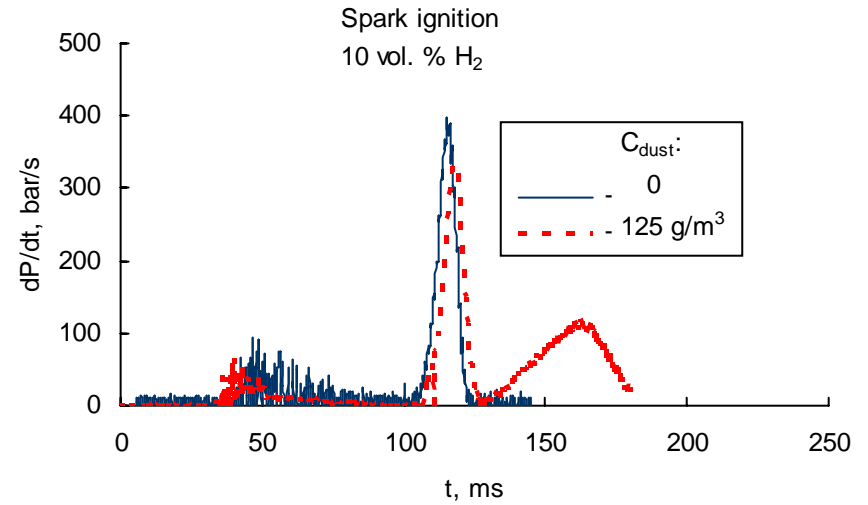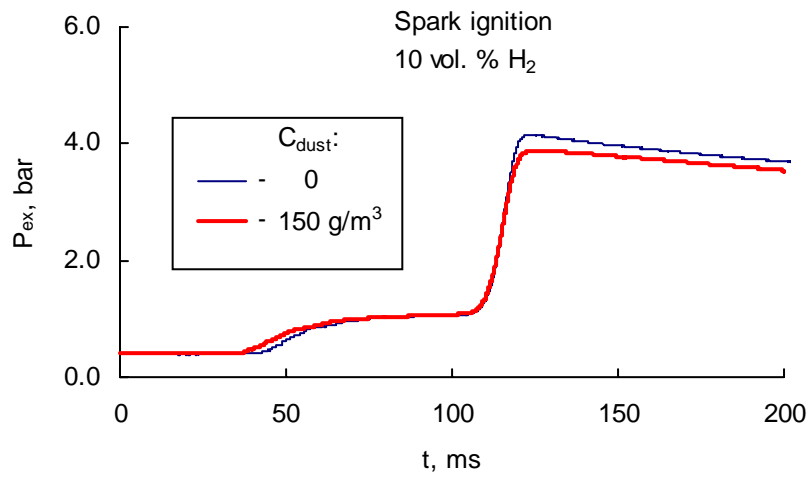
(b)

Figure 42. Pressure-time curve (a) and its derivative (b) for combined hydrogen/graphite dust explosion. $[H_2]$=8 vol. %, C_{dust}= 100 and 200 g/m^3.
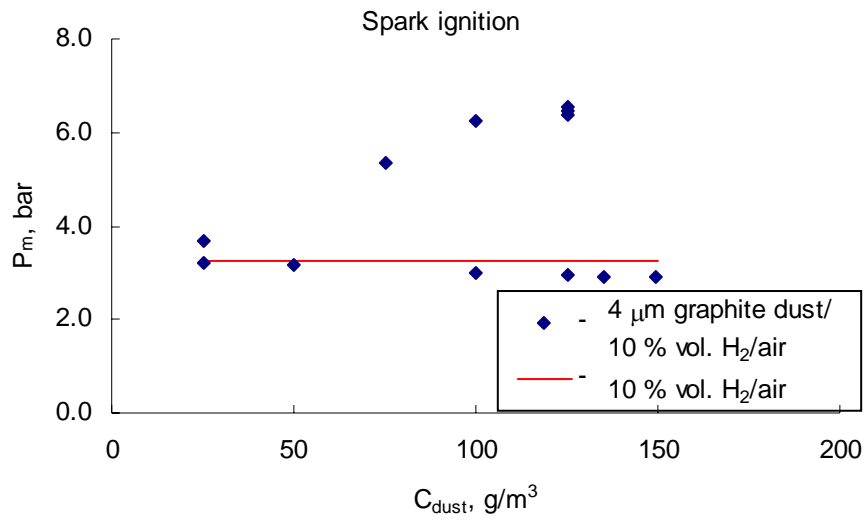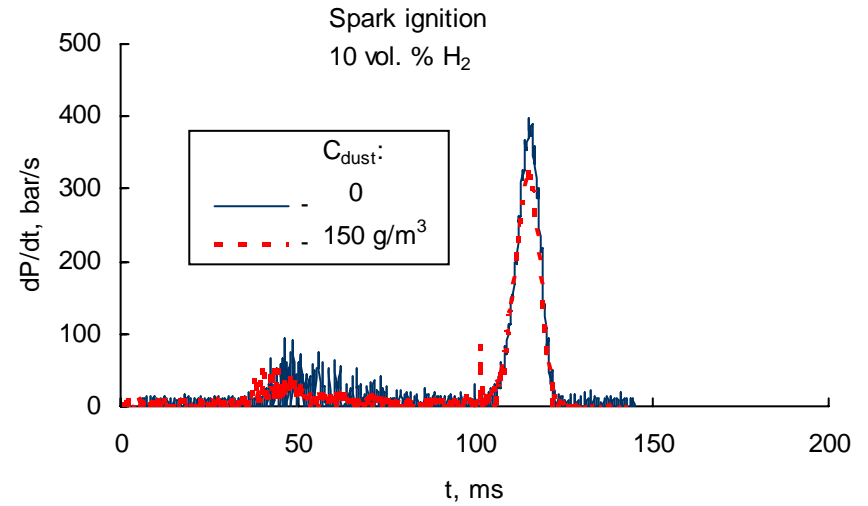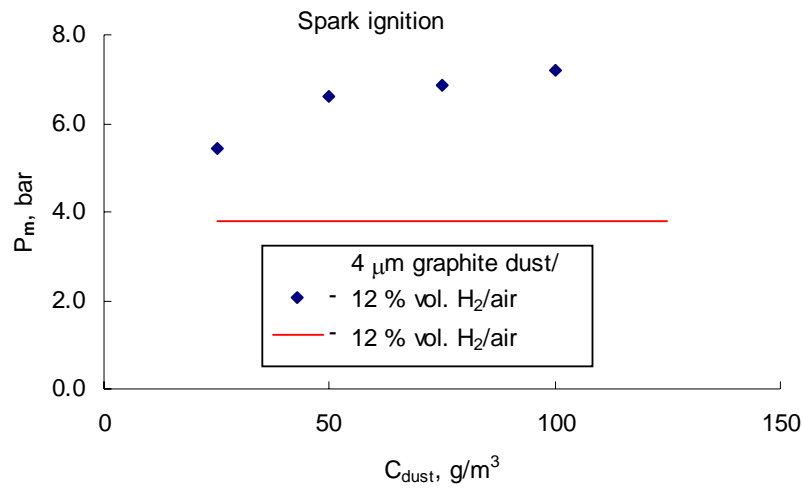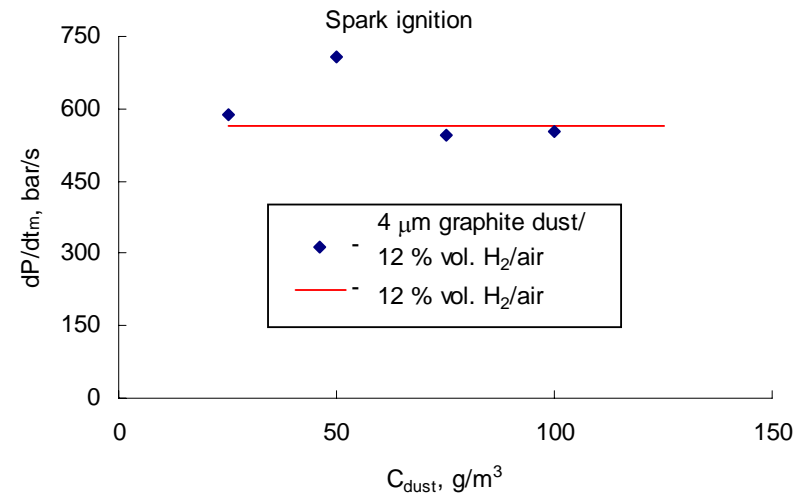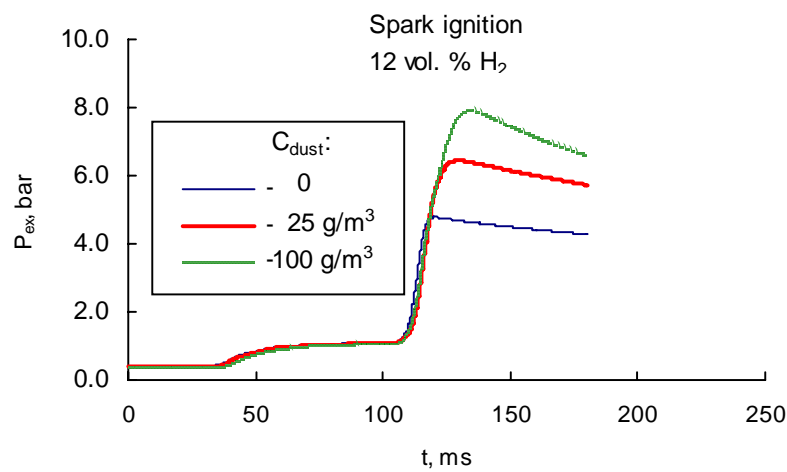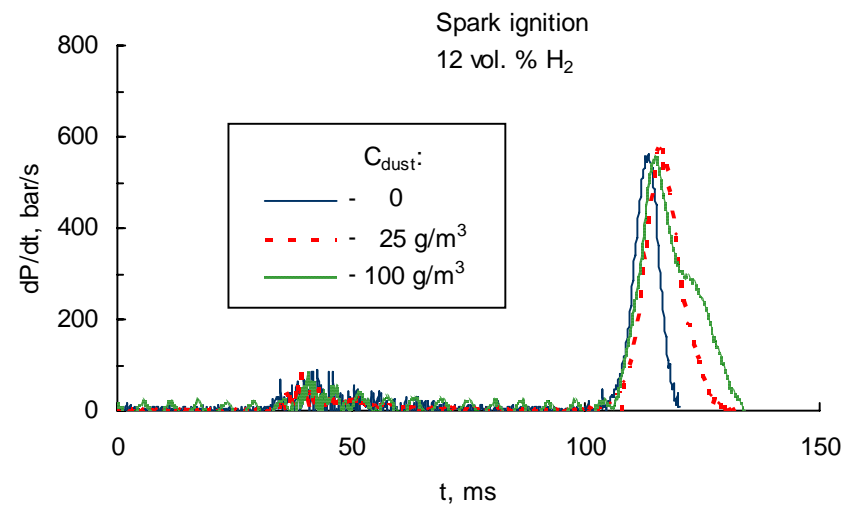
(a)
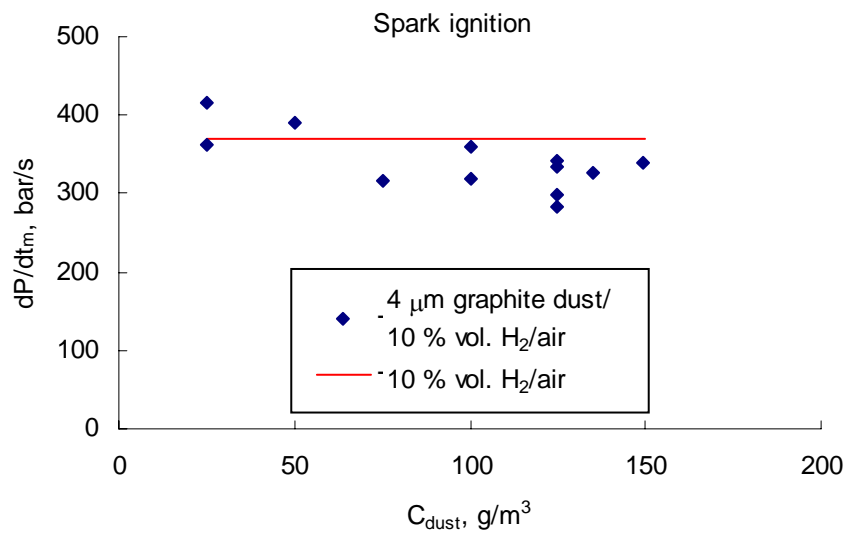
(b)

Figure 43. Maximum overpressures (a) and rates of pressure rise (b) measured in combined
hydrogen/graphite dust (4μm) explosions.
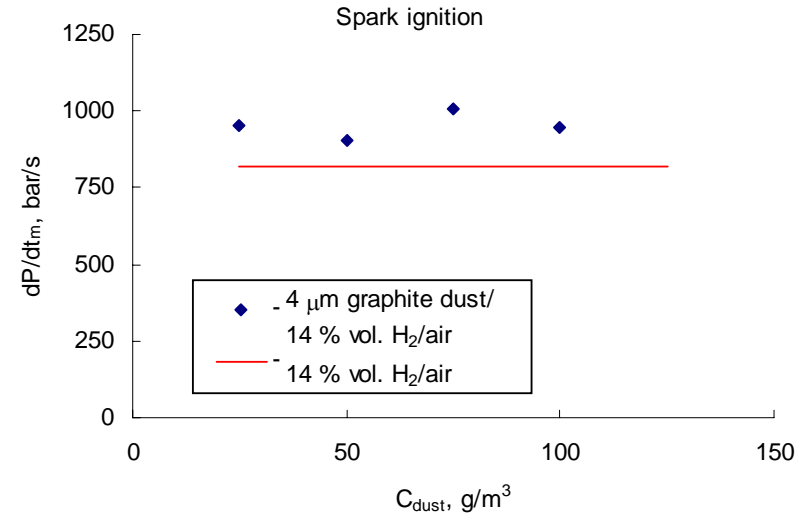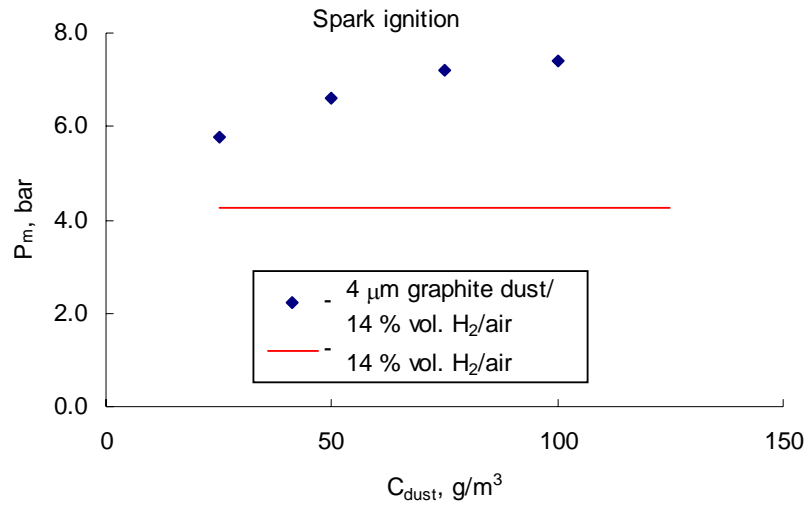Hydrogen concentration – 10 vol. %, ignition – electric spark.
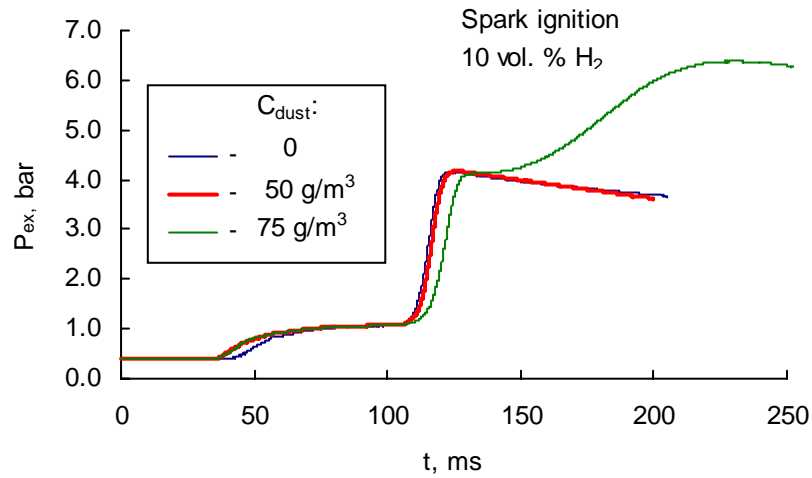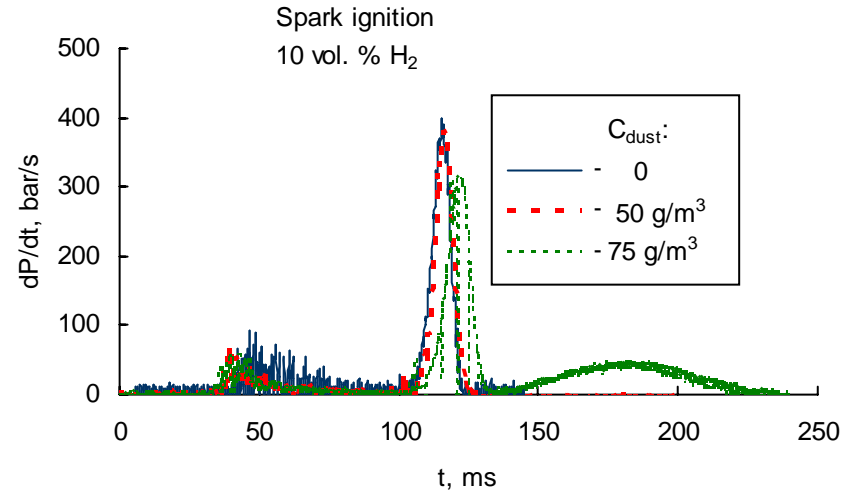
(a)　　　　　　　　　　　　　　　　　　(b)

Figure 44. Pressure-time curve (a) and its derivative (b) for combined hydrogen/graphite dust explosion. $[H_2]$=10 vol. %, C_{dust}= 50 and 75 g/m^3.

(a)　　　　　　　　　　　　　　　　　　(b)

Figure 45. Pressure-time curve (a) and its derivative (b) for combined hydrogen/graphite dust explosion. $[H_2]$=10 vol. %, C_{dust}= 100 g/m^3.

(a)

(b)

Figure 46. Pressure-time curve (a) and its derivative (b) for combined hydrogen/graphite dust explosion. [H$_2$]=10 vol. %, C$_{dust}$= 125 g/m^3.

(a)

(b)

Figure 47. Pressure-time curve (a) and its derivative (b) for combined hydrogen/graphite dust explosion. [H$_2$]=10 vol. %, C$_{dust}$= 150 g/m^3.

(a)

(b)

Figure 48. Maximum overpressures (a) and rates of pressure rise (b) measured in combined hydrogen/graphite dust (4μm) explosions. Hydrogen concentration – 12 vol. %, ignition – electric spark.
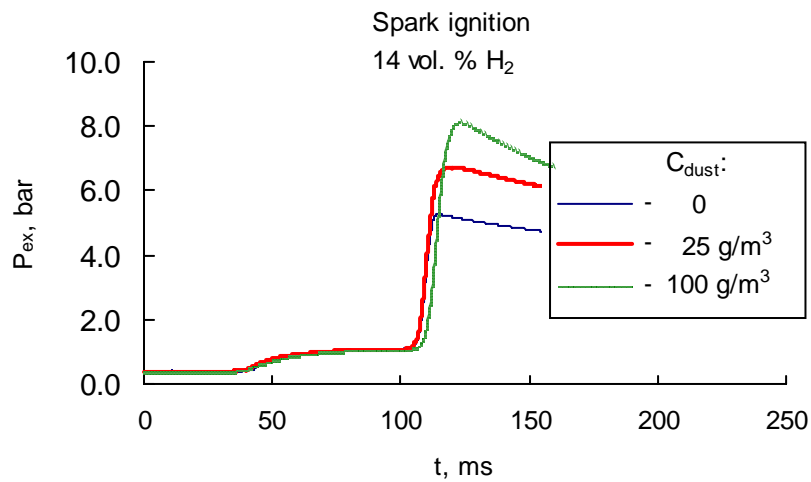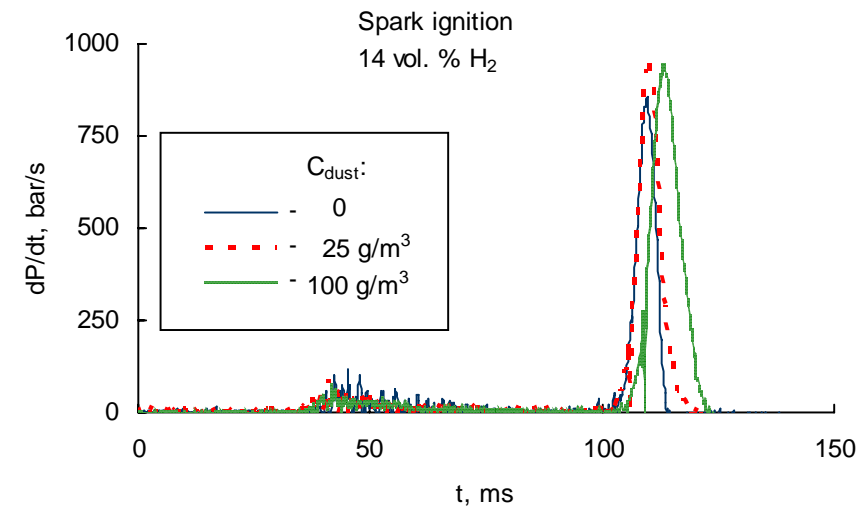

(a)

(b)

Figure 49. Pressure-time curve (a) and its derivative (b) for combined hydrogen/graphite dust explosion. [H_2]=12 vol. %, C_{dust}= 25 and 100 g/m^3.

(a)   (b)

Figure 50. Maximum overpressures (a) and rates of pressure rise (b) measured in combined hydrogen/graphite dust (4μm) explosions. Hydrogen concentration – 14 vol. %, ignition – electric spark.
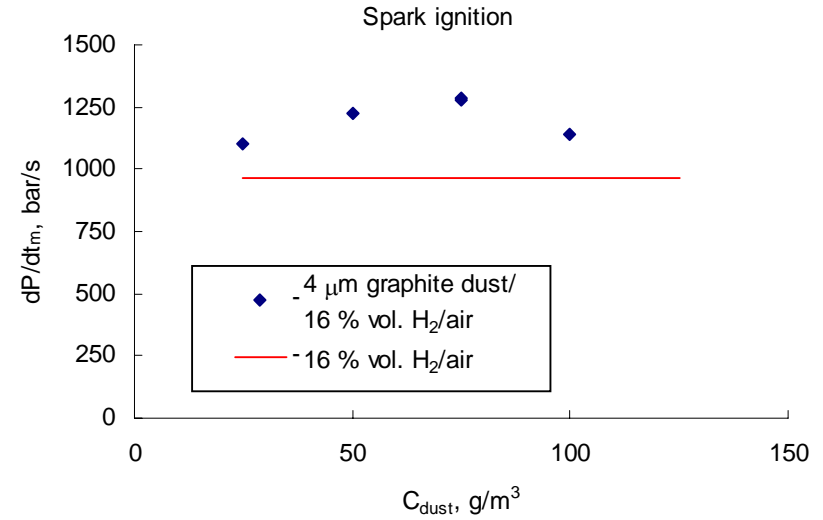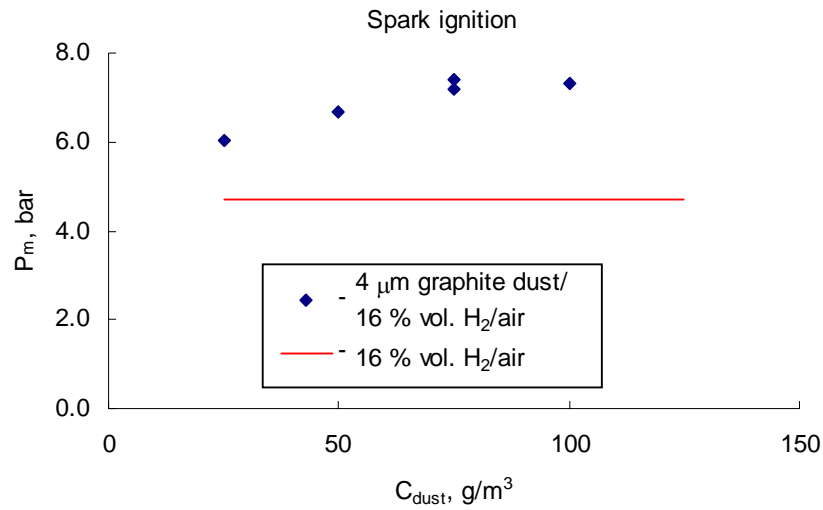

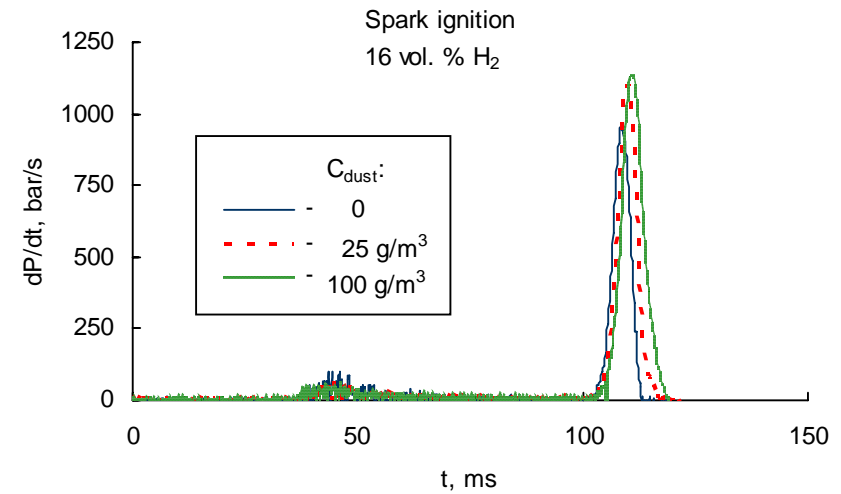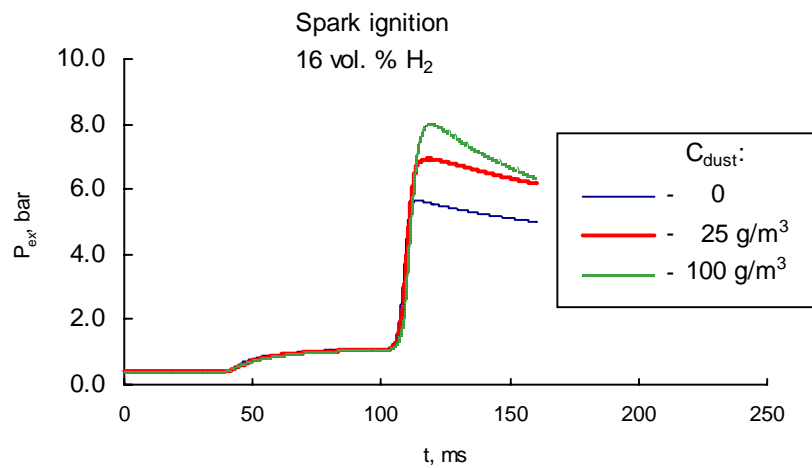(a)   (b)

Figure 51. Pressure-time curve (a) and its derivative (b) for combined hydrogen/graphite dust explosion. $[H_2]$=14 vol. %, C_{dust}= 25 and 100 g/m^3
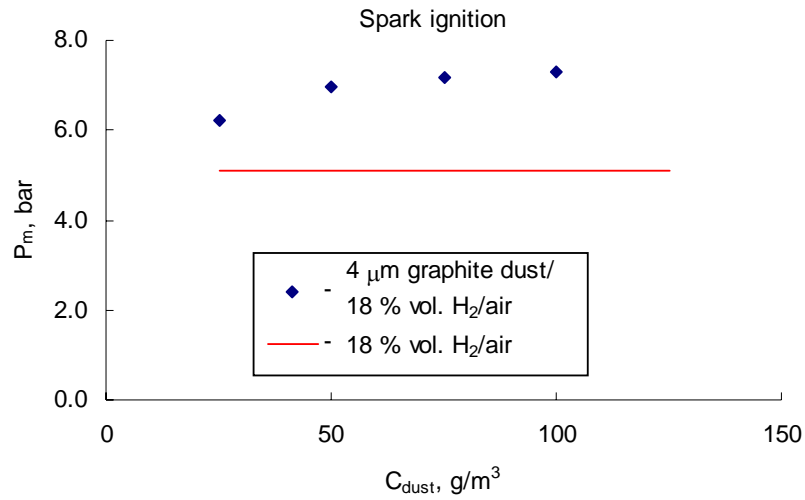
(a)   (b)

Figure 52. Maximum overpressures (a) and rates of pressure rise (b) measured in combined hydrogen/graphite dust (4μm) explosions. Hydrogen concentration – 16 vol. %, ignition – electric spark.

(a)   (b)

Figure 53. Pressure-time curve (a) and its derivative (b) for combined hydrogen/graphite dust explosion. $[H_2]$=16 vol. %, C_{dust}= 25 and 100 g/m^3.

(a)

(b)

Figure 54. Maximum overpressures (a) and rates of pressure rise (b) measured in combined hydrogen/graphite dust (4μm) explosions. Hydrogen concentration – 18 vol. %, ignition – electric spark.
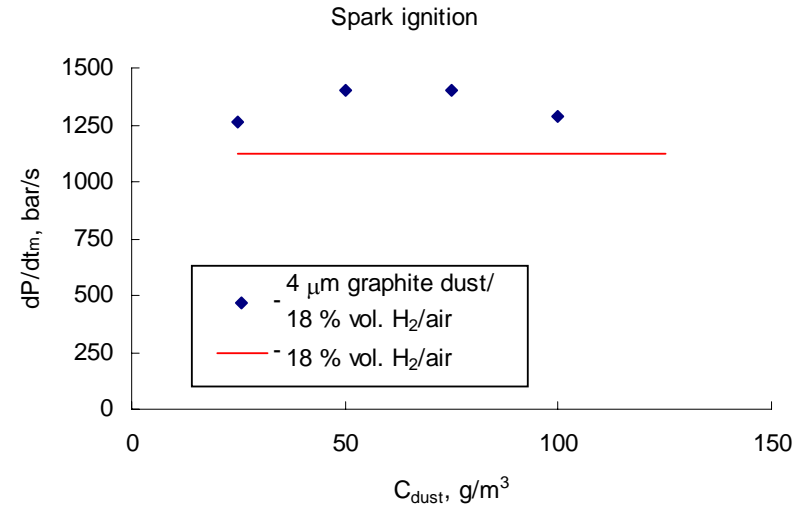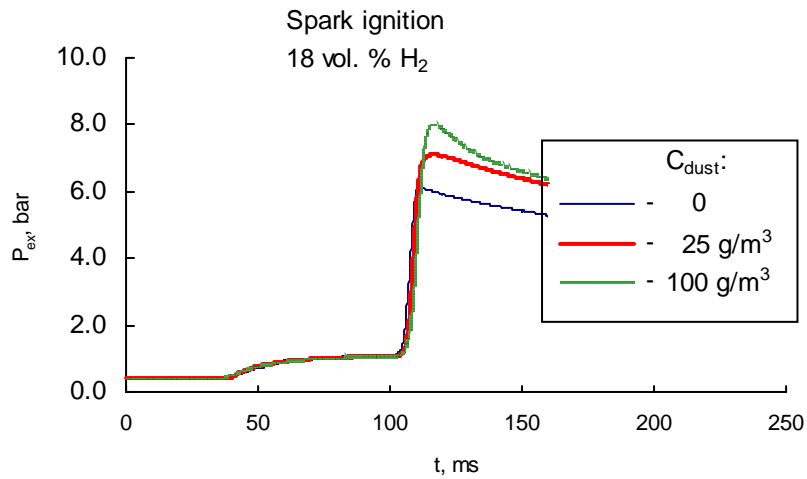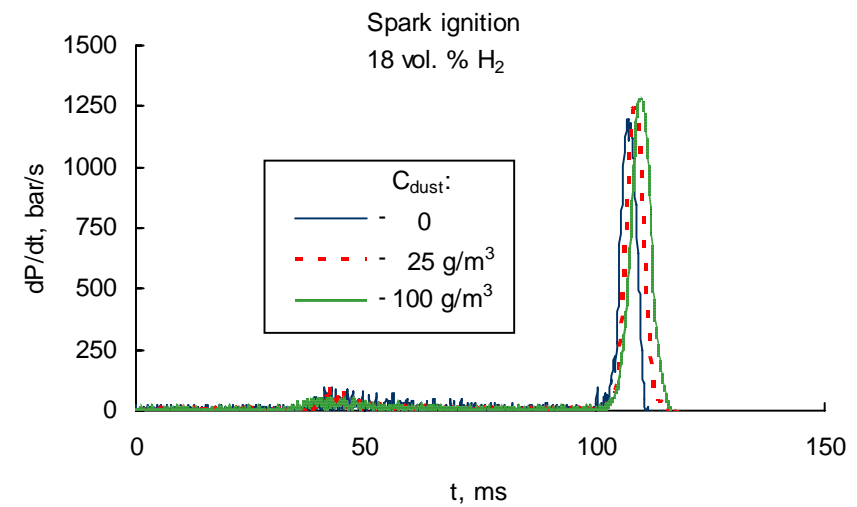

(a)

(b)

Figure 55. Pressure-time curve (a) and its derivative (b) for combined hydrogen/graphite dust explosion. [H_2]=18 vol. %, C_{dust}= 25 and 100 g/m^3.

To investigate in more detail the hydrogen concentration range where the graphite dust becomes involved in the explosion process, 10.5 and 11 vol. % [H₂] were tested additionally. The maximum overpressure and the maximum pressure rise rates measured for the hydrogen/graphite dust/air mixtures at **10.5 vol. % hydrogen** are presented in Fig. 56. The tests have been performed with 25, 50, 75, 100, 125, 150, and 175 g/m^3 dust concentrations. In the tests with 25 and 50 g/m^3 dust concentrations the dust does not participate markedly in the combustion process. The pressure-time curve for the test with 50 g/m^3 (Fig. 57) is almost identical the curve recorded in the hydrogen test without dust. In the test with 75 g/m^3 of the graphite dust the dust is ignited and explodes. The overpressure is 2 bar higher than generated by the hydrogen alone. The pressure-time curve (Fig. 58) shows two distinct stages of pressure rise: a first one of 25 ms duration, followed by a second one of 80 ms. The amplitude of the first peak of pressure rise is 320 bar/s; the amplitude of the second one is 50 bar/s. At 100 g/m^3 dust concentration the explosion regime is similar: the first fast stage, where the pressure evolution is almost the same as in the test with hydrogen without dust, and a much slower second stage. The first stage lasts 25 ms and the second 60 ms; the rate of pressure rise at the first stage is 350 bar/s and 80 bar/s at the second (Fig. 59). At 125 g/m^3 dust concentration the explosion regime differs from the previous one in the following details: the first pressure rise peak has 320 bar/s amplitude and 25 ms duration, the second one has 100 bar/s and is about 5 ms shorter. At this dust concentration the maximum overpressure is 6.4 bar, which is the maximum value over the tested dust concentration range. The explosion becomes weaker at 150 g/m^3. It still features the two stages, but both are weaker. The maximum overpressure is 5.8 bar; the first and second pressure-rise peaks have 250 and 50 bar/s amplitude, 30 and 70 ms duration, respectively (Fig. 60). The dust concentration of 175 g/m^3 can be considered as the Upper Explosion concentration Limit at 10.5 vol. % hydrogen concentration. This mixture behaves almost like the corresponding hydrogen/air mixture, since there is no second combustion stage. The difference is only that the generated overpressure and the maximum rate of pressure rise are lower due to unburned dust. The pressure-time curves have quite similar shapes. (Fig. 61).

In all dust/hydrogen/air tests with 10.5 vol. % H₂ concentration the maximum rates of pressure rise are lower than in the corresponding hydrogen/air test. A stable dust reaction is observed from 75 to 150 g/m^3.

The explosions of the graphite dust with **11 vol. % hydrogen** added are qualitatively the same as with 10 and 10.5 %. The maximum overpressures and rates of pressure rise are presented in Fig. 62. Twelve different dust concentrations ranging from 25 to 300 g/m^3 have been tested. At 25 g/m^3 dust concentration the mixture explosion is almost identical to the one without dust

(Fig 63). The second stage appears now at 50 g/m^3 (Fig. 64). It is detectable only in P(t) curve as a secondary very slow pressure rise just after the fast hydrogen explosion, adding about 0.6 bar to the cumulative overpressure. The second peak on the dP/dt(t) curve appears first in case of the 75 g/m^3 dust concentration (Fig. 65), having 100 bar/s amplitude and 40 ms duration, growing to 120 bar/s at 100 g/m^3 (Fig. 66) and to 145 bar/s at 125 g/m^3 (Fig. 67) and then degrading to 100 bar/s at 150 g/m^3 (Fig. 68) and to 40 bar/s at 250 g/m^3 (Fig. 69). Again, at all dust concentrations the maximum rate of pressure rise are lower than that measured without dust.

The last tested dust concentration was 300 g/m^3. In this case no explosion occurred, because there was no spark. The reason seems to be a shortening of the electrode rods by the graphite dust which settled down nearby onto the chamber wall. After this test the bayonet flange assembly together with the rods was disconnected from the chamber, and the spark unit was initiated to check the spark visually. There was no spark at all, which only appeared again after cleaning the flange assembly between the electrode rods.

The dependence of P$_m$ on the dust concentration is (Fig. 62a) has a weak local minimum at 175 g/m^3, which may be due to experimental scatter. It should be noted that only one test was performed for each 'dust/hydrogen concentration' value. These data require check reproducibility.
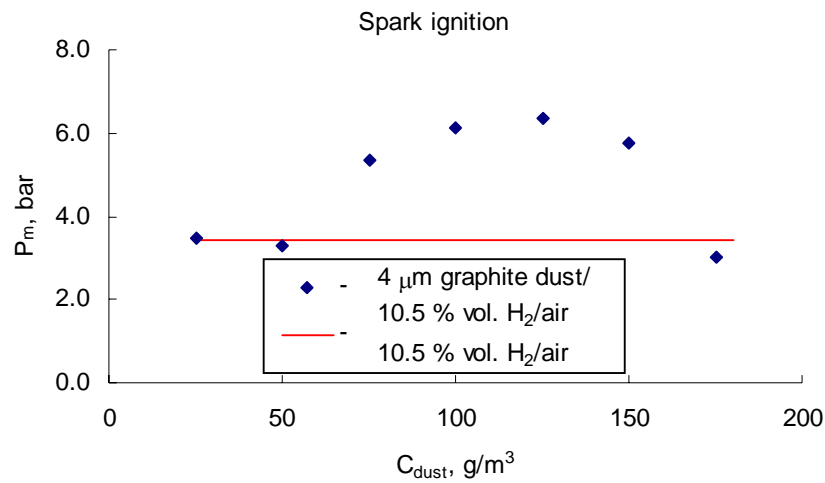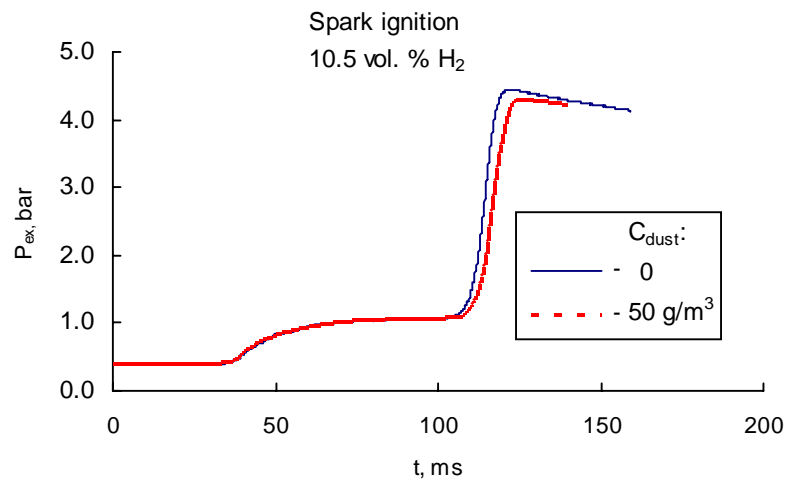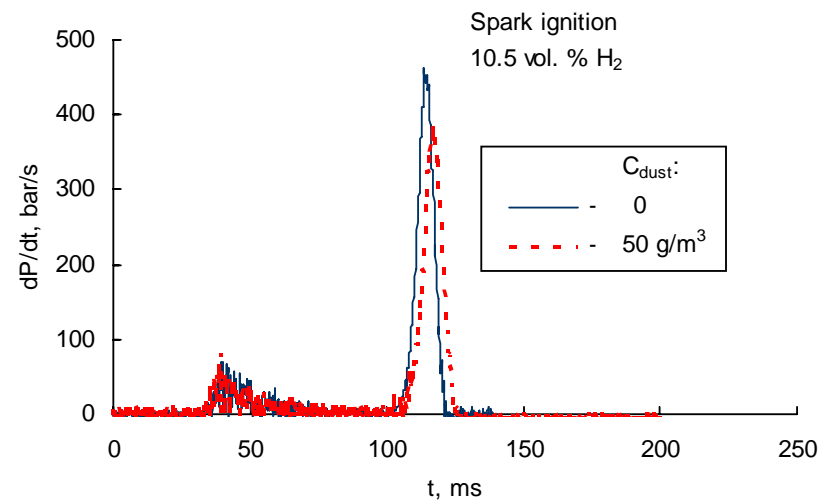
(a)
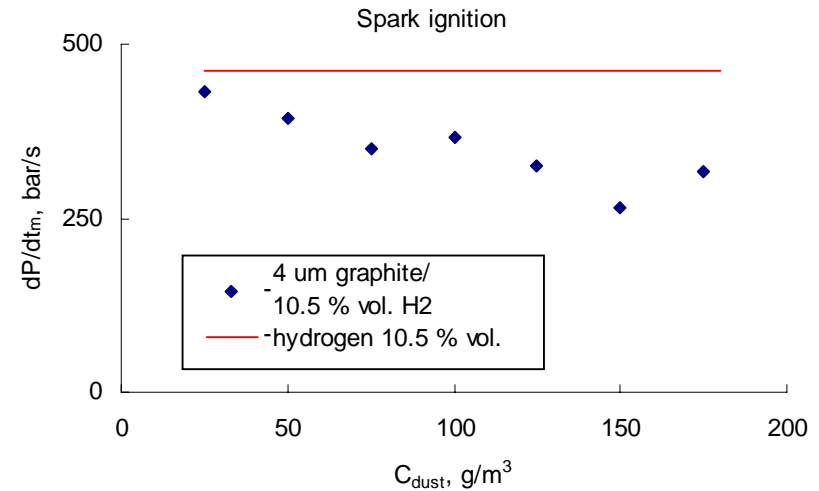
(b)

Figure 56. Maximum overpressures (a) and rates of pressure rise (b) measured in combined hydrogen/graphite dust (4μm) explosions. Hydrogen concentration – 10.5 vol. %, ignition – electric spark.
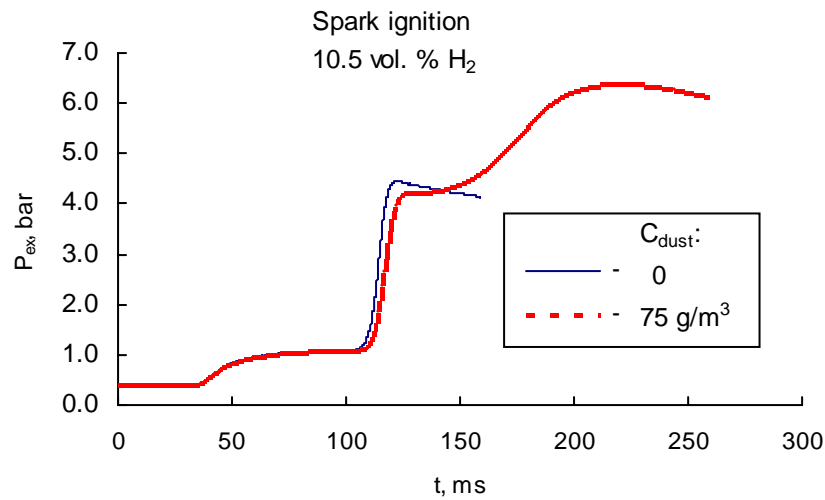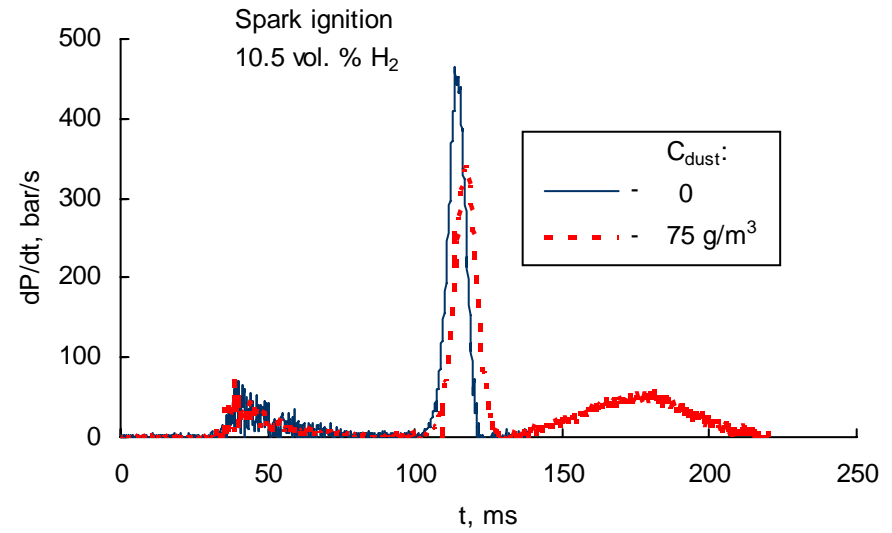

(a)

(b)

Figure 57. Pressure-time curve (a) and its derivative (b) for combined hydrogen/graphite dust explosion. $[H_2]$=10.5 vol. %, C_{dust}= 50 g/m^3.

(a)   (b)

Figure 58. Pressure-time curve (a) and its derivative (b) for combined hydrogen/graphite dust explosion. $[H_2]$=10.5 vol. %, C_{dust}= 75 g/m^3.

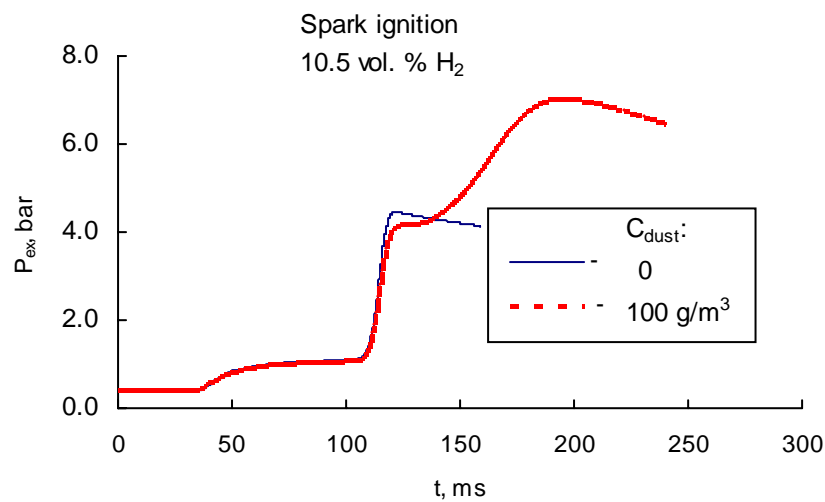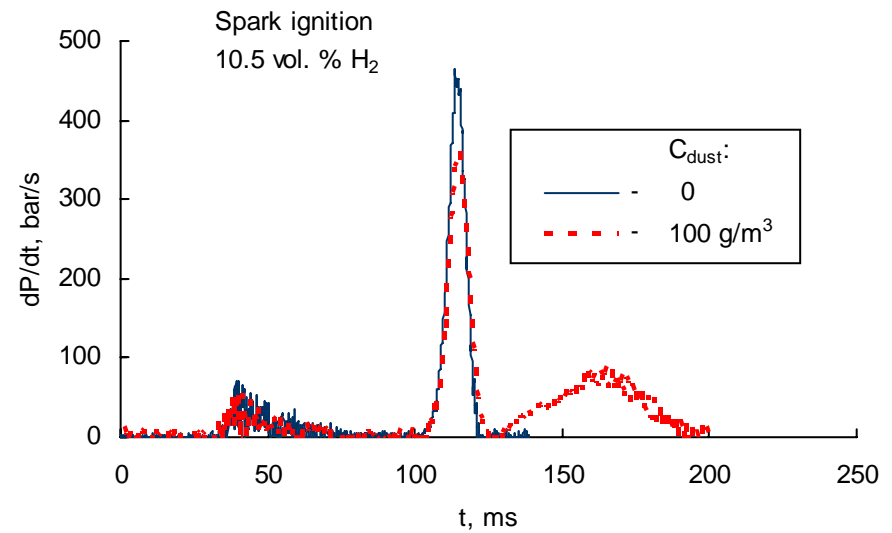(a)   (b)

Figure 59. Pressure-time curve (a) and its derivative (b) for combined hydrogen/graphite dust explosion. $[H_2]$=10.5 vol. %, C_{dust}= 100 g/m^3.
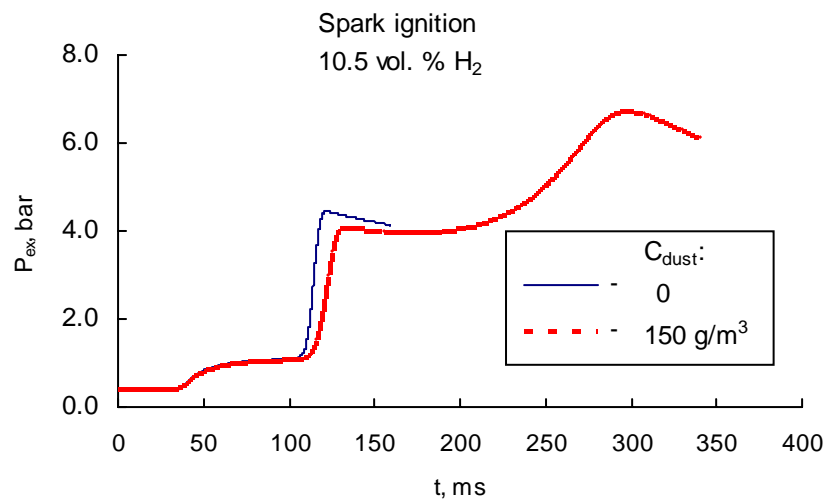
<p align="center">(a)</p>
<p align="center">(b)</p>

Figure 60. Pressure-time curve (a) and its derivative (b) for combined hydrogen/graphite dust explosion. $[H_2]$=10.5 vol. %, C_{dust}= 150 g/m^3.
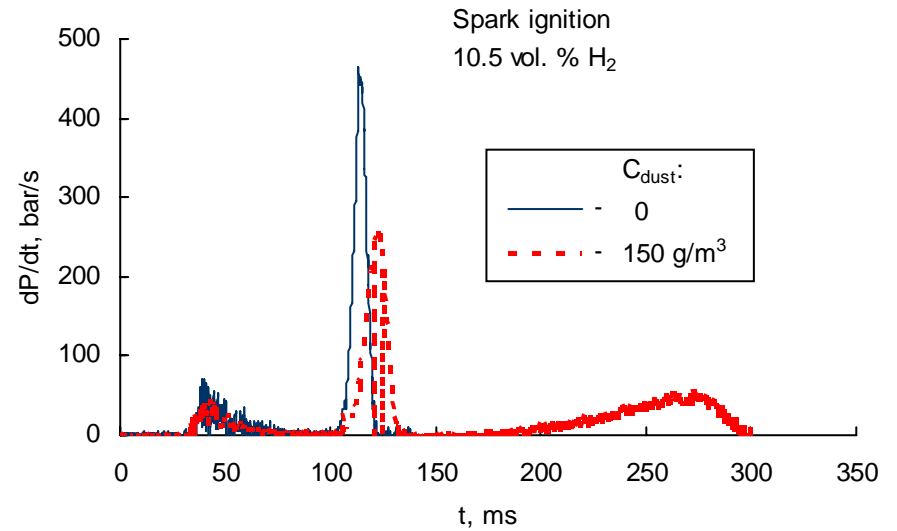

<p align="center">(a)</p>
<p align="center">(b)</p>

Figure 61. Pressure-time curve (a) and its derivative (b) for combined hydrogen/graphite dust explosion. $[H_2]$=10.5 vol. %, C_{dust}= 175 g/m^3.

(a)

(b)

Figure 62. Maximum overpressures (a) and rates of pressure rise (b) measured in combined hydrogen/graphite dust (4μm) explosions. Hydrogen concentration – 11 vol. %, ignition – electric spark.
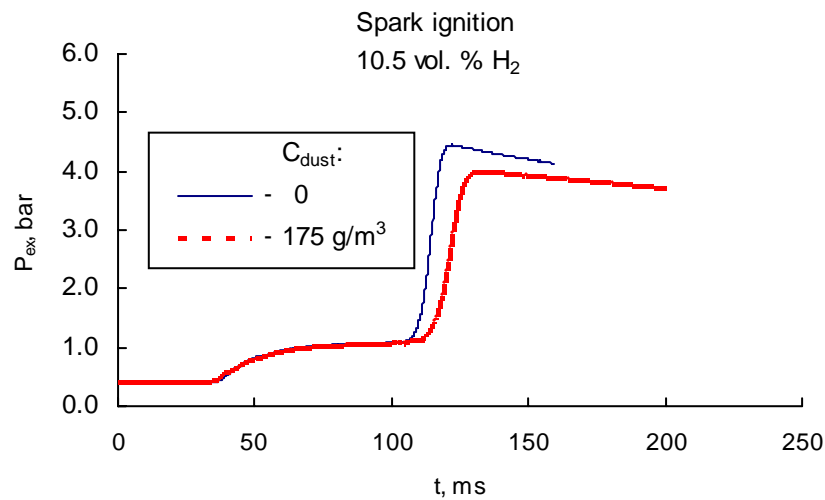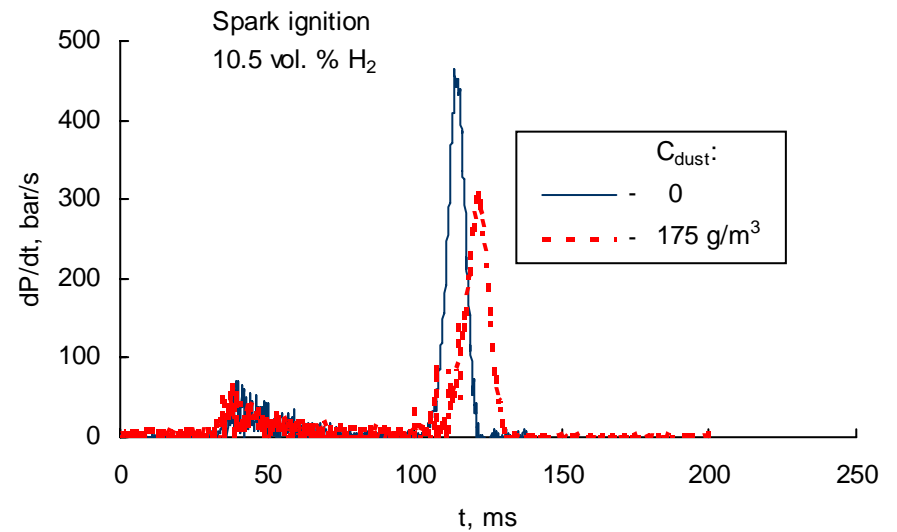

(a)

(b)

Figure 63. Pressure-time curve (a) and its derivative (b) for combined hydrogen/graphite dust explosion. $[H_2]$=11 vol. %, C_{dust}= 25 g/m^3.

<p style="text-align:center">(a)</p> <p style="text-align:center">(b)</p>

Figure 64. Pressure-time curve (a) and its derivative (b) for combined hydrogen/graphite dust explosion. [H$_2$]=11 vol. %, C$_{dust}$= 50 g/m^3.

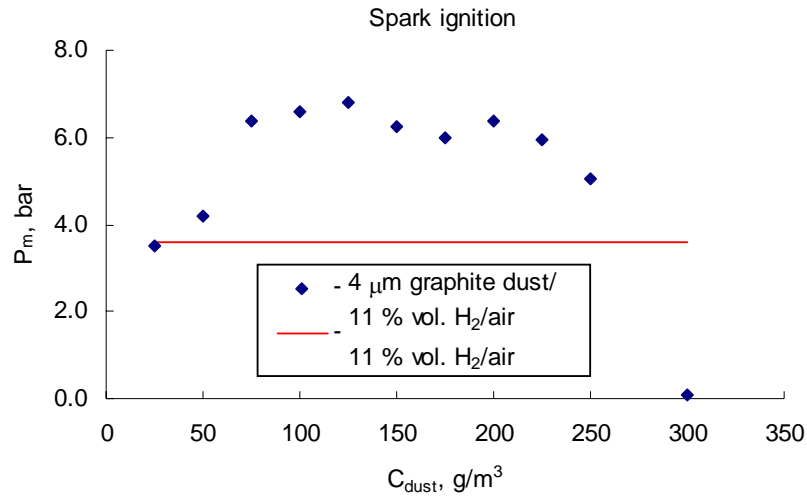<p style="text-align:center">(a)</p> <p style="text-align:center">(b)</p>
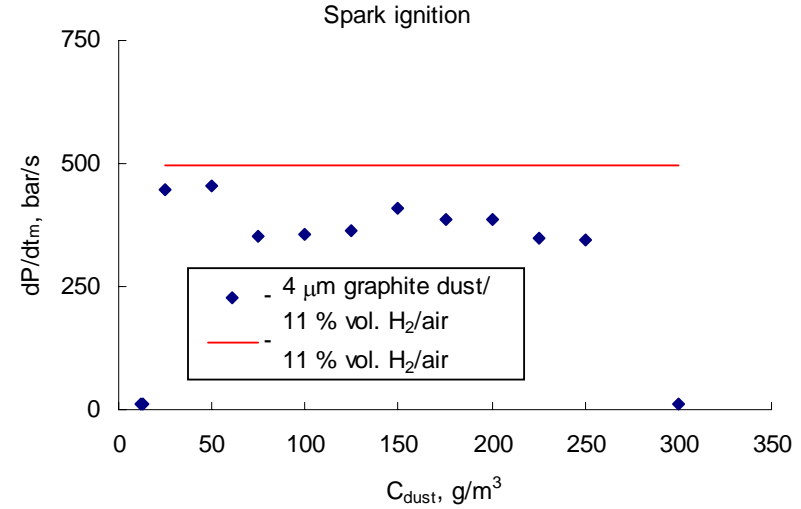
Figure 65. Pressure-time curve (a) and its derivative (b) for combined hydrogen/graphite dust explosion. [H$_2$]=11 vol. %, C$_{dust}$= 75 g/m^3.
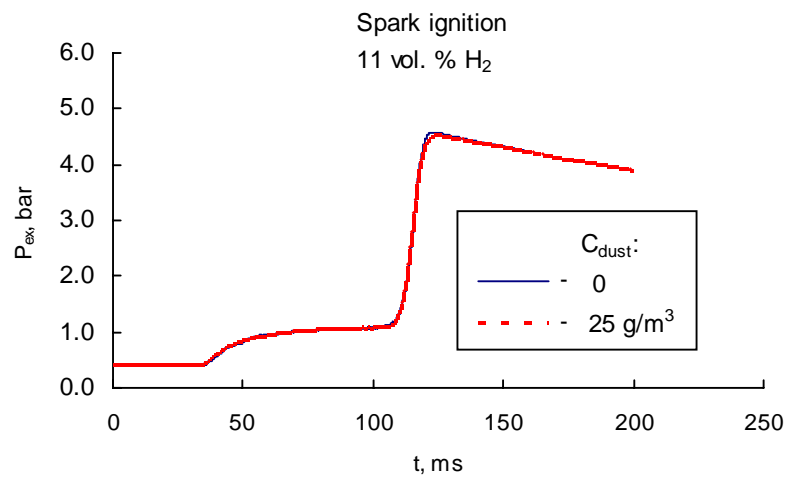
Figure 66. Pressure-time curve (a) and its derivative (b) for combined hydrogen/graphite dust explosion. $[H_2]$=11 vol. %, C_{dust}= 100 g/m^3.

Figure 67. Pressure-time curve (a) and its derivative (b) for combined hydrogen/graphite dust explosion. $[H_2]$=11 vol. %, C_{dust}= 125 g/m^3.
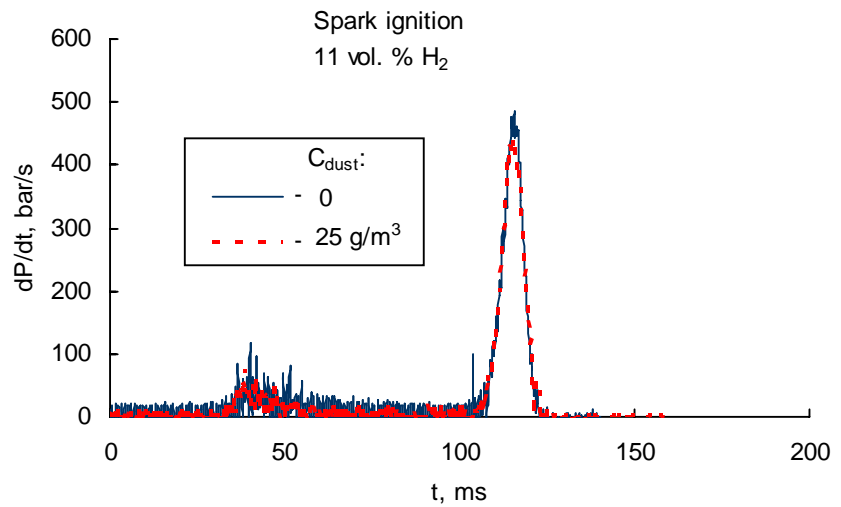
(a)

(b)

Figure 68. Pressure-time curve (a) and its derivative (b) for combined hydrogen/graphite dust explosion. $[H_2]$=11 vol. %, C_{dust}= 150 g/m^3.
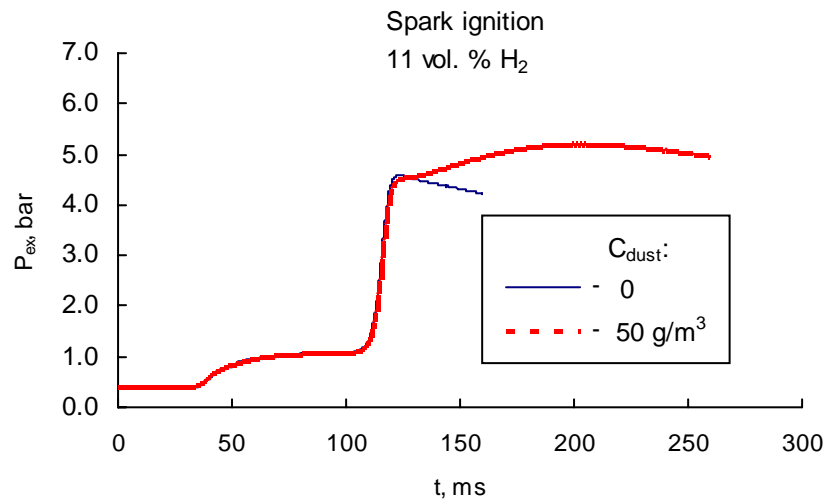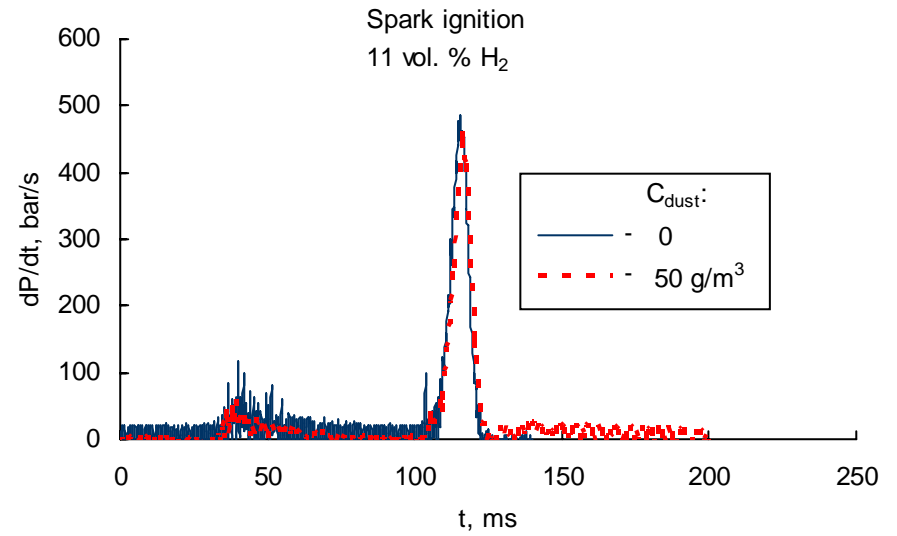

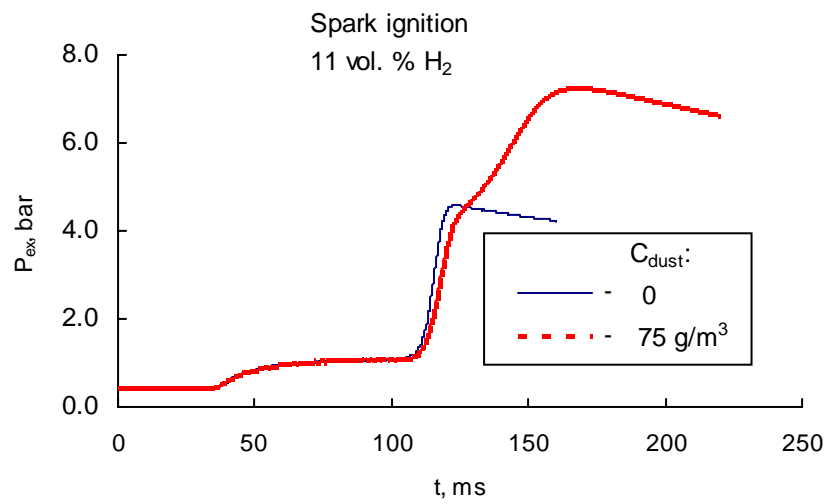(a)
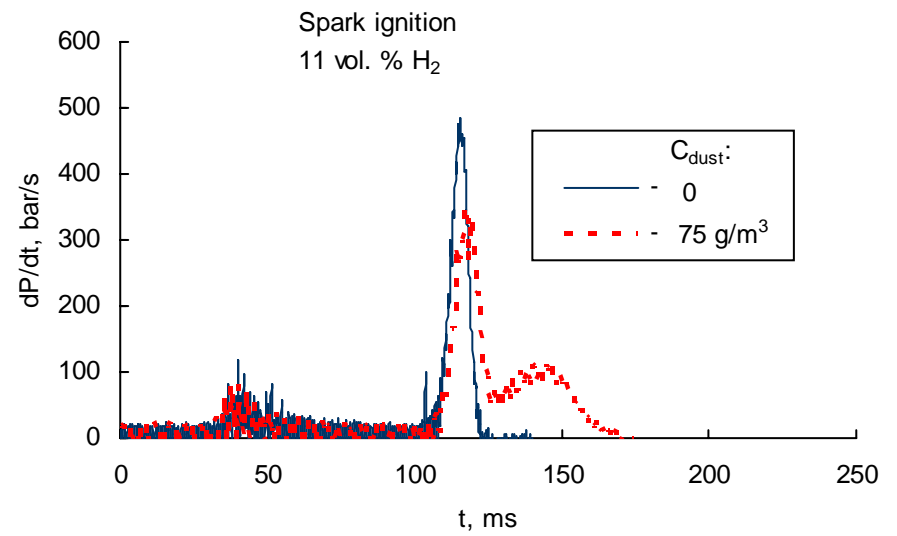
(b)

Figure 69. Pressure-time curve (a) and its derivative (b) for combined hydrogen/graphite dust explosion. $[H_2]$=11 vol. %, C_{dust}= 250 g/m^3.
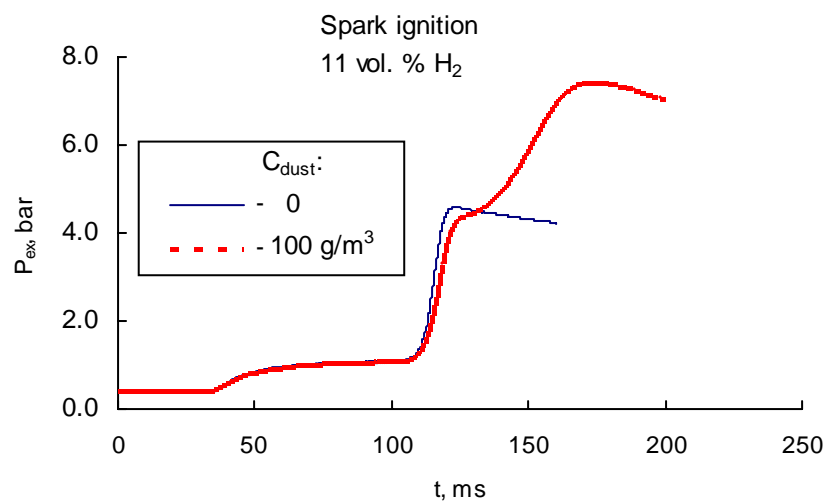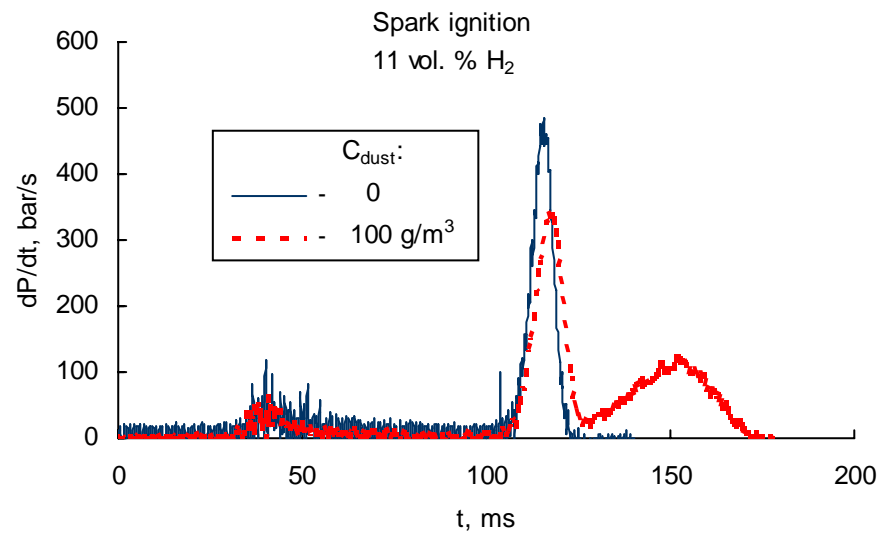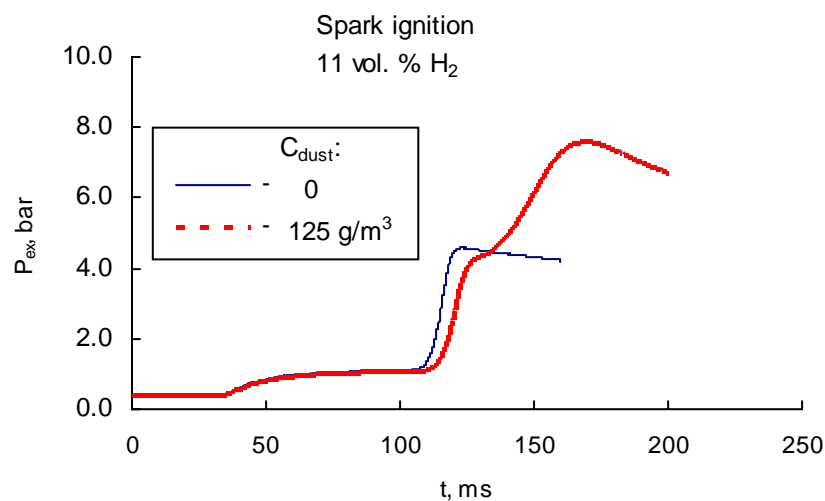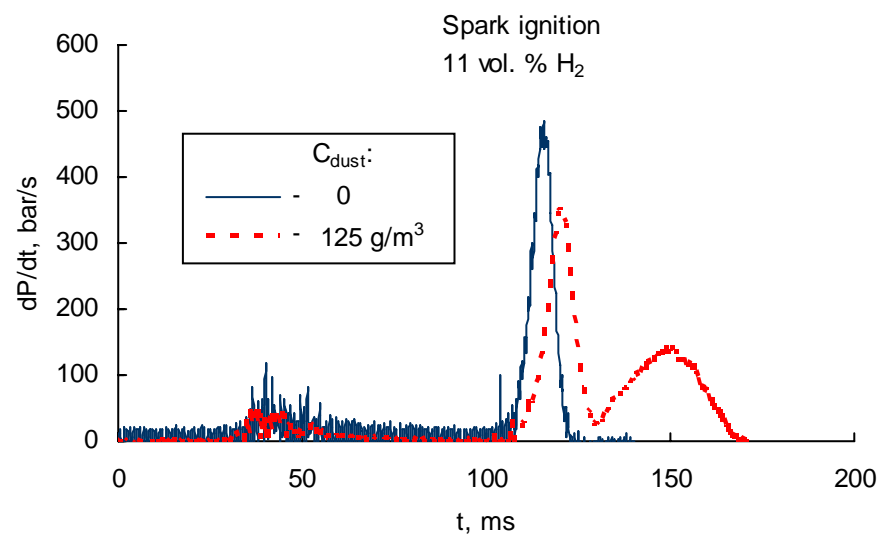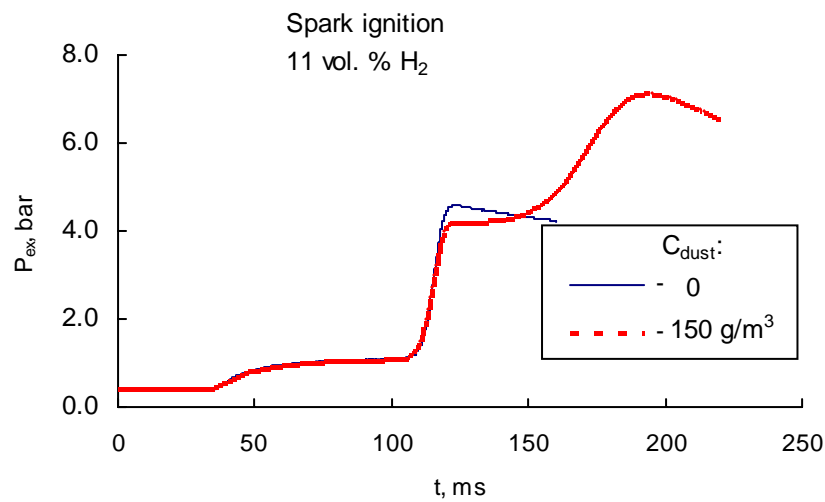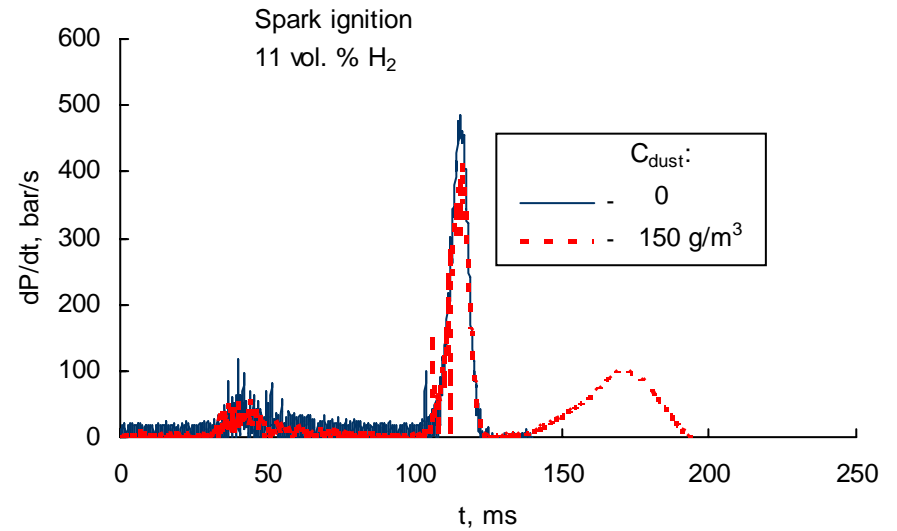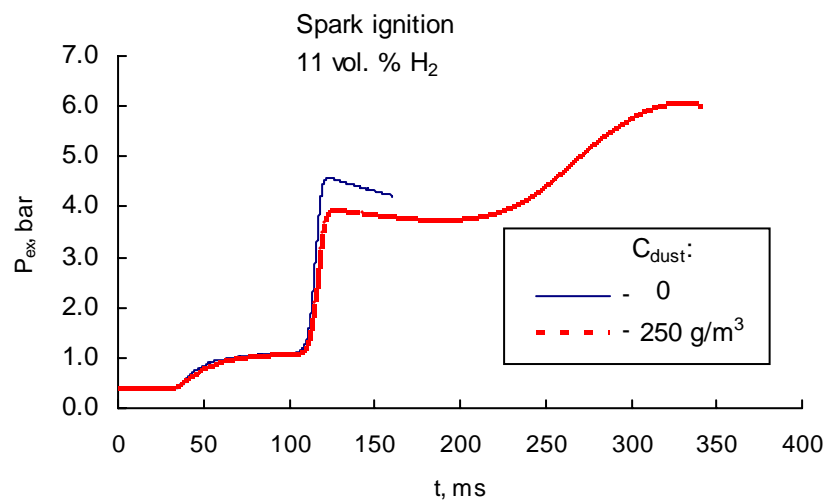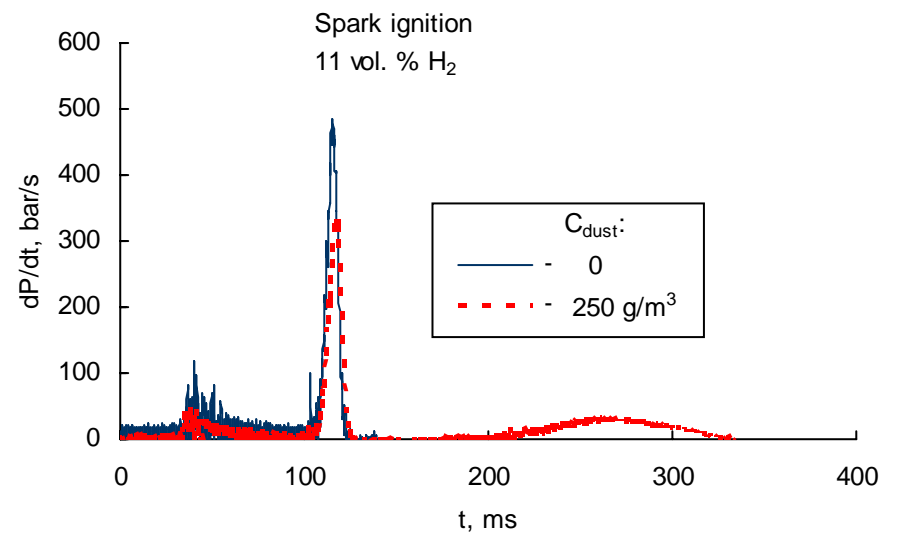
Combined hydrogen/dust explosion tests: Summary and conclusions

About 180 tests have been performed to investigate the combined dust/hydrogen explosion hazard in ITER. The explosion behaviour of fine graphite dust/hydrogen/air mixtures was studied using a standard method with a 20-l sphere. The explosion indices of four-micron graphite dust were measured in hydrogen-containing atmospheres at 1 bar initial pressure and room temperature. The dust was tested in 25-300 g/m3 concentration range, the hydrogen content varied from 4 to 18 vol. %. Both strong 10-kJ chemical igniters and electric spark were used to ignite the mixtures. The maximum overpressures generated during the explosions and maximum rates of pressure rise were measured as functions of hydrogen content and dust-cloud concentrations.

The use of strong chemical igniters provides pressure loads that can be expected if a strong local hydrogen explosion ignites hydrogen/dust/air cloud. Furthermore, such data can help to determine the dust effect on pressure loads in case of developed hydrogen flame propagation, namely, whether the dust amplifies the explosion or mitigates it by acting as a heat-sink agent. Tests with electric spark ignition address the issue if a cloud of ITER-relevant dust can be ignited by a weak ignition source in presence of hydrogen.

Strong chemical igniters. Adding hydrogen to a graphite dust cloud atmosphere makes the dust explosible by 10 kJ igniters at any tested concentrations. At low concentrations, from 4 to 8 vol. %, hydrogen acts like an additional igniter. The explosion process of the hybrid dust/hydrogen/air mixture is similar to the explosion of a dust/air mixture. It consists of a fast combined explosion of the chemical igniter and hydrogen followed by the dust explosion phase. With increasing dust concentrations, the dust-explosion phase becomes faster, and, near the optimum dust-in-air concentrations, it overlaps the ignition phase. At medium hydrogen concentrations, from 8 to 12 vol. %, some part of the dust explodes together with hydrogen participating in the fast explosion phase. At higher hydrogen concentrations, from 14 to 18 vol. %, most of the dust is involved in the fast phase; dust and hydrogen explode together like a monofuel.

At all tested combinations of hydrogen/dust concentrations the measured maximum overpressures are higher than those produced by hydrogen or dust alone (Fig 35a). The maximum rates of pressure rise for the hybrid mixtures at low hydrogen concentrations (4 and 6 vol. %) are lower than for the corresponding hydrogen/air mixtures. In this sense one can say that dust slows down the combustion of hydrogen. At higher hydrogen concentrations the

maximum rates of pressure rise in the hybrid mixtures can be higher than those featuring hydrogen/air mixtures (see Fig. 35b).

Electric spark ignition. Hybrid hydrogen/graphite dust mixtures can be induced to explode by an electric spark only at hydrogen concentrations higher than 8 vol. %. In case of 8 vol. % hydrogen the used electric spark ignites only the hydrogen constituent of the mixtures; the graphite dust is not involved in the explosion process at any tested dust concentrations. In this case the dust acts as a heat-sink decreasing the maximum overpressure and rate of pressure rise. At medium hydrogen concentrations (10-12 vol. %) both hydrogen and graphite dust can be induced to explode by electric spark ignition. Like in the case of strong ignition, the hybrid explosion consists of two phases. Initially the spark triggers the hydrogen which reacts similar to the case without dust. Then the graphite dust combustion follows, if the dust concentration is high enough. The LEL is 75 g/m^3 for 10 and 10.5 vol. % hydrogen content. With increasing dust concentrations the dust constituent explodes faster generating higher overpressures. For the medium hydrogen concentrations there are also upper dust concentrations limiting the dust explosion development; these UELs are 150 and 175 g/m^3 at 10 and 10,5 vol. % of hydrogen, respectively. With 11 vol. % of hydrogen added, the dust/air mixtures can explode in the dust concentration range from 50 to 250 g/m^3.

At low hydrogen concentrations the maximum rates of pressure rise in the hybrid mixtures are generally lower that the corresponding values of hydrogen/air mixtures, indicating a slower reaction than without dust.

At hydrogen concentrations from 14 to 18 vol. % both reactions proceed at the same time scale resulting in only one fast phase of the hybrid hydrogen-dust explosion. The maximum rates of pressure rise are higher than those measured without dust.

Open-end dust combustion tube

The purpose of the facility is to measure the effective flame velocities (EFV) in dust-air mixtures. The dusts under consideration are pure C, W, Al and/or Mg, and their mixtures. The dependence of the EFV is to be studied as function of the characteristic dust particle size, dust concentration, turbulence level, and the parameters of the oxidizing gas, namely, oxygen content and pressure. The influence of hydrogen addition is also to be studied. The measurements will be performed at room temperature.

The measurement method is to create a dust-air cloud in a long cylindrical tube placed horizontally, where one of its ends is open to atmosphere. The cloud is ignited at the open end, and the process of the flame propagation towards the closed end of the tube is investigated. Ideally, a thin flame front is formed after the dust cloud ignition, and the flame travels some distance along the tube. If the combustion products can flow out freely to the atmosphere at the open end, the flame front propagates toward the closed end of the tube in an undisturbed reagent mixture. The propagation of the flame front along the tube is recorded by front-arrival-time measurements, and the flame velocity is extracted from the measurement results.

The dust cloud is formed by dispersion of a dust layer, which has been deposited on the bottom of the tube prior to testing, which can be suspended by an array of jets of compressed air from a dispersion pipe with a row of holes. This method was used in [17]. The dispersion pipe is fixed inside the tube slightly above the tube bottom; the blow holes point downwards onto the dust layer. To obtain the desired pressure inside the tube after the dust dispersion, the tube is pre-evacuated. A thin-film diaphragm closing the 'open' end of the tube provides the necessary vacuum before the dust dispersion and keeps the cloud inside the tube. At the moment of ignition the diaphragm is ruptured. The dust cloud atmosphere immediately after dust dispersion is highly turbulent; but the turbulence level decays with time. Varying the delay between dust dispersion and ignition allows measurements at different turbulence levels.

To measure the parameters of flame propagation, a number of gauges need to be installed along the tube and at the end flange of the tube. A set of ports is arranged to fix the gauges. Subsidiary ports are arranged to fix the igniter feedings and the dispersion pipe.

In practical work the tube cannot be opened to the atmosphere directly, because the combustion products can be aggressive, hot, etc. To keep the environment safe and clean, the test tube is connected to a dump tank of 0.5 m^3 inner volume and 2 bar design overpressure.

A very important issue in this measurement method is the spatial homogeneity of the dust cloud concentration. So at first pre-tests on the dust dispersion process will be performed to define the optimum operating parameters for the cloud homogeneity For these tests the tube must be transparent.

The open-end dust combustion facility has been designed and fabricated (Fig. 70). The facility consists of a metal dump tank *1* to receive the combustion products, a plexiglas tube *2* of 150 mm i.d. connected to the tank by a joint-flange assembly *3*, and dust dispersion system (not shown). The tube and the tank are fixed on the frame *4* by two ring holders *5*. The tube consists of two parts, a 1 m and a 2 m long pieces, that makes it possible to vary the tube length. The parts are joint together by flange *6* and rods *7*. The rods also fix the tube to the tank. The tube is closed by the end flange *8* with outlet *9* for evacuation and port *10* for a pressure gauge, see also Fig. 71.

The dispersion system consists of a dispersion pipe *11* placed inside the combustion tube, a pressure reservoir, and an electromagnetic valve. The dispersion pipe of 14 mm diameter is made of stainless steel. The pipe is fixed inside the tube at 5 mm distance above the tube bottom. The holder design makes it possible to vary the height of the dispersion pipe in the test tube. The pipe has a row of holes pointing down towards the bottom of the test tube. The holes have 1 mm diameter and placed 30 mm apart.

The air-pressure reservoir is a stainless-steel vessel of about 7 l volume. It is pressurized with compressed air to 20 bar overpressure (design overpressure is 30 bar). The reservoir inlet is connected with a pipe to a standard compressed-air bottle, and the reservoir outlet is connected by a pipe with an electromagnetic valve.

The electromagnetic valve serves to open the outlet of the pressure reservoir to let the compressed air flow through the dispersion pipe into the combustion tube and then to close the outlet to prevent backflow of the combustion products. The operation of the electromagnetic valve must provide a certain volume of air to the dispersion system in order to fill the combustion tube with air to a pre-specified pressure. This is achieved by precise timing of the valve operation. A typical example of the operation is as follows: the valve opens in less than 5 milliseconds, remains open for 10 to 100 ms, and then closes the line in less than 5 ms. The design operation pressure of the valve is 30 bar. A special controlling system has been fabricated to supply the valve with 24 V up to 4 A and to control valve and ignition operation.
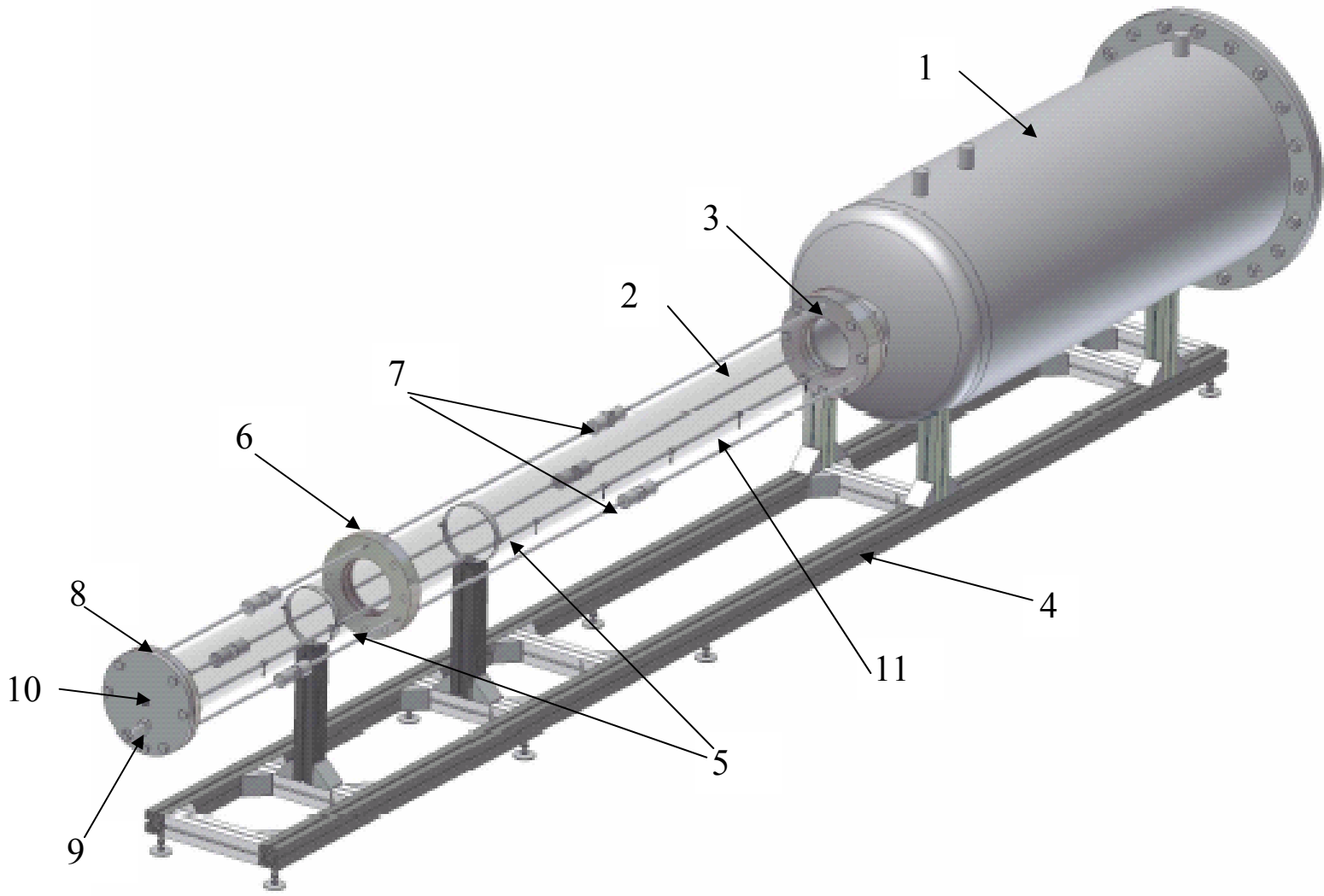
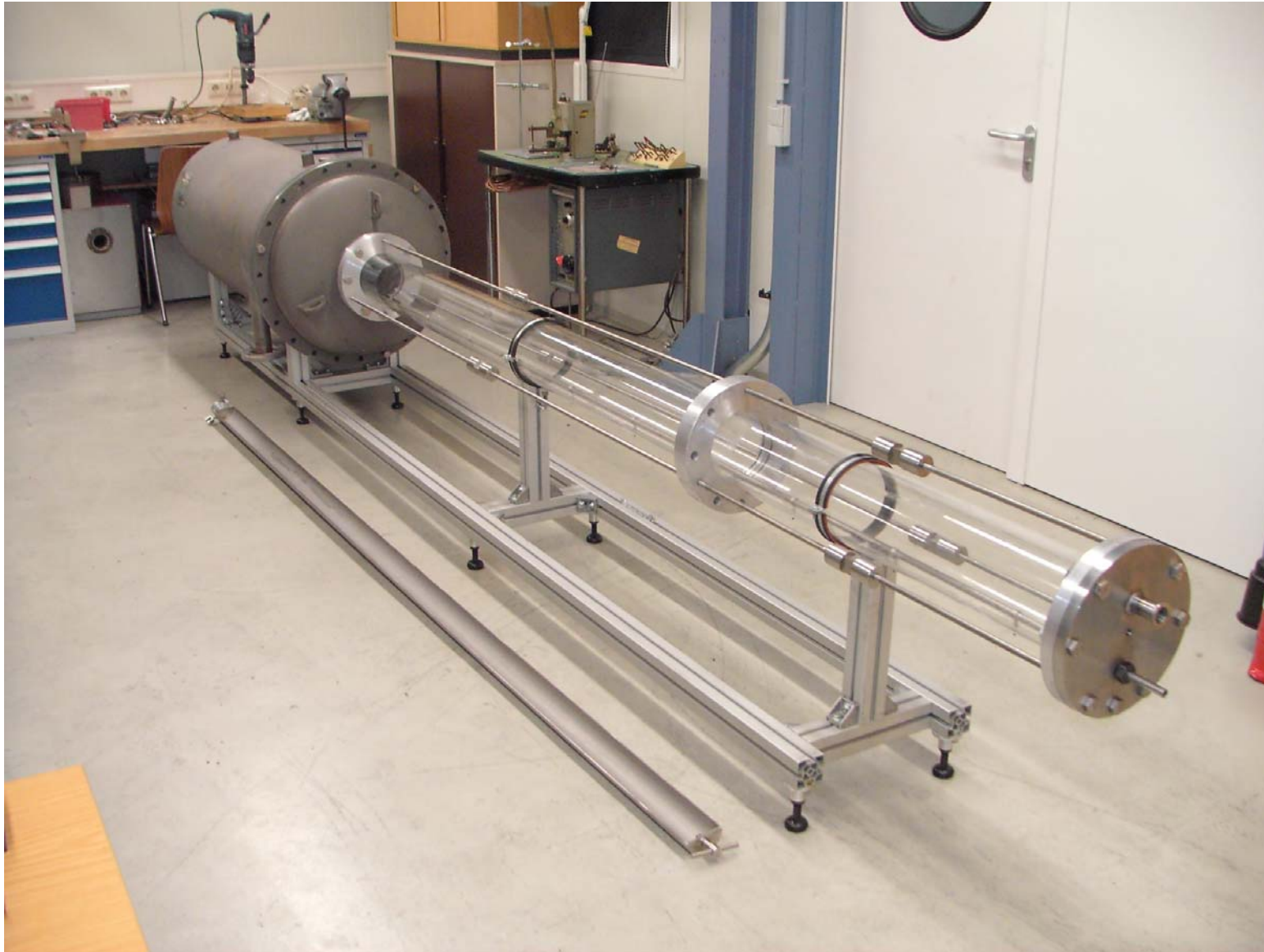Figure 70. Open-end combustion tube. Design view.

Figure 71. Open-end combustion tube. The tube is transparent to perform dispersion tests.

References

1. A. Denkevits, S. Dorofeev. Dust explosion experiments: measurements of explosion indices of graphite dusts. FZK Report FZKA 6872, 2003.

2. A. Denkevits, S. Dorofeev. Dust explosion experiments: measurements of explosion indices of tungsten dusts and graphite-tungsten dust mixtures. FZK Report FZKA 6987, 2004.

3. 17. VDI-Richtlinien. Staubbrände und Staubexplosionen Gefahren-Beurteilung-Schutzmaßnahmen. Beuth Verlag GmbH, Berlin, 1990.

4. R. Siwek, Determination of technical safety indices and factors influencing hazard evaluation of dusts, J. Loss Prev: Process Ind. 9 (1996) 21-31.

5. W. Breitung, A. Denkevits, M. Kuznetsov, R. Redlinger, feasibility study for hydrogen and dust explosion experiments on ITER-relevant scale, Report on EFDA Task TW4-TSS-SEA5.5, July 2004.

6. R. K. Eckhoff, Dust Explosions in the Process Industries (3rd edition). Gulf Professional Publishing, Amsterdam, 2003, pp. 50-56.

7. R. Foniok, Hybrid dispersive mixtures and inertized mixtures of coal dusts. Explosiveness and ignitability, Staub Reinhalt. Luft 45 (1985) 151-154.

8. M. Hertzberg, K.L. Cashdollar, Introduction to dust explosions, in Industrial Dust Explosions, ed. K.L. Cashdollar and M. Hertzberg, ASTM Special Technical Publication 958, Philadelphia: ASTM (1987) 5-32.

9. P. Cardillo, E.J. Anthony, The flammability limits of hybrid gas and dust systems, La Rivista dei Combustibili 32 (1978) 390-395.

10. H. Franke, Bestimmung der Mindestzündenergie von Kohlenstaub/Methan/Luft-Gemischen (Hybride Gemische), VDI-Berichte 304 (1985) 69-72.

11. J.G. Torrent, J.C. Fuchs, Flammability and explosion propagation of methane/coal dust hybrid mixtures, 23rd Int. Conf. of the Safe Mining Research Institute, Washington DC, September 1989.

12. W. Bartknecht, Explosionen-Ablauf und Schutzmassnahmen, Berlin, Springer-Verlag, 1978.

13. C. J. Dahn, Contribution of low-level flammable level concentrations to dust explosion output, 2nd Int. Colloquium on Dust Explosions, Warsaw, Poland, 1986.

14. R. Siwek, Determination of technical safety indices and factors influencing hazard evaluation of dusts, J. Loss Prev. in Process Ind. 9 (1996) 21-31.

15. Ch. Cesana, R. Siwek. Operating Instructions for 20-l-Apparatus. Adolf Kühner AG, Birsfelden, Switzerland, 2001 (http://www.kuhner.com/DOCUMENT/KSEP_E.pdf).

16. A. Bezmelnitsyn et. al., Experimental study on laminar burning velocities for nuclear safety applications, RRC Kurchatov Institute Report for FZK-INR, Contract No 315/20116757/INR, Moscow, 1999

17. F. Zhang and H. Groenig. Detonation structure of corn starch particles-oxygen mixtures. 12th ICDERS, Ann Arbor, MI, 1989.